

**REGULATING PRE-MRNA SPLICING AND TRANSCRIPTION USING SMALL
MOLECULES FOR CANCER THERAPY**

by

Yang Gao

B.S., Yantai University, 2004

M.S., Lanzhou University, 2007

Submitted to the Graduate Faculty of

Kenneth P. Dietrich School of Arts and Sciences in partial fulfillment
of the requirements for the degree of
Doctor of Philosophy

University of Pittsburgh

2014

UNIVERSITY OF PITTSBURGH
DIETRICH SCHOOL OF ARTS AND SCIENCES

This dissertation was presented

by

Yang Gao

It was defended on

March 11, 2014

and approved by

Paula Grabowski, Professor, Department of Biological Sciences

Steve Weber, Professor, Department of Chemistry

Michael Trakselis, Assistant Professor, Department of Chemistry

Dissertation Advisor: Kazunori Koide, Associate Professor, Department of Chemistry

Copyright © by Yang Gao

2014

REGULATING PRE-MRNA SPLICING AND TRANSCRIPTION USING SMALL MOLECULES FOR CANCER THERAPY

Yang Gao, PhD

University of Pittsburgh, 2014

Eukaryotic gene expression is an integral network encompassing chromatin packaging, transcription, capping, polyadenylation, splicing, mRNA nuclear export, and translation. Pre-mRNA splicing removes non-coding RNA sequences, generates proteomic diversity, and even affects other gene expression processes. Hence, dysregulated splicing has emerged as the origin of various diseases including cancer, representing an attractive therapeutic target. FR901464 is a natural bacterial metabolite that arrests tumor growth by interfering with the spliceosomal SF3b subcomplex. Meayamycin B, an FR901464 analogue synthesized by the Koide group, exhibited picomolar anti-proliferative activity in a broad spectrum of tumor cell lines.

The first goal of this thesis project was to further characterize the biological activity of meayamycin B and identify downstream effectors, thereby discovering novel combination therapeutics for cancer. To that end, we first optimized a cell-based reporter system for splicing inhibition, which was subsequently used for a comprehensive comparison of meayamycin B with recently reported splicing modulators, including spliceostatin A, herboxidiene, and meayamycin. This study provides a handy guide in terms of the splicing inhibitory activity of these widely utilized compounds in both basic and translational research.

To identify downstream effectors and their therapeutic applications, we focused on examining the B-cell lymphoma 2 (Bcl-2) family members that control the mitochondria-

mediated cell death pathway — apoptosis. This effort led us to myeloid cell leukemia sequence-1 (Mcl-1), a Bcl-2 family member that is recurrently correlated with drug resistance and tumor refractory. Meayamycin B reversed the dominant splicing isoform from Mcl-1_L to Mcl-1_S, resulting in a proapoptotic cellular environment. Taking advantage of this effect, we combined meayamycin B with Bcl-x_L inhibitor ABT-737 to trigger apoptosis in cancer cell lines that were otherwise resistant to either single agent. This potent combination was characterized *in vitro* in non-small-cell lung carcinoma (NSCLC) and head and neck squamous cell carcinoma (HNSCC) models.

The second part of this thesis project was devoted to the biological characterization of a fungal metabolite TMC-205 and its stable analogs. These indole derivatives are both activators of Simian virus 40 (SV40) promoter and inhibitors of firefly luciferase, representing a new generation of anticancer agents with a multifactorial mode of action.

TABLE OF CONTENTS

LIST OF ABBREVIATIONS	XIV
ACKNOWLEDGEMENTS	XVIII
1.0 BACKGROUND	1
1.1 PRE-MRNA SPLICING AND CANCER	1
1.1.1 Spliceosome-mediated splicing	1
1.1.2 Alternative splicing and cancer	5
1.1.2.1 Regulation of alternative splicing.....	5
1.1.2.2 Splicing regulatory proteins as anticancer drug targets.....	9
1.2 TARGETING SF3B SUBUNIT 1 (SF3B1).....	10
1.2.1 SFEB1 in constitutive splicing	10
1.2.2 SF3B1 in alternative splicing	12
1.2.3 SF3B1 alterations in cancer	14
1.2.4 SF3b modulators	16
1.2.4.1 FR901464 and its analogs.....	16
1.2.4.2 Pladienolides, E7107 and their analogs	21
1.2.4.3 Sudemycins.....	23
1.2.4.4 Herboxidiene/GEX1A.....	24
1.2.5 Summary.....	25

2.0	SF3B MODULATOR MEAYAMYCIN B FOR CANCER THERAPY	28
2.1	MEAYAMYCIN B—POTENT SPLICING MODULATOR.....	28
2.1.1	Research Design	28
2.1.2	Results and Discussion.....	29
2.1.2.1	Cell-based splicing inhibition assay	29
2.1.2.2	Evaluation of natural and synthetic SF3b inhibitors	33
2.1.2.3	Are simple electrophiles sufficient to inhibit splicing?.....	36
2.1.3	Conclusion.....	37
2.1.4	Experimental	38
2.2	MEAYAMYCIN B SENSITIZES NON-SMALL CELL LUNG CARCINOMA TO BCL-X_L/BCL-2 INHIBITOR	43
2.2.1	Research design	43
2.2.2	Results and Discussion.....	44
2.2.2.1	Dose-dependent modulation of alternative splicing of Mcl-1	44
2.2.2.2	Time-dependent modulation of alternative splicing of Mcl-1.....	46
2.2.2.3	Meayamycin B does not regulate alternative splicing of Bcl-x.....	48
2.2.2.4	Meayamycin B sensitizes A549 and H1299 cells to ABT-737	49
2.2.2.5	Mcl-1 abundance correlates with meayamycin B-sensitivity.....	50
2.2.2.6	Meayamycin B and ABT-737 combination synergistically causes apoptosis	52
2.2.3	Conclusion.....	54
2.2.4	Experimental	54

2.3 MEAYAMYICN B SENSITIZES HEAD AND NECK SQUAMOUS CELL CARCINOMA TO BCL-X_L/BCL-2 INHIBITOR.....	58
2.3.1 Introduction.....	58
2.3.2 Results and Discussion.....	61
2.3.2.1 Meayamycin B and ABT-737 combination causes apoptosis	61
2.3.2.2 Basal level of MCL-1 correlates with meayamycin B sensitivity ...	67
2.3.2.3 Regulation of the splicing of Mcl-1 pre-mRNA	69
2.3.2.4 Cell type-dependent inhibition of HPV-16 E6 splicing	74
2.3.2.5 SF3B1 inhibition is not the only activity of meayamycin B	77
2.3.3 Discussion.....	80
2.3.4 Conclusion.....	82
2.3.5 Experimental	83
2.4 MEAYAMYCIN B IN OTHER IN VITRO CELL MODELS.....	87
2.4.1 Cisplatin-resistant ovarian cancer cells	87
2.4.2 Cervical cancer model cell lines	89
2.4.3 Experimental	90
3.0 ACTIVATION OF SV40 PROMOTER AND INHIBITION OF LUCIFERASE BY TMC-205 AND ANALOGS	92
3.1 RESEARCH PLAN.....	92
3.2 RESULTS AND DISCUSSION.....	93
3.2.1 Viral promoter activation.....	94
3.2.2 Luciferase inhibition	96
3.3 CONCLUSION.....	99

3.4 EXPERIMENTAL	99
BIBLIOGRAPHY	103

LIST OF TABLES

Table 1-1 Human genes controlled by SF3b components	27
Table 2-1 Primer sequences for RT-PCR experiments in NSCLC system.....	57
Table 2-2 GI50 values for 72-h antiproliferation assays in HNSCC cells.....	62
Table 2-3 Primer sequences for RT-PCR experiments in HNSCC system	86
Table 3-1 Antiproliferative activity of TMC-205 and its analogs against HCT-116	94

LIST OF FIGURES

Figure 1-1 Spliceosome assembly and activation along pre-mRNA	3
Figure 1-2 The chemistry of splicing.....	4
Figure 1-3 Patterns of alternative splicing.....	6
Figure 1-4 Exon definition mediated by splicing machinery and RBPs.....	8
Figure 1-5 SF3B1 mediates U2 snRNP assembly in constitutive splicing.....	11
Figure 1-6 SF3B1 regulates Bcl-x alternative splicing in response to ceramide signaling	13
Figure 1-7 Structures of FR901464 and its derivatives	17
Figure 1-8 Structures of thailanstatin A and spliceostatin B	18
Figure 1-9 Structures of pladienolides and their analogs.....	22
Figure 1-10 Structures of sudemycin F1 and D6.....	24
Figure 1-11 Structure of herboxidiene.....	24
Figure 2-1 TPI minigene constructs for splicing inhibitor screening	30
Figure 2-2 Meayamycin B in HEK293-II and HEK293-III.....	31
Figure 2-3 Optimization of cell density	32
Figure 2-4 Z-factor calculation of the splicing inhibition assay in a 96-well format	33
Figure 2-5 Splicing inhibition of TPI minigene by SF3b inhibitors for 16 h	34
Figure 2-6 Time-dependence of splicing inhibition by SF3b inhibitors.....	35

Figure 2-7 Correlation between splicing inhibitory and antiproliferative activities.....	36
Figure 2-8 Epoxides and Michael acceptors do not inhibit splicing.....	37
Figure 2-9 Structures of meayamycin B and ABT-737	44
Figure 2-10 Dose-dependent regulation of Mcl-1 alternative splicing.....	46
Figure 2-11 Time-dependent regulation of Mcl-1 alternative splicing.....	47
Figure 2-12 Meayamycin B inhibits the constitutive splicing of Mcl-1	48
Figure 2-13 Mcl-1 abundance correlates with meayamycin B-sensitivity	51
Figure 2-14 Rapid onset of apoptosis triggered by the combination in NSCLC cells.....	52
Figure 2-15 Apoptosis activation monitored with Annexin V-FITC and PI staining.....	53
Figure 2-16 Generation of HPV16 E6 and E7 oncoproteins	60
Figure 2-17 Antiproliferation assays of meayamycin B and ABT-737 in HNSCC cells	63
Figure 2-18 Bliss Independence evaluation of meayamycin B and ABT-737 combination	64
Figure 2-19 Apoptosis activation monitored with Annexin V-FITC and PI staining.....	65
Figure 2-20 Bak/Bax-mediated apoptosis.....	67
Figure 2-21 Basal expression of anti-apoptotic Bcl-2 proteins at the protein level.....	68
Figure 2-22 Anti-proliferative activity of meayamycin B in HNSCC cell lines	69
Figure 2-23 RT-PCR analysis of the alteration of Mcl-1 alternative splicing.....	70
Figure 2-24 Western blotting analysis of the alteration of Mcl-1 alternative splicing	71
Figure 2-25 Enhanced Mcl-1 elimination by meayamycin B and ABT-737 combination.....	72
Figure 2-26 Meayamycin B inhibits constitutive splicing Mcl-1	73
Figure 2-27 Meayamycin B does not regulate Bcl-x alternative splicing	74
Figure 2-28 Meayamycin B regulates HPV16 E6/E7 splicing.....	76
Figure 2-29 SF3B1 knockdown switches the pattern of Mcl-1 alternative splicing.....	77

Figure 2-30 SF3B1 knockdown in UM-SCC47 and 93-VU-147T	78
Figure 2-31 SF3B1 controls splicing patterns of HPV16 E6 and Mcl-1	79
Figure 2-32 Meayamycin B and ABT-737 combination overcomes cisplatin resistance	88
Figure 2-33 Antiproliferative and caspase 3/7 assays in cervical cancer cells	90
Figure 3-1 SV40 enhancer-dependent activation of SV40 promoter.....	95
Figure 3-2 TMC-205 activates SV40 promoter independent of enhancer.....	95
Figure 3-3 Compounds 12, 14 and resveratrol activate SV40 promoter	96
Figure 3-4 Absorption spectra of compound 12	97
Figure 3-5 Compound 12 and resveratrol non-competitively inhibit luciferase.....	98
Figure 3-6 Activation of Luciferase expression at the mRNA level	99

LIST OF ABBREVIATIONS

7-AAD	7-aminoactinomycin D
ATCC	American Type Culture Collection
ATP	adenosine triphosphate
Bak	Bcl-2-antagonist/killer-1
Bax	Bcl-2 associated X protein
BCA	bicinchoninic acid
Bcl-2	B-cell lymphoma 2
Bcl-x _L	B-cell lymphoma-extra large
BH3	Bcl-2 homolgy domain 3
BODIPY	boron dipyrromethene
BSA	bovine serum albumin
Cdc25A	cell division cycle 25A
CDK	cyclin-dependent protein kinase
cDNA	complementary DNA
CLL	chronic lymphocytic leukemia
CMV	cytomegalovirus
CRCE-1	ceramide-responsive <i>cis</i> -element 1
DMEM	Dulbecco's Modified Eagle Medium
DMSO	dimethyl sulfoxide
ED ₅₀	half maximal effective dose
EJC	exon junction complex
ESE	exonic splicing enhancer
ESS	exonic splicing silencer

FADD	Fas-associated death domain protein
FAS	apoptosis stimulating fragment
FIR	FUSE-binding protein interacting repressor
FITC	fluorescein isothiocyanate
FUSE	far-upstream element
GI ₅₀	half maximal growth inhibitory concentration
HDACi	histone deacetylase inhibitor
HEAT	huntington, elongation factor 3, PR65/A, TOR
HEK293	Human embryonic kidney 293
hnRNP	heterogeneous nuclear ribonucleoprotein
HNSCC	head & neck squamous cell carcinoma
HPLC	high-performance liquid chromatography
HPV	human papillomavirus
HRP	horseradish peroxidase
IC ₅₀	half maximal inhibitory concentration
IL-2	interleukin 2
ISE	intronic splicing enhancer
ISS	intronic splicing silencer
I κ B α	nuclear factor of kappa light polypeptide gene enhancer in B-cell inhibitor, alpha
MAMB	meayamycin B
Mcl-1	myeloid cell leukemia sequence 1
MDM2	murine double minute 2
MDS	myelodysplastic syndrome
Me	methyl
MEF	mouse embryonic fibroblast
MM	multiple myeloma
mTOR	mammalian target of rapamycin
MTS	3-(4,5-dimethylthiazol-2-yl)-5-(3-carboxymethoxyphenyl)-2-(4-sulfophenyl)-2 <i>H</i> -tetrazolium
NF κ B	nuclear factor of kappa light polypeptide gene enhancer in B-cell

NIPP1	nuclear inhibitor of protein phosphatase 1
NMD	nonsense-mediated mRNA decay
NOK	normal oral keratinocyte
NSCLC	non-small cell lung carcinoma
NTD	N-terminus domain
PHF5A	plant homeodomain (PHD)-finger domain protein
PI	propidium iodide
PI3K	phosphatidylinositol-3-kinase
PMS	phenazine methosulfate
PMSF	phenylmethylsulfonyl fluoride
Pre-mRNA	precursor messenger RNA
Puf60	poly(U)-binding-splicing factor 60
PUMA	p53 upregulated modulator of apoptosis
RBP	RNA-binding protein
RLU	relative luminescence unit
ROS	reactive oxygen species
RPMI-1640	Roswell Park Memorial Institute-1640
RRM	RNA-recognition motif
RSV	resveratrol
RT-PCR	reverse transcription-polymerase chain reaction
S.D.	standard deviation
SAR	structure-activity relationship
SCLC	small-cell lung cancer
SDS	sodium dodecyl sulfate
SF3a	splicing factor 3a
SF3b	splicing factor 3b
SF45	splicing factor 45
siRNA	small interfering RNA
Sm protein	Smith protein

snRNA	small nuclear RNA
snRNP	small nuclear ribonucleoprotein
SR protein	serine/arginine-rich protein
SRSF1	serine/arginine-rich splicing factor 1
SV40	Simian virus 40
THF	tetrahydrofuran
TM domain	transmembrane domain
TPI	triose phosphate isomerase
U2AF	U2 snRNP auxiliary factor
UHM	U2AF-homology motif
ULM	UHM-ligand motif
UV	ultraviolet
VEGF	vascular endothelial growth factor

ACKNOWLEDGEMENTS

I would like to define this long journey of graduate training as my belated, genuine maturation process as a human being. What did I learn? I learned to appreciate limitations, where, paradoxically, happiness and creativity stem from; I learned making compromises is merely another term for seeking alternative solutions so that many others can also benefit; most importantly, I learned that a life-long learning process is how I prefer to spend the rest of my life. Everyone that has touched my life is my teacher; I hope I have influenced them in a similar, positive manner.

I would like to thank Dr. Koide for recognizing me and taking me, a student with pure biology background, into this organic chemistry group and providing me both opportunities and challenges that have been fundamental for my intellectual growth. During this training, I transformed from a student merely with some basic bench skills to a scholar with a clear view of her future career path.

I would like to thank the members of my dissertation committee, Professor Paula Grabowski, Professor Steve Weber and Professor Michael Trakselis, and my proposal mentor Professor Seth Horne. I appreciated every moment of communication with these passionate scientists.

I have also been honored to work with Dr. Andrea Vogt, Dr. Robert Ferris, and Dr. Sumita Trivedi. This thesis would have still been a blueprint had it not been for your help. I would also like to thank Dr. Joel Gillespie at the Materials Characterization Laboratory and the UPCI flow cytometry facility.

I am indebted to my labmates and friends in the chemistry department. An environment without you would never have become my 'second home' where I truly enjoy working hard.

Finally, I would like to thank my family with their unconditional support and love. As a single child, it's beyond my imagination how much uneasiness I have put my parents through by coming to the other side of the globe alone. I hope I can make them proud.

1.0 BACKGROUND

1.1 PRE-MRNA SPLICING AND CANCER

1.1.1 Spliceosome-mediated splicing process

Eukaryotic genes undergo a multi-step processing prior to forming messenger RNAs (mRNAs) that are subsequently exported into cytoplasm for translation.¹ One pivotal step is precursor mRNA (pre-mRNA) splicing, in which non-coding sequences (introns) are removed and protein-coding sequences (exons) are joined to produce the mRNAs. In eukaryotes, splicing of protein-coding gene transcripts is mostly carried out by the spliceosome, a macromolecular machinery composed of five small nuclear ribonucleoproteins (snRNPs) (the U1, U2, U4, U5 and U6) and more than 200 polypeptides.² Self-splicing introns exist in rRNA, tRNA, mRNA of organelles (chloroplasts and mitochondria) in fungi plants and protists, and in bacterial mRNA.³

The excision of an intron commences with the intricately regulated assembling of snRNPs onto pre-mRNAs to form an active spliceosome (Figure 1-1).⁴ This spliceosome is directed by special sequences at the intron/exon junctions called splice sites.⁵ Four consensus sequences at the splice sites define the exon-intron boundaries and direct the assembly of snRNPs. These sequences encompass GU/C at the intronic 5' splice site that marks the exon/intron junction and three conserved sequence elements at the 3' splice site region: the

branchpoint with the consensus adenine, the polypyrimidine tract, and the conserved AG at the 3' end of the intron.⁶

To initiate the assembly of the spliceosome, U1 snRNP interacts with the 5' end of the intron through RNA-RNA base-pairing.⁷ Various serine/arginine-rich (SR) proteins assist in the recognition process. For 3' splice site recognition, splicing factor-1 (SF-1) recognizes the branchpoint, and the 65 kDa and 35 kDa subunits of the U2 snRNP auxiliary factor (U2AF) bind to the polypyrimidine tract and 3' AG, respectively.⁸⁻⁹ These interactions give rise to the spliceosomal complex E. U2 snRNP is also involved in complex E, but is only loosely attached, without direct interaction with pre-mRNA. Subsequently, U2 snRNP becomes stably bound to pre-mRNA at the expense of an ATP, completing the transition from complex E to complex A. Next, extensive ATP-dependent conformational changes within complex A facilitate the incorporation of U4-U5-U6 tri-snRNP to form the spliceosomal complex B.¹⁰⁻¹² The U1 and U4 snRNPs are then released,¹³ leaving behind the activated form of spliceosomal complex B* after further dynamic conformational changes, which performs the first step of splicing catalysis. Subsequently, complex C is formed and catalyzes the second transesterification reaction.¹⁴

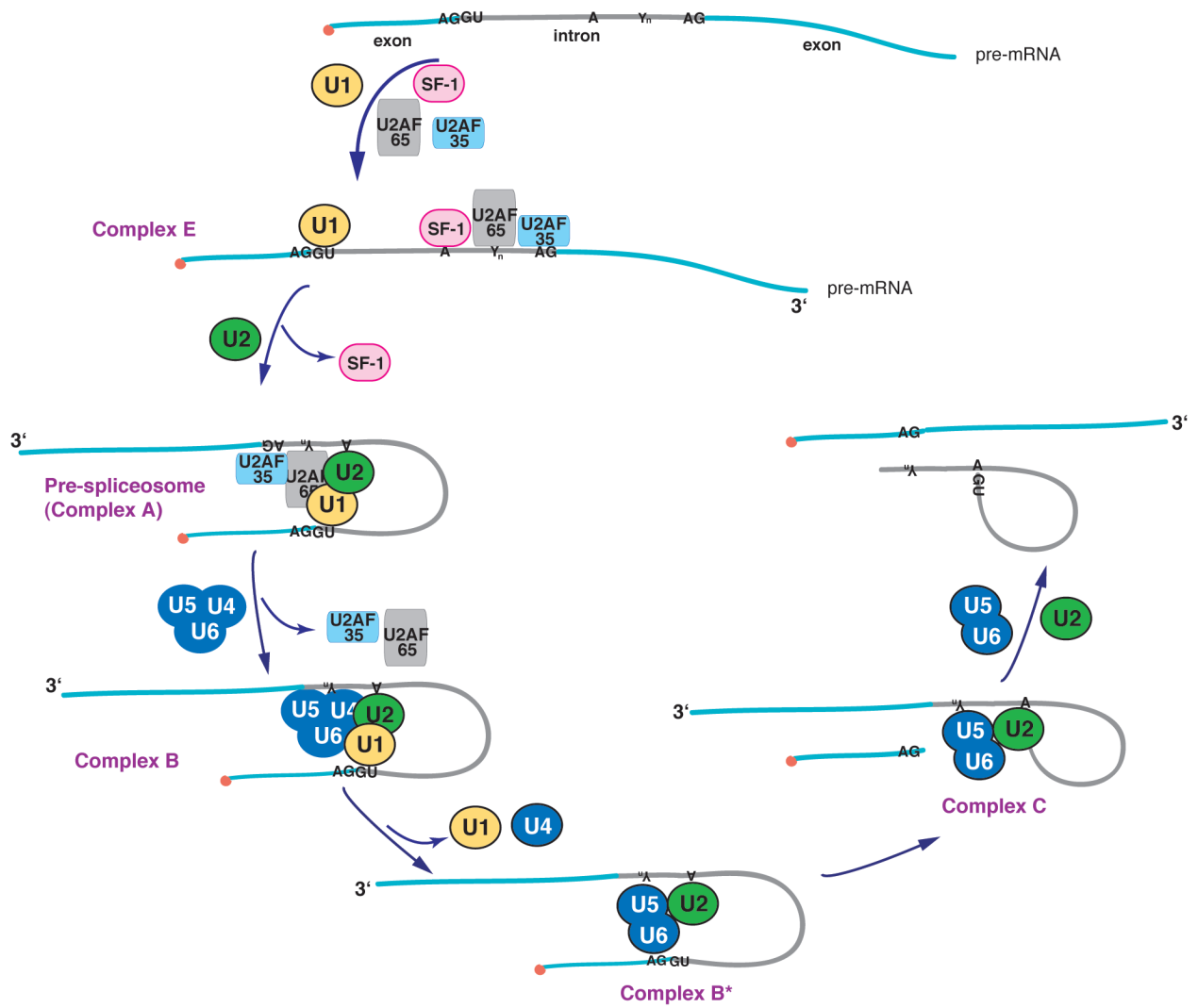


Figure 1-1 Spliceosome assembly and activation along pre-mRNA

In splicing catalysis, which comprises two sequential transesterification reactions, spliceosomal complex C brings crucial sequences in close proximity (Figure 1-2). During the first transesterification, the 2' hydroxyl group of the adenine residue at the branchpoint sequence attacks the 5' end of the intron as a nucleophile, forming a branched intermediate called an intron lariat. During the second transesterification, the 3' hydroxy group of the newly released 5' exon attacks the 3' splice site, thereby releasing the lariat and joining the exons.¹³

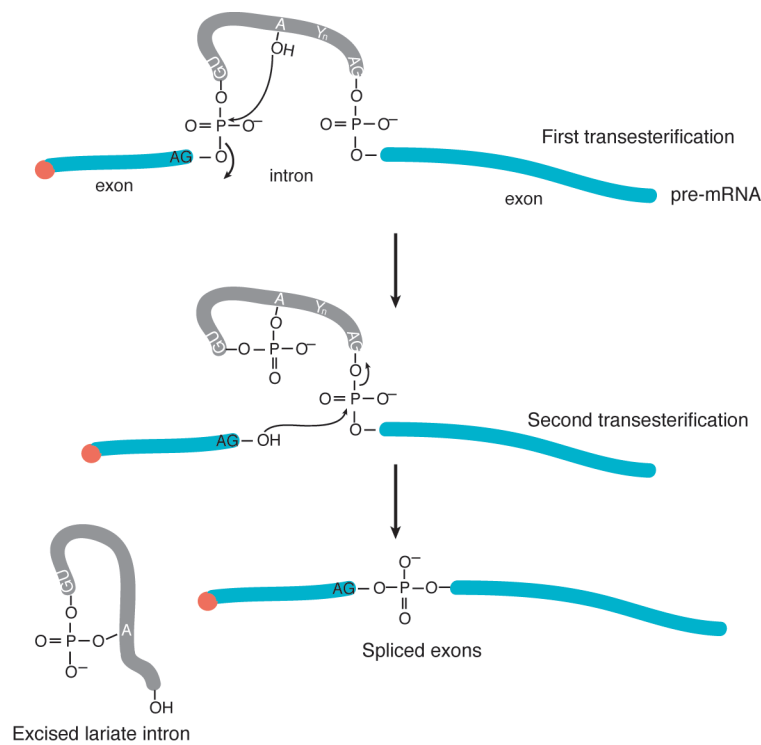


Figure 1-2 The chemistry of splicing

1.1.2 Alternative splicing and cancer

1.1.2.1 Regulation of alternative splicing

Alternative splicing generates multiple mRNAs and the corresponding proteins from a single primary transcript, furnishing the complexity of the human proteome. The protein isoforms that are generated from the same transcript may have different, or even antagonistic, functions.¹⁵⁻¹⁶ On average, each human gene contains 8.7 exons, and >90% of the genes are alternatively spliced.¹⁷ Normal cells rely on alternative splicing to adjust protein diversity during development and differentiation;¹⁸ conversely, misregulated alternative splicing evokes diseases, including cancer.¹⁹ Indeed, evidence in support of this notion has emerged in many aspects of cancer progression, including cell proliferation, programmed cell death, cancer cell metabolism, angiogenesis and invasion.²⁰⁻²¹

The alternative splicing pattern can be altered in many different ways (Figure 1-3).²² Most exons are constitutive and included in the final mRNAs. Cassette exons are sometimes excluded from the mRNA (Figure 1-3A). On occasions, multiple cassette exons are mutually exclusive — only one can be selected (Figure 1-3B). Exons can also be shortened or lengthened by altering the position of one of their splice sites (Figure 1-3C and D), resulting in alternative 5' and 3' splice sites. The 5'-terminal exons of an mRNA can be switched through the use of alternative promoters and alternative splicing (Figure 1-3E). Similarly, the 3'-terminal exons can be switched by combining alternative splicing with alternative polyadenylation sites (Figure 1-3F). In addition, a failure to remove an intron may occur, causing a splicing pattern called intron retention (Figure 1-3G).

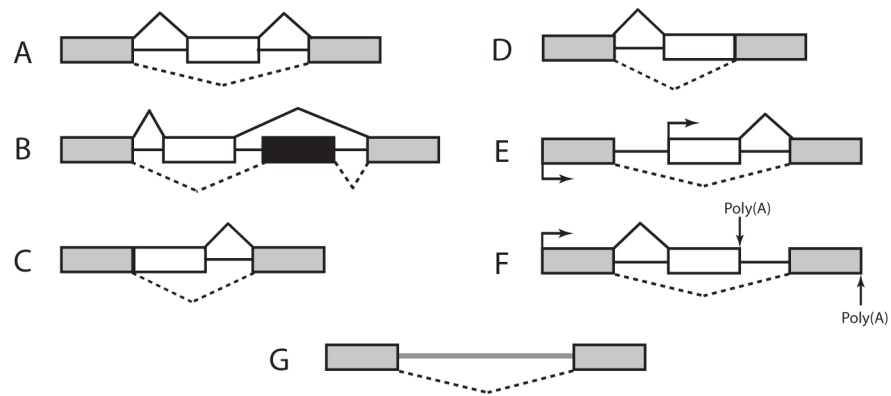


Figure 1-3 Patterns of alternative splicing

Despite the diverse patterns of alternative splicing, most of the information necessary to decide which sections of pre-mRNA will be included is present in the sequence of the pre-mRNA.²³ To understand the complexity of alternative splicing, we must study how changes in splice site choice take place. Introns can range from <100 nucleotides (nt) to hundreds of thousands of nucleotides. In contrast, exons are generally as short as 50–300 nt (~150 nt on average).²⁴ The challenge for correctly choosing the splice sites is that splicing machinery must locate small exon sequences within vast stretches of intronic RNA. Although very few patterns of alternative splicing have been mechanistically characterized in detail to explain the precision they possess, a general outline is understood. Figure 1-4 shows exon definition, a process that entails the binding of spliceosomal components on opposite sides of an exon to stimulate the excision of an intron.²⁵⁻²⁶ Factors that can strongly influence this process include splice-site strength, exon size and RNA secondary structure.

Moreover, in most of the complex pre-mRNAs in higher eukaryotes, the intronic sequences are not sufficiently conserved for exon definition. Hence, varied regulatory RNA-binding proteins (RBPs) with RNA sequence specificity also mediate the assembly of snRNPs and subsequently stimulate or repress exon inclusion. RBPs bind directly to 5' or 3' splice sites,

or to other pre-mRNA sequences called exonic or intronic splicing enhancers (ESEs or ISEs) and silencers (ESSs or ISSs). The enhancers and silencers stimulate or repress splice-site selection, respectively.²⁷⁻²⁹

The RBPs that recognize ESEs or ISEs are SR proteins, which contain one or more RNA-recognition motifs (RRMs) and an arginine/serine-rich (RS) protein-protein interaction domain on the C-terminal.³⁰ To date, nine classical SR proteins have been identified, including SRSF1 (SRp30a), SRSF3(SRp20), SRp30b (SC35), SRp30c, SRp40, SRSF6 (SRp55), SRp54, SRp75 and 9G8. SR proteins are required at different steps of spliceosome assembly and are constantly migrating between nuclear speckles—the subnuclear domains in which certain splicing factors are stored—and sites of active transcription.²⁸ To facilitate splicing, they mediate the crucial initiation of ‘cross-intron’ and ‘cross-exon’ interactions in both constitutively and alternatively spliced pre-mRNAs (Figure 1-4). Briefly, once bound to ESEs or ISEs, different SR family protein members recruit U1 snRNP to the 5’ splice sites, forming spliceosome complex E.³¹ Complex E subsequently promotes the splicing factor U2AF65 and U2AF35 to bind to the polypyrimidine tract (Yn) and the AG dinucleotide of the upstream 3’ splice site, respectively. In turn, U2AF coordinates with SR proteins to recruit U2 snRNP to the branchpoint sequence (A). The exact mechanism that SR proteins use to engage both 5’ and 3’ splice site-selection is unclear and is still an area of intense investigation.

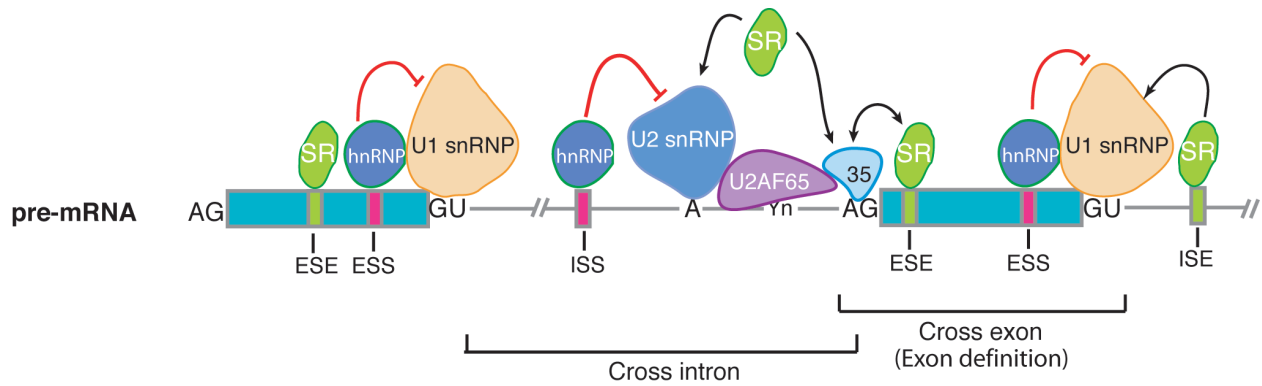


Figure 1-4 Exon definition mediated by splicing machinery and RBPs

On the other hand, ESSs and ISSs are recognized by members of the heterogeneous nuclear ribonucleoproteins (hnRNP) family. Unlike SR proteins, which co-localize with other splicing factors in nuclear speckles, the hnRNPs are diffusely distributed throughout the nucleus.³² Structurally, besides RNA-binding motifs, hnRNPs have auxiliary domains that are enriched with unusual distributions of amino acids, which are hypothesized to mediate protein-protein interactions. In addition, hnRNPs produce strikingly diverse isoforms through alternative splicing and post-translational modifications. The resulting complexity of hnRNP family members is reasonable given their diverse duties throughout the whole network of gene expression, ranging from chromatin-architecture remodeling, telomere maintenance, transcript packaging, mRNA export, cytoplasmic mRNA trafficking, pre-mRNA 3'-end processing, and alternative splicing, to translation.³³ The unifying theme for such functional diversity is the inherent DNA/RNA sequence specificity of each hnRNP. Upon tethering to the *cis*-elements, the resulting hnRNP complexes may modulate the accessibility and/or interaction of *trans*-acting factors. In the case of alternative splicing (Figure 1-4), the ESS sequences or ISS sequences possibly promote exon exclusion through interacting with hnRNPs bound to distal sites and loop formation.³⁴⁻³⁵

1.1.2.2 Splicing regulatory proteins as anticancer drug targets

In light of their crucial role in regulating alternative splicing, aberrant regulation of RBPs likely results in the deregulation of splicing in cancer. In keeping with this notion, deep sequencing has revealed that various hnRNPs and SR proteins are expressed in a proliferation-associated manner; much higher expression levels were observed in tumor than non-tumor tissues in a wide variety of cancers.^{20, 36} Furthermore, *SRSF1*, encoding the most well known SR protein SRSF1 (also called ASF/SF2), was recently described as a proto-oncogene, when its overexpression transformed rodent fibroblasts into sarcoma in nude mice.³⁷ The mechanism involved in the transformation is likely multifactorial, affecting pathways of proliferation, survival and invasion.³⁸ In skin tissue, *SRSF6*, normally promotes wound healing, can cause hyperplasia when overexpressed.³⁹ *SRSF3*, another newly defined proto-oncogene that encodes the smallest member in SR protein family, is amplified in both epithelial carcinoma and mesenchymal tissue tumors. The tumorigenic mechanism of *SRSF3* involves the overexpression of regulators of G2/M transition.⁴⁰

More recently, overexpression of core spliceosome components was also observed in malignancy. Each spliceosomal snRNP (U1, U2, U4, U5, and U6) consists of a uridine-rich small nuclear RNA (snRNA) and seven Sm (Smith) proteins. The Sm proteins (B/B', D1, D2, D3, E, F and G) form a 7-membered ring core structure that surrounds the snRNA. The overexpression of these Sm proteins was identified in a large number of tissues from ovarian, non-small cell lung carcinoma, and breast cancers. Further, the overexpression was correlated with more aggressive phenotypes. Mechanical studies showed that a deletion of Sm proteins led to the mammalian target of rapamycin (mTOR)-mediated autophagic cell death in tumor cells, while sparing non-tumorigenic cells.⁴¹

Altogether, these recent discoveries suggest that overexpression of splicing-related proteins could be a hallmark of cancer and therefore a therapeutic target.

1.2 TARGETING SF3B SUBUNIT 1 (SF3B1)

1.2.1 SFEB1 in constitutive splicing

The U2 snRNP is a key spliceosome subunit that recognizes the 3' intronic splice sites during spliceosome assembly. Besides U2 snRNA, seven Sm proteins are common to the spliceosomal snRNPs. U2 snRNP possesses two unique subcomplexes, splicing factor 3a (SF3a) and splicing factor 3b (SF3b), both being required for the interaction between U2 snRNP and pre-mRNA.⁴² SF3a is composed of three subunits of 60, 66, and 120 kDa;⁴³ SF3b consists of SF3B1 (SAP155), SF3B2 (SAP145), SF3B3 (SAP130), SF3B4 (SAP49), SF3B5 (10 kDa), SF3B14 (p14) and PHF5A.⁴⁴⁻⁴⁷

Among the SF3b components, the amino acid sequence of SF3B1 is highly conserved from *Schizosaccharomyces pombe* (52.4% identity) to human (99.6%) and composed of two regions: the N-terminal domain (NTD, amino acids 1–430) and C-terminus (amino acids 431–1304). The C-terminus shows even higher identity and comprises 22 tandem HEAT (Huntington, Elongation Factor 3, PR65/A, TOR)-like repeats, each consisting of approximately 40 amino acids to afford two antiparallel α -helices. These HEAT repeats are essential for protein-protein interactions, wrapping around—hence stabilizing—several other components of the U2 snRNP (Figure 1-5).⁴⁸ The N-terminal of SF3B1 is less conserved and has binding sites for splicing

factors U2AF65, U2AF35,⁴⁹ and SF3B14,⁴⁶ as well as for the regulatory proteins cyclin E⁵⁰ and Nipp1⁵¹, which mediate the phosphorylation of SF3B1.

SF3b facilitates the stable assembly of U2 snRNP, an early event during spliceosome formation that requires both RNA-RNA and protein-RNA interactions with 3' end of the intron. SF3B14 and SF3B1⁴⁹ are the SF3b components that directly bind pre-mRNA. SF3B14 binds to the branchpoint adenine. SF3B1 wraps SF3B14 inside so that it accurately localizes on the adenine (Figure 1-5).⁵²⁻⁵³ Further downstream on the intron, U2AF65 binds the polypyrimidine tract and U2AF35 binds the 3' splice site. The N-terminus of SF3B1 forms an elongated, unstructured conformation that extensively interacts with U2AF65 and U2AF35 for efficient recruitment of other U2 snRNP components.⁵⁴⁻⁵⁵ Of note, U2AFs rely on an RNA recognition motif (RRM) to bind their partners; these RRM are accordingly named U2AF-homology motifs (UHMs).⁵⁶ U2AF UHMs recognize tryptophan-containing linear peptide motifs, so-called UHM-ligand motifs, which were identified in SF-1 and SF3B1.^{54, 57-58} SF3B1 was predicted to have five HLMs, indicating that it might be involved in extensive protein-protein interactions. Collectively, these conserved interactions coordinate the assembly of early complexes of a spliceosome and might have more profound implications in alternative splicing regulation, where similar protein-protein interactions are desired.

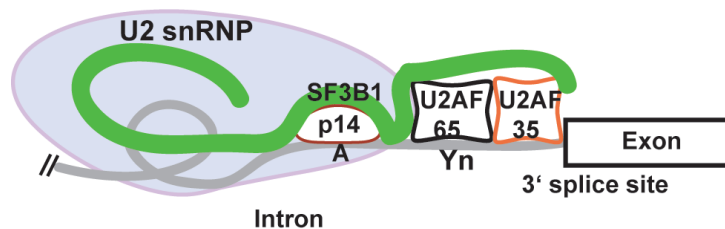


Figure 1-5 SF3B1 mediates U2 snRNP assembly in constitutive splicing

SF3a and b complexes are also believed to mediate the timing for catalytic activation of splicing complexes.⁵⁹⁻⁶⁰ This is reinforced by the fact that SF3B1 is the only U2 component known to experience reversible phosphorylation concomitant with, or right after, the first catalytic step.⁶¹⁻⁶³

Altogether, SF3B1 acts as a modulator of the integrity of U2 snRNP by interacting with multiple snRNP and non-snRNP proteins; it might be a key switch for the whole splicing machinery for faithful 3' pre-mRNA binding.

1.2.2 SF3B1 in alternative splicing

As explained above, the sequence selectivity of SF3B1 during constitutive splicing is achieved through protein-protein interactions. SF3B1 may broadly interact with splicing factors to regulate alternative splicing events. However, accumulating evidence indicates SF3B1 might function as an independent splicing factor to regulate alternative splicing as well as will be discussed as follows.

The sequence specificity of SF3B1 as a *trans*-acting splicing factor was first discovered in the alternative splicing regulation of B-cell lymphoma 2 (Bcl-2) family member Bcl-x in response to ceramide. Bcl-2 family proteins control programmed cell death (apoptosis)-mediated cell fate. Bcl-x generates anti-apoptotic Bcl-x_L and pro-apoptotic Bcl-x_S via the alternative selection of 5' splice sites. This study demonstrated that phosphorylated SF3B1 binds to ceramide-responsive *cis*-element 1 (CRCE-1) upstream of the alternative 5' splice site, thereby blocking the selection of the alternative proximal 5' splice site that generates Bcl-x_S (Figure 1-6). Ceramide activates protein phosphatase 1 (PP1), which dephosphorylates SF3B1, releasing the alternative 5' splice site. Accordingly, knockdown of *SF3B1* decreased the ratio of Bcl-x_L/Bcl-x_S

and sensitized A549 lung cancer cells to the chemotherapeutic agent daunorubicin. This study provided the first proof that SF3B1 exhibits sequence-specific binding in alternative splicing regulation; down-regulation of U2AF65, SF3B2, SF3B3, SF3B4, the splicing factors typically interacting with SF3B1 in constitutive splicing, did not affect the splicing pattern of Bcl-x.⁶⁴

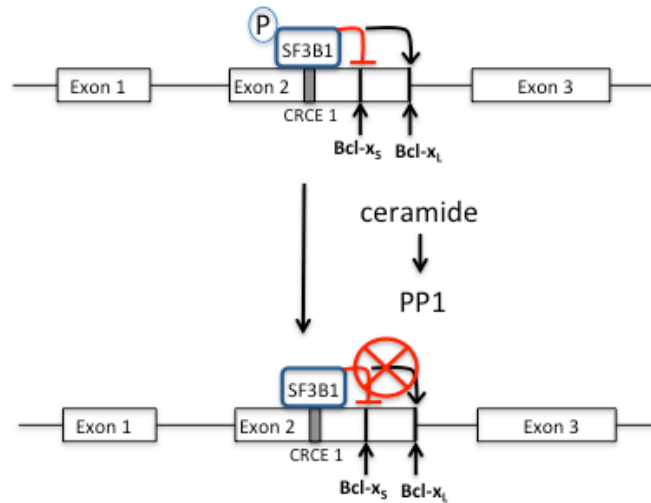


Figure 1-6 SF3B1 regulates Bcl-x alternative splicing in response to ceramide signaling

In addition to direct binding to RNA sequences, SF3B1 was also shown to mediate alternative splicing through protein-protein interactions. Sattler and coworkers demonstrated the significance of the structural units for SF3B1 to regulate alternative splicing. Specifically, by selective binding to SF-1, U2AF65, and splicing factors SFP45 or the poly(U)-binding-splicing factor (Puf60) via different HLMs, SF3B1 regulates the alternative splicing of the apoptosis regulatory gene *FAS*, resulting in exon 6 skipping.⁶⁵⁻⁶⁶ Among these binding partners, Puf60 might also play a role in spliceosome assembly by replacing SF1 from the branch point and then acting as a loading dock for SF3B1 to recognize/bind to U2AF65.⁶⁷ A splicing variant of Puf60, the far-upstream element (FUSE)-binding protein-interacting repressor (FIR), represses *c-myc*

transcription by suppressing the TFIIH/P89/XBP helicase. In colon cancer tissues, enhanced expression of SF3B1 increases both FIR and FIR Δ exon2, a splicing variant of FIR without the transcriptional repression domain. In turn, FIR Δ exon2 interacts with FIR and SF3B1, disturbing their *c-myc* expression suppressing and splicing regulatory functions, respectively.⁶⁸⁻⁷⁰ SF3B1 knockdown decreased the expression of *c-myc*, apparently by breaking up the FIR/FIR Δ exon2/SF3B1 complexes.

Besides these genes verified through biological approaches, small-molecule modulators of SF3b significantly expanded the pool of target genes regulated by SF3B1, as will be discussed in detail later. Considerably more cancer-related genes are under the surveillance of key splicing factors like SF3B1 at the alternative splicing level. For that reason, targeting splicing factors may become a new generation of chemotherapeutic strategy.

1.2.3 SF3B1 alterations in cancer

Unlike other oncogenic splicing-related proteins, the only type of genetic alteration in *SF3B1* in diseases is somatic mutation, which has been mainly studied in hematologic malignancies since 2011. The first SF3B1 somatic mutation was observed in myelodysplastic syndromes (MDSs). MDSs are heterogeneous hematologic cancers characterized by low blood cell counts (mostly anemia) and a risk of progression to acute myeloid leukemia. Pre-mRNA splicing-related genes are recurrently mutated in >60% of MDS patients, and in up to 87% for those with high-count ring sideroblasts.⁷¹⁻⁷² Interestingly, the mutations are invariably heterozygous substitutions and it appears *SF3B1* mutation is associated with longer survival free of disease.⁷³

In chronic lymphocytic leukemia (CLL), the most common adult leukemia in Western countries, *SF3B1* mutation also ranks as the most frequently mutated gene, ranging from 5% –

18% depending on the composition of the cohorts. In striking contrast to MDS, *SF3B1* mutation has been consistently correlated with poorer clinical outcomes.⁷⁴ Temporally, *SF3B1* mutation occurred only in certain populations of tumor cells, indicating that it appeared later in the disease development, promoting the malignancy's progress instead of initiating it.⁷⁵ In the future, *SF3B1* mutation might be incorporated into prognostic schema in combination with current biologic markers to better predict CLL progression. Meanwhile, when knocked out in mouse embryos and silenced with shRNA in human cell (HEK293T) models, *SF3B1* was also shown to be essential for cell survival.⁷⁶⁻⁷⁷

The mutations within *SF3B1* are mainly located at six hotspot codons E622D, R625H, H662D, K666E, K700E, and G742D; K700E accounts for over 50% of the cases. Combined with other less common mutations, they are all located in the conserved C-terminal region, clustering between the fifth and eighth HEAT repeats. Quesada *et al.* constructed a tentative model of SF3B1 and suggested that these hotspot mutations might occur at the inner surfaces of the structure (Figure 1-5), where interactions between SF3B1 and its binding partners occur.⁷⁵ The mutated amino acids were predicted to be spatially adjacent to one another. Hence, these mutations might have the similar functional impact of significantly disturbing the normal protein-protein interactions of SF3B1. SF3B1 mutation was also detected in 3 out of 77 breast cancer patients (2 K700E and 1 K666E),⁷⁸ 4 out of 99 pancreatic cancer patients (1 R568H, 1 Q699H and 2 K700E)⁷⁹ and 19 out of 102 uveal melanoma patient (all R625C).⁸⁰

The causative link between *SF3B1* mutation and tumorigenesis is still elusive. The co-occurrence of SF3B1 alteration and these malignancies further supports this splicing factor as a cancer therapeutic target. In CLL, *SF3B1* was recently categorized as a proto-oncogene.⁷⁶

1.2.4 SF3b modulators

The modulation of core spliceosomal components would most likely result in a loss of critical proteins and expression of splice variants with aberrant functions; therefore, inhibiting spliceosomal components would be a highly deleterious event in all cells. However, as will be explained here in detail, using SF3b as an example, spliceosome modulators generally affect selective subgroups of genes in a tumor-specific manner.⁸¹ This selectivity supports further exploiting alternative splicing as a new class of tumor vulnerability.

Up to now, three bacterial natural products, FR901464,⁸²⁻⁸⁴ pladienolides⁸⁵⁻⁸⁶ and herboxidiene/GEX1A,⁸⁷ have been confirmed to target SF3b. These three originated from distantly related bacterial genera (FR901464 and herboxidiene from *Pseudomonas* sp. and pladienolides from *Streptomyces* sp.). Ironically, bacterial genomes are devoid of introns as well as the genes that code for spliceosomal components.

1.2.4.1 FR901464 and its analogs

In 1996, FR901464 was by the Fujisawa Pharmaceutical Company from *Pseudomonas* sp. No. 2663 in efforts to discover transcription factor modulators. FR901464 exhibited antiproliferative activity against human solid tumor cell lines as well as against murine tumors in mice.⁸²⁻⁸⁴ Phenotypic characterization of the cells exposed to FR901464 showed that FR901464 increased the expression of SV40 promoter-driven reporter genes stably expressed in MCF-7 breast cancer cells (M-8), arrested cell cycles at G1 and G2/M phases, and induced internucleosomal DNA fragmentation. These distinctive phenomena are similar to those caused by histone deacetylase inhibitors.⁸⁸ Soon it was confirmed that this molecule, unlike histone deacetylase inhibitors, did not cause an accumulation of acetylated histones, indicating a novel unknown mode of action.⁸⁹

The interesting biological profile of FR901464 uncovered from these preliminary studies has prompted researchers to synthesize this natural product. The Jacobson group reported the first total synthesis of FR901464 in 2001.⁹⁰ The Kitahara group reported second and third syntheses of FR901464, and subsequently prepared spliceostatin A and its biologically active biotinylated probe.⁹¹⁻⁹³ More recently, the Koide group synthesized FR901464 and obtained two analogs — meayamycin and meayamycin B (Figure 1-7) — that are at least two orders of magnitude more potent than FR901464 in terms of antiproliferative activity in *in vitro* models, with GI₅₀ as low as single digit picomolar.⁹⁴⁻⁹⁵ In 2013, the Ghosh group reported a more concise enantioselective synthesis of FR901464 in 10 linear steps.⁹⁶

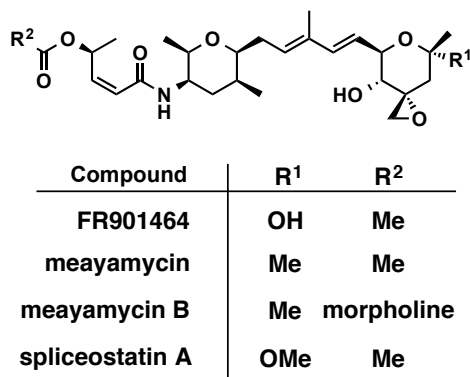


Figure 1-7 Structures of FR901464 and its derivatives

In 2013, the Cheng group discovered two groups of FR901464-related natural product. Thailanstatin A (Figure 1-8),⁹⁷ isolated from the culture broth of *Burkholderia thailandensis* MSMB43, differs from FR901464 in that it lacks a destabilizing hydroxyl group on C17 and has a methylene group instead. Moreover, in pH 7.4 buffer at 37 °C, more than 60% of thailanstatin A remained after 78 h, while FR901464 decayed to and remained at a total level of 38%. Furthermore, thailanstatin A was shown to be equipotent in its *in vitro* splicing inhibition and

anti-proliferative activity in comparison to FR901464. Serendipitously, while trying to purify FR901464 from *Pseudomonas* sp. 2663 as a reference for the characterization of thailanstatins, Cheng et al. isolated spliceostatin B (Figure 1-8).⁹⁸ Compared with FR901464, spliceostatin B is missing a hydroxyl group on C4. Similar to thailanstatins, the hydroxyl moiety at C17 is substituted with a carboxyl moiety on spliceostatin B. In addition, the epoxide on C3 is replaced by a terminal methylene moiety. Clearly, multiple substitutions on spliceostatin B, such as C3 and C4, were deleterious to its potency, since it was nearly three orders of magnitude less potent than FR901464.

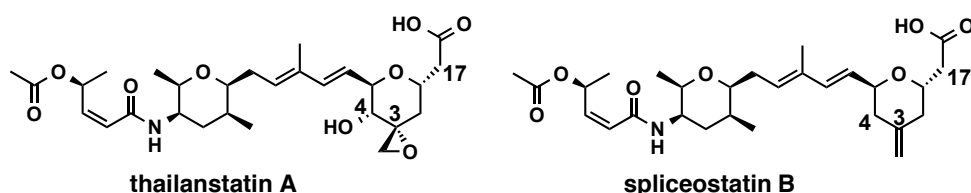


Figure 1-8 Structures of thailanstatin A and spliceostatin B

In 2005, FR901464 was identified with inhibitory activity against transmembrane thioredoxin-related protein, which has not been proved by further investigations.⁹⁹ In 2007, Yoshida and coworkers discovered that spliceostatin A (SSA), a methoxy ketal analog of FR901464, targeted the SF3b subcomplex of the spliceosome U2 snRNP.¹⁰⁰ The specific binding target within this complex was elusive, but it was presumed to be SF3B1 or SF3B3. FR901464 and its analogs targeted the SF3b sub-complex and subsequently blocked splicing before the first transesterification reaction.¹⁰⁰ Roybal and Jurica used spliceostatin A to show that besides being critical for spliceosome assembly, the SF3b sub-complex was required for the maturation of the spliceosome from complex A to B.¹⁰¹ This conclusion, however, is questionable because the

concentration of heparin in the quenching buffer for the *in vitro* splicing reactions was much lower than required (0.125 mg/mL versus 1.25 mg/mL or higher). Such defected procedures would inevitably cause nonspecific binding of components in the nuclear extract to the negatively charged pre-mRNA substrates.¹⁰²

In 2011, Valcárcel et al. proved that spliceostatin A prevented the correct base-pairing between U2 snRNA and pre-mRNA branch point via an interruption of the SF3B1 function, bringing our understanding of the impact of SF3b inhibition on spliceosome dynamics to another level. In addition, this study also unveiled that when spliceostatin A binds to SF3B1, sequences at 5' upstream of the branch point are invariantly selected as alternative binding partners to U2 snRNA, with varying sequence-dependent affinity. In HeLa cells, spliceostatin A (3-h exposure) mimicked the effect from SF3B1 siRNA and altered alternative splicing of ~2% of the endogenous genes that were examined by a splicing-sensitive microarray. A majority of the affected genes code for cell cycle-related proteins, which is consistent with the results from the knockdown of spliceosome components.^{40, 100, 103}

Spliceostatin A inhibited *in vitro* splicing, accumulating pre-mRNA at nuclear speckles.¹⁰⁰ Through an unknown mechanism, spliceostatin A resulted in the production of a C-terminally truncated product of p27 splice variant with a retained intron 1. This truncated variant evaded nonsense-mediated mRNA decay (NMD), leaked into cytoplasm, and was translated into protein. Both of these p27 isoforms blocked the G1 to S phase transition by inhibiting cyclin-dependent protein kinases (CDKs). The mechanism of the leakage is clearly related with the inhibition of SF3b via an unknown mechanism.

A misprocessed RNA molecule is subject to NMD because of a premature termination codon. If an intron is retained after splicing, an in-frame stop codon (either UAA “ochre” or

UGA “opal”) will likely appear in the splicing product because of the consensus sequence AG/GURAGU (R = A or G) on the intronic 5' splice sites. When such a stop codon is >50 nt upstream of the final exon-exon splice junction in the mRNA transcript, a premature termination codon is defined and this mRNA becomes an NMD candidate. Growing evidence suggests that the coupling of alternative splicing and NMD provides a prominent means of gene expression regulation.¹⁰⁴ Accompanying the regulation of alternative splicing by spliceostatin A, the introduction of premature termination codon causes widespread NMD and subsequent decreased mRNA and protein levels.¹⁰⁵ Therefore, SF3b inhibition would produce diverse genes that are subject to NMD.

The cytoplasmic leakage of abnormally spliced pre-mRNA might play a role in the cytotoxicity caused by SF3b inhibitors. In support of this notion, it was discovered that splicing factors, crucial for early spliceosome assembly, directly interact with RNA binding proteins from the exon junction complex (EJC). EJCs are typically assembled ~20 to 24 nt upstream of splice junctions and are in charge of mRNA export in the NMD pathway. In nematode *Caenorhabditis elegans*, depletion of any of the core components of an EJC, which is typically left on the spliced mRNA for exporting mRNA into cytoplasm, leads to cytoplasmic leakage of unspliced RNAs. Importantly, several splicing factors, including SF3b complex, interact with key EJC subunits.¹⁰⁶ The actions of FR901464 thus probably interfere with a correct coupling of alternative splicing and the NMD pathway, mimicking the deletion of these EJC subunits. In turn, EJCs can influence alternative splicing. Core (Y14 and eIF4A3) and auxiliary (RNPS1, Actin, and SAP18) components of EJCs promote the proapoptotic Bcl-x_s, Bim, Mcl-1.¹⁰⁷ All together, these data present FR901464 derivatives as attractive chemical tools to probe the complex interaction between splicing and RNA surveillance mechanisms.

As another significant example of the splicing modulatory effect of spliceostatin A, Yoshida et al. demonstrated that spliceostatin A impaired the expression of vascular endothelial growth factor (VEGF) at both mRNA and protein levels in cervical cancer HeLa cells.¹⁰⁸ Specifically, at the RNA level, both splicing and transcription were inhibited by spliceostatin A, but its effects on the alternative splicing was elusive since the short variant (VEGF_{165b}) was undetectable. For the translation pathway, spliceostatin A suppressed both initiation and elongation by an unknown mechanism that blocked the phosphorylation of the C-terminal domain of polymerase II. This suppression of VEGF was sufficient to inhibit angiogenesis *in vivo*. Furthermore, a global gene expression in HeLa cells using a DNA microarray revealed that nearly 25% of genes were downregulated when exposed to spliceostatin A for 3 h, indicating the existence of a previously unappreciated level of coupling of splicing and transcription pathways.

1.2.4.2 Pladienolides, E7107 and their analogs

Pladienolides (first reported in 2004) are seven 12-membered macrolides identified from *Streptomyces platensis* Mer-11107 via a cell-based assay for suppressing hypoxia-induced, human VEGF promoter-mediated expression.⁸⁵ Similar to FR901464, pladienolides arrest cells at the G1 and G2/M phases. The most potent pladienolides B and D (Figure 1-9), exhibited low nanomolar range IC₅₀ in inhibiting the growth of a variety of cancer cell lines and even caused tumor regression in several human cancer xenograft models, demonstrating a broad therapeutic window. A COMPARE analysis of a panel of 39 human cancer cell lines indicated a mode of action different from current anticancer drugs.⁸⁶ E7107, a urethane derivative of pladienolide D that showed enhanced *in vivo* potency and pharmacochemical properties, quickly advanced to phase I a clinical trial for solid tumors.¹⁰⁹⁻¹¹¹

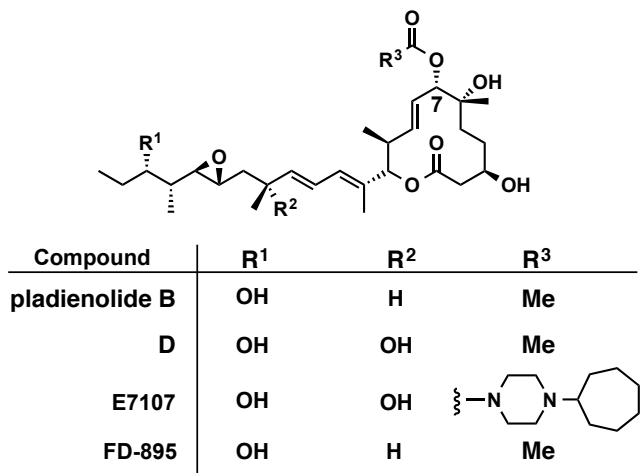


Figure 1-9 Structures of pladienolides and their analogs

Kotake et al. completed the first total synthesis of pladienolides B and D.¹¹² Subsequently, by using ³H-labeled, BODIPY-tagged, and photoaffinity- and biotin-tagged pladienolide B derivatives, they discovered that SF3B3, from the SF3b subcomplex, was the binding target of pladienolides. However, they could not eliminate the possibility that the compound can fit into a binding pocket composed of SF3B1 and SF3B3.¹¹¹ As a support for the importance of SF3B1, colorectal cancer cell lines WiDr and DLD1 with acquired resistance to pladienolide B developed the same R1074H mutation in *SF3B1*.¹¹³ These arginines are required for the conformation of HEAT repeats during protein-protein interactions.¹¹⁴ Therefore, this mutation likely alters the crucial conformation of the C-terminal of SF3B1. Taken together, the divergent conclusions about the specific binding target of pladienolides indicate that pladienolides may bind to an interface of multiple SF3b components.

The necessity of epoxide for the activity of pladienolides has been debated. Recently, via synthesizing analogs of a pladienolide-like natural product FD-895 (Figure 1-9), Burkart et al. showed that replacing the epoxide with cyclopropane stabilized the compound with moderate

compromise of the potency, indicating the dispensability of epoxide for pladienolide.¹¹⁵ This is in contrast to the epoxide of FR901464—the same substitution led to a complete abrogation of the biological activity of FR901464.⁹⁰ This discrepancy in the importance of the epoxide moiety between the derivatives of FR901464 and pladienolides is non-trivial and needs to be fully elucidated.

1.2.4.3 Sudemycins

The structural complexity of FR901464 and pladienolides has considerably hindered the synthetic efforts to improve their stability, potency, and their application in extensive biological studies. Interestingly, Webb et al. reported that although structurally dissimilar, FR901464 and pladienolides shared common key features that could be overlapped in low energy conformation in three-dimensions. These features include a carbonyloxy group (two hydrogen-bond acceptors), a well-restrained (hydrophobic) diene linker, and a secondary epoxide (a nucleophilic hydrogen-bond acceptor). Hence, a series of derivatives of FR901464, called sudemycins (the most active analogs shown in Figure 1-10) were synthesized, which are much more synthetically accessible (bearing only three of the nine stereocenters in FR901464) with improved stability. Importantly, they retained the biological activities of the parent compounds, including splicing inhibition and cell cycle arrest. Preliminary SAR analyses afforded analogs with IC₅₀ in the range of ~80 – 500 nM against various cell lines, especially in mantle cell lymphoma.¹¹⁶⁻¹¹⁷ Sudemycins also regulated alternative splicing of MDM2, caspase 2, and caspase 9, but not Bcl-x, *in vitro* and *in vivo*. It appeared that the regulation of MDM2 alternative splicing is more prominent in cancer cells versus normal myoblast cells (LHCN-M2), which might result from a relatively lower baseline expression of this gene in normal cells.⁸¹

Subsequently, the Webb group chose to screen for potential combinations using sudemycin D6 (low double-digit nanomolar IC_{50} values, structure shown in Figure 1-10) in *in vitro* and *in vivo* melanoma models. It synergized with a dual inhibitor of phosphatidylinositol-3-kinase/mammalian target of rapamycin (PI3K/mTOR) BEZ235, and epoxide hydrolase inhibitors. The epoxide hydrolase inhibitors presumably enhanced the stability of sudemycins.¹¹⁸

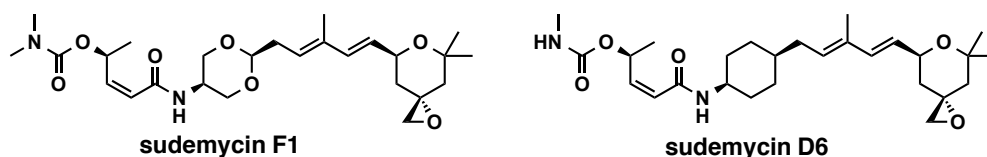


Figure 1-10 Structures of sudemycin F1 and D6

1.2.4.4 Herboxidiene/GEX1A

Herboxidiene (Figure 1-11) was originally isolated in 1992 from *Streptomyces chromofuscus* A7847 as a herbicide.¹¹⁹ In 1997, Koguchi and colleagues implemented a luciferase reporter driven by a low density lipoprotein receptor promoter stably transfected into Chinese hamster ovarian cells and identified herboxidiene and trichostatin A from a butanol microbial extract.¹²⁰

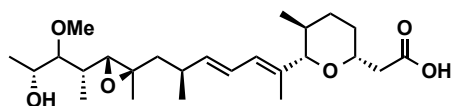


Figure 1-11 Structure of herboxidiene

In 2002, herboxidiene was isolated as an anti-tumor agent. This compound arrested the cell cycle at the G1 and G2/M phases of human normal fibroblast cells WI-38 and activated the

expression of the luciferase reporter driven by the promoters of E2F, c-myc, DNA polymerase α , c-fos, Interleukin 2 (IL-2) and SV40 early genes in human osteosarcoma cell line Saos-2. The strength of gene activation activity of the compounds correlated with that of their cytotoxicity. Unexpectedly, herboxidiene decreased the level of endogenous genes including E2F-1 (cell cycle-related transcription factor gene), cdc2, cyclin D1, cyclin A (cell cycle related kinase genes), p21/waf1, p27/kip1 (inhibitors of cell cycle related kinase genes), cdc25A (cell cycle related phosphatase gene), Bcl-x_L, Bax (apoptosis-related genes), c-myc and c-fos (cell proliferation-related genes) at sub- to single digit micromolars after a 2–8 h exposure. Particularly with cdc25A, a shorter product of unknown identity was induced by herboxidiene post an 8-h treatment, with a simultaneous decrease in the major product, indicating a regulation of alternative splicing by herboxidiene.^{87, 121}

In 2011, Mizukami and coworkers identified SF3B1 as the molecular target of herboxidiene and demonstrated its function as a splicing inhibitor.¹²² In contrast to their reports in 2002, herboxidiene induced the production of C-terminal truncated p27 (so called p27*) by intron 1 retention. P27* was also found to be a functional inhibitor of cyclin E-Cdk2, like its full-length counterpart p27, but is not targeted for degradation by the proteasome. Most importantly, a photoaffinity-labeled derivative labeled SF3B1 as the only target of herboxidiene.

1.2.5 Summary

The biological studies of SF3b inhibitors reveal the extent and significance of the influence that spliceosomal components have in the expression of subgroup of human genes, especially in cancer biology. Progress in the regulation of alternative splicing has been benefiting from the efforts using both biological and chemical tools. Known human genes under the regulation of

SF3b components, especially SF3B1, are summarized in Table 1-1. Modulating the corresponding splicing-regulatory proteins, therefore, can allow for novel therapeutic targets to reverse the cancerous phenotype caused by these misregulated genes.

Table 1-1 Human genes controlled by SF3b components

Gene product	Function	Cellular pathway	Experimental tools (condition)	References
p27/kip1	Kinase inhibitor	Cell cycle (CDK-cyclin)	SSA (14 h)	100
p21/waf1			FR (16 h)/Herb (2 h)	84, 87
E2F-1	Transcription factor		Herb (8 h)	87
Cdc25A	Phosphatase		Herb (2 h)	122
Cdc2	Kinase		Herb (8 h)	87
Cyclin D1	Kinase		Herb (8 h)	87
I κ B α	NF κ B inhibitor		Cell cycle (transcription)	SSA (14 h)
c-myc	Transcription factor	SF3B1 siRNA (72 h)/FR (48 h)		68, 84
FIR	Transcription suppressor	SF3B1 siRNA (72 h)/SSA (48 h)		68, 84
VEGF	Angiogenesis	Microenvironment	SSA (6 h)	108
Bcl-x	Apoptosis-related	Cell death	SF3B1 siRNA (24 h)/Herb (8 h)	64, 87
Mcl-1			SF3B1 siRNA (24 h)	123
FAS			SF3B1 deletion-mutation (24 h)	65
MDM2			sudemycins (8 h)	81
Caspase-9			sudemycins (8 h)	81
Caspase-2			sudemycins (8 h)	81
Bax			Herb (8 h)	87

2.0 SF3B MODULATOR MEAYAMYCIN B FOR CANCER THERAPY

2.1 MEAYAMYCIN B—POTENT SPLICING MODULATOR

This section is taken from “Gao, Y., Vogt, A., Forsyth, C. J., and Koide, K. (2013) Comparison of splicing factor 3b inhibitors in human cells, *ChemBioChem* **14**, 49-52.”

2.1.1 Research Design

The correct assembly of spliceosomal snRNPs, especially U1 and U2 snRNPs that respectively define the locations of spliceosome on 5' and 3' splice sites of introns, onto pre-mRNAs is essential for pre-mRNA splicing. The binding fidelity of U2 at 3' splice site relies on the U2-associated SF3b subcomplex. In 2007, the SF3b complex was found to be directly inhibited by FR901464,¹⁰⁰ a natural product isolated from the culture broth of a bacterium of *Pseudomonas* sp. No.2663 (Figure 1-7).⁸³ Since then, some of the readily available FR901464 analogs — spliceostatin A⁹² and meayamycin¹²⁴, among others^{81, 116-117} — have been widely used to elucidate the mechanisms of pre-mRNA splicing and SF3b-related diseases.^{100-101, 105, 108, 125-134} In 2011, herboxidiene (a.k.a., GEX1A)^{87, 121} was also found to be an inhibitor of SF3b,^{119, 122} and our group reported meayamycin B as a new FR901464 analogue.

Meayamycin B was more synthetically accessible than meayamycin and the most potent among the known FR901464 analogs as an antiproliferative agent,^{94, 135} however, it has not yet

been studied as a splicing inhibitor. Meanwhile, despite their widespread use, FR901464 analogs have not been directly compared within the same splicing system. With the addition of new SF3b inhibitors such as meayamycin B and herboxidiene, a direct comparison of these two compounds, FR901464, spliceostatin A, and meayamycin in a splicing assay would enable rational selection of an SF3b inhibitor for specific experimental designs.

In addition, it should be noted that there appears to be confusion in the literature about the identity of FR901464 analogs. For example, in a recent review article, FR901464, spliceostatin A, and meayamycin were listed as if they were unrelated compounds.¹³⁶ Both spliceostatin A and meayamycin are synthetic analogs of FR901464⁹² and should be treated as such^{129, 137-138} and not as natural products.¹³⁹

2.1.2 Results and Discussion

2.1.2.1 Cell-based splicing inhibition assay

In this study, we used a splicing reporter developed by the Moore group (Figure 2-1).¹²⁹ Briefly, this screening construct consists of an exon 6-intron 6-exon 7 cassette from the human triose phosphate isomerase (TPI) minigene upstream of a firefly luciferase open reading frame. To ensure that the expressed luciferase activity is positively correlated with the splicing inhibitory capability of the test compounds, the constitutive in-frame stop codon in the intron was removed and a G was inserted in TPI exon 7 so that the downstream luciferase gene is in-frame when the intron is retained.

In addition to the screening construct, there are also positive and negative controls (Figure 2-1). A negative control construct contains the same minigene but with a mutated 5'-splice site; therefore, it constantly expresses high levels of luciferase. A positive control contains

unmodified TPI minigene and a functional luciferase is translated only when the intron is spliced. These constructs were stably transfected into the human embryonic kidney 293 (HEK293) cell line, and the resulting cell lines were called HEK293-II and HEK293-III, respectively. The Z-scores of a splicing assay using HEK293-II paired with HEK293-III were reported.¹²⁹ However, the Z-score of an assay using the HEK293-II cell line by itself and a potent SF3b inhibitor as a positive control for splicing inhibition has not been reported.

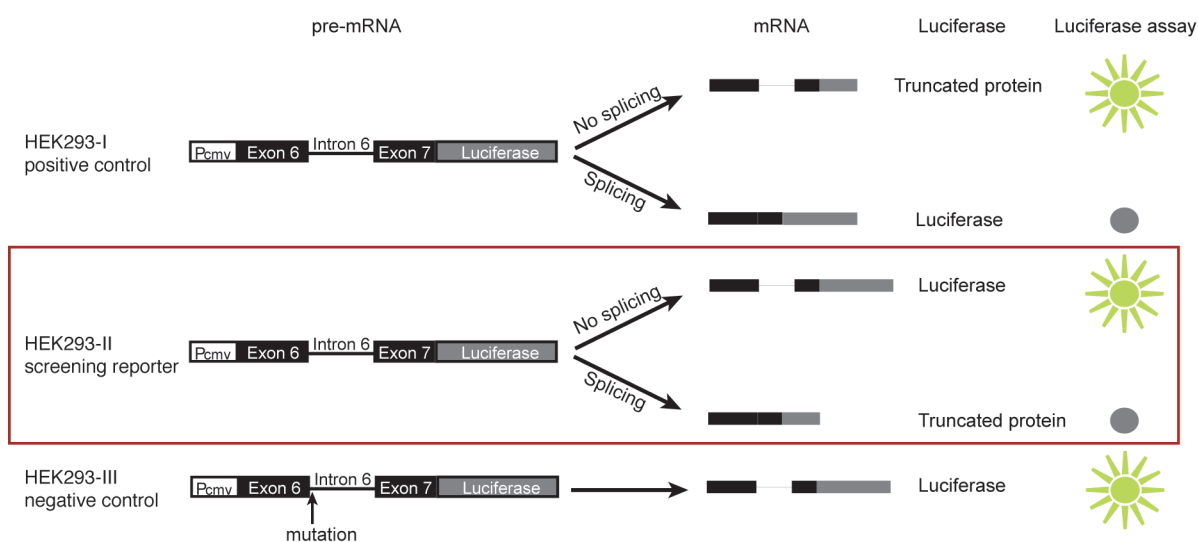


Figure 2-1 TPI minigene constructs for splicing inhibitor screening

To configure the cellular assay for compound screening using a small-molecule control, we set out to further optimize and validate the HEK293-II-based splicing assay to meet the accepted high throughput criteria in a 96-well format.¹⁴⁰ To this end, meayamycin B was chosen as a pre-mRNA splicing inhibitor because it is the most potent among known FR901464 analogs against various human cancer cell lines and is structurally similar to the known splicing modulators meayamycin, spliceostatin A, and FR901464.⁹⁴ To find a convenient end-point of the splicing assay, the inhibitory activity of meayamycin B (10 nM, ED₉₅) and DMSO (0.5% v/v)

was monitored over time. This study revealed that meayamycin B caused a linear increase in luciferase activity that plateaued at around 36 h. Sixteen hours was the shortest period of exposure that was in the linear range of the curve, showing a reasonably large signal-to-background ratio (Figure 2-2A); hence, 16 h was chosen for further assay development. It is noteworthy that our assay system did not include HEK293-III (negative control) cell line, but a dose-dependence study showed that a 16-h exposure of meayamycin B elicited negligible increase of luciferase activity, indicating the absence of other influence such as transcription and translation (Figure 2-2B).

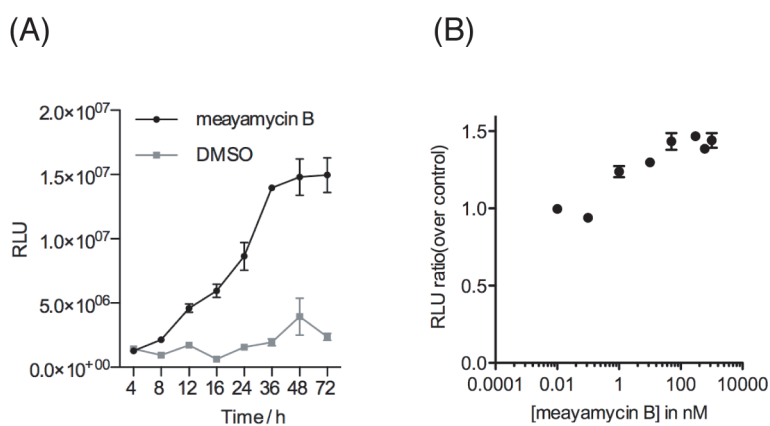


Figure 2-2 Meayamycin B in HEK293-II and HEK293-III

We then determined the optimal cell density at the 16-h time point. In the presence of meayamycin B (10 nM, ED_{95}), luciferase activity showed a linear correlation with cell numbers over a wide range of cell densities. We chose 1.6×10^4 cells per well as judged by the lowest standard deviation of luciferase expression (Figure 2-3A, left panel) and a calculated coefficient of variation of less than 7% (Figure 2-3A, right panel). This optimal cell density was in agreement with previously reported data in a 384-well format.¹²⁹

Meayamycin B is also an antiproliferative agent; therefore, we assessed the growth inhibition of the HEK293-II cells by meayamycin B to ensure that the luciferase data would not be skewed by cell growth inhibition, and therefore would truly reflect the splicing inhibition. To this end, we employed a total protein assay using bicinchoninic acid (BCA) and a cell proliferation assay using 3-(4,5-dimethylthiazol-2-yl)-5-(3-carboxymethoxyphenyl)-2-(4-sulfophenyl)-2*H*-tetrazolium inner salt (MTS) after a 16-h incubation of HEK293-II cells with meayamycin B (10 nM). The BCA assay was used to assess cell proliferation because in our experiments, cell number correlated with total protein concentrations (Figure 2-3B). Meayamycin B (10 nM) induced a 15% inhibition of growth in HEK293-II cells (Data not shown). Hence, further luciferase assays were normalized with total protein concentrations.

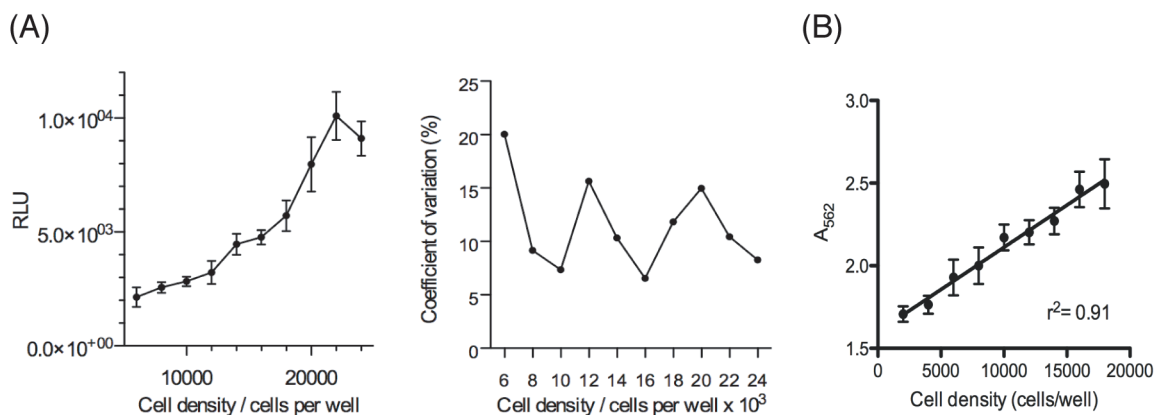


Figure 2-3 Optimization of cell density

With the optimized conditions in hand, we proceeded to determine the Z-score of the splicing inhibition assay. The HEK293-II cells (1.6×10^4 cells per well) in 96 wells were treated with meayamycin B (10 nM) or DMSO for 16 h. As shown in Figure 2-4, a half-plate minimum/half plate maximum signal design produced a Z-score of 0.56 ± 0.04 ($n = 3$), validating

high throughput compatibility.¹⁴⁰⁻¹⁴¹ Dotted lines for each set of data indicate $3 \times$ standard deviations.

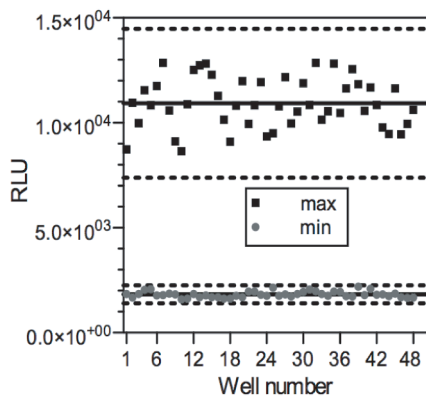


Figure 2-4 Z-factor calculation of the splicing inhibition assay in a 96-well format

2.1.2.2 Evaluation of natural and synthetic SF3b inhibitors

With this validated method, we investigated the potencies of FR901464, spliceostatin A, meayamycin, meayamycin B, and synthetic¹⁴² herboxidiene. As shown in Figure 2-5A, 16-h treatments with these compounds resulted in a dose-dependent splicing inhibition with ED₅₀ values of 3.5 ± 0.75 , 4.7 ± 1.7 , 1.6 ± 0.4 , 0.23 ± 0.12 , and 257 ± 11.1 nM, respectively. The relative luminescence unit (RLU) is defined as the ratio of luminescence intensities from compound-treated and DMSO-treated normalized by the corresponding cell density. Data points represent average values of triplicate experiments \pm standard deviations. The splicing inhibition was further verified by a semi-quantitative RT-PCR experiment that showed the relative amounts of both spliced and unspliced TPI mRNA (Figure 2-5B). In both assays, meayamycin B was found to be the most potent splicing inhibitor among the compounds tested.

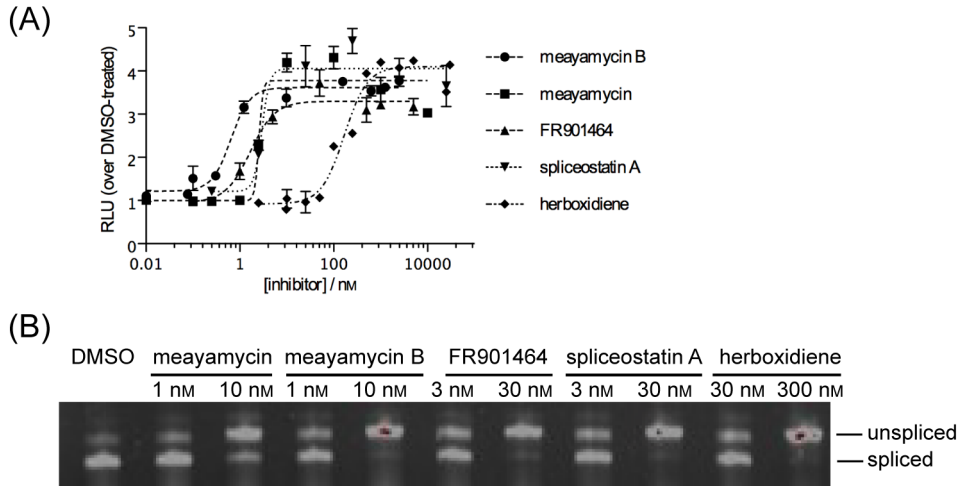


Figure 2-5 Splicing inhibition of TPI minigene by SF3b inhibitors for 16 h

We next studied the time-dependence of splicing inhibition using the ED₉₅ concentrations calculated from the 16-h assays. Since these compounds are potent antiproliferative agents, cell viability (see Figure 2-6A) under each treatment was measured and factored into the evaluation of splicing inhibition over time. As shown in Figure 2-6B, the luciferase activity (i.e., splicing inhibitory activity) increased to a similar extent (relative luminescence unit, RLU = 5–10-fold increase over vehicle control) for the first 24–48 h in the presence of FR901464, spliceostatin A, and herboxidiene before it dropped back to near baseline in 72 h. The magnitude of luciferase activity was much larger in the presence of meayamycin and meayamycin B (RLU = 20–30-fold increase over vehicle increase) and remained as such for 72 h. We postulated that the prolonged effect of the meayamycins was partly due to their superior stability in cell culture medium.^{124, 143}

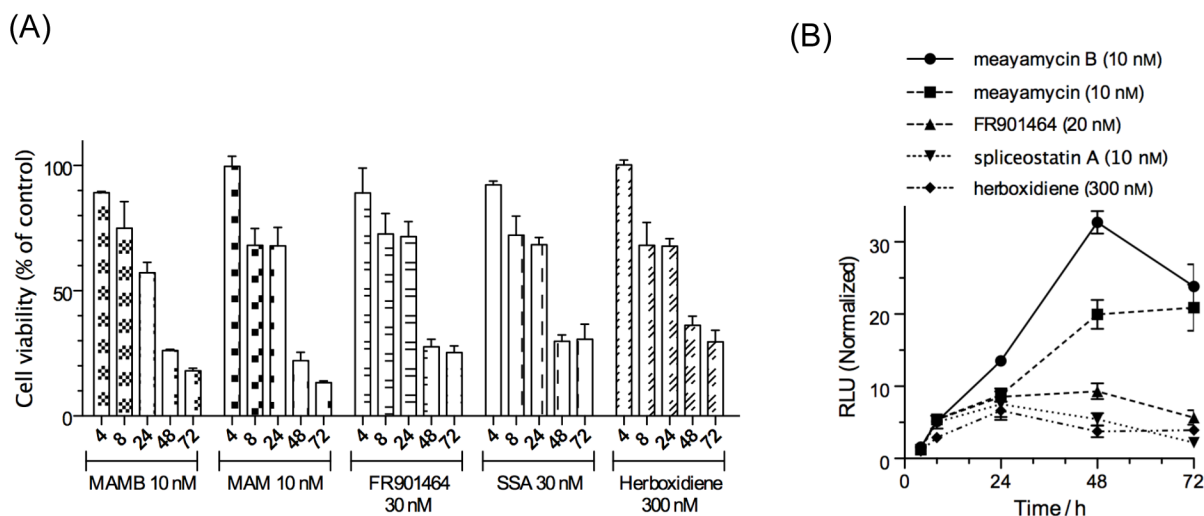


Figure 2-6 Time-dependence of splicing inhibition by SF3b inhibitors

Thus far, we have discussed FR901464, its analogs, and herboxidiene as SF3b inhibitors. However, these compounds are also antiproliferative agents.^{83-84, 87, 91, 117, 121-122, 135, 143} Surprisingly, the relationship between these two activities has not been evaluated by the Pearson correlation. To determine how well splicing inhibition and cell growth inhibition caused by meayamycin B and herboxidiene correlate with each other, HEK293-II cells were exposed to meayamycin B and herboxidiene for 16 h, and the luciferase activity and cell proliferation were measured. The results are shown in Figure 2-7. The Pearson correlation coefficients (r) for meayamycin B and herboxidiene were determined to be -0.944 ± 0.01 ($p < 0.0001$) and -0.603 ± 0.17 ($p < 0.0008$), respectively. Therefore, the splicing inhibition and antiproliferative activities for both compounds are correlated in these transformed HEK293 cells, with a stronger correlation for meayamycin B.

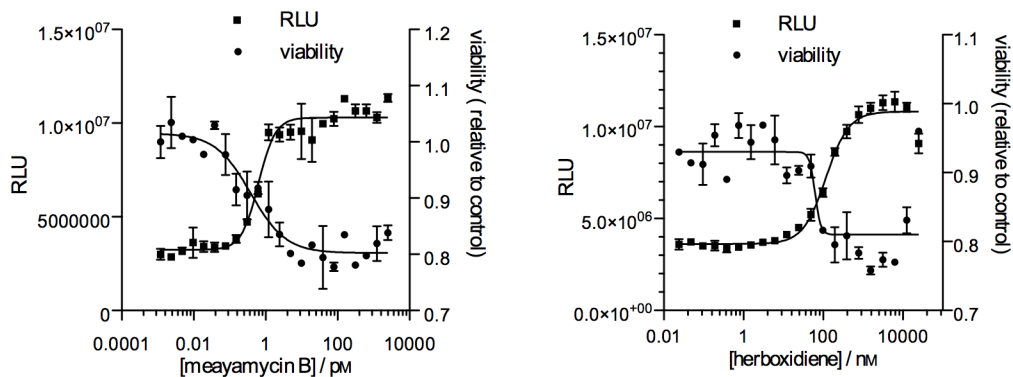


Figure 2-7 Correlation between splicing inhibitory and antiproliferative activities

2.1.2.3 Are simple electrophiles sufficient to inhibit splicing?

Many of the natural products that inhibit pre-mRNA splicing (FR901464,¹⁰⁰ pladienolides,¹¹¹ herboxidiene,¹²² and isoginkgetin¹²⁹) are endowed with either an epoxide or a Michael acceptor. However, a complete understanding of these important electrophilic functional groups remains elusive.⁹⁰ Thus, we screened a panel of epoxides and Michael acceptors (Figure 2-8) in the HEK293-II-based assay; none of these compounds inhibited splicing (1, 10, and 50 μ M) as determined by the luciferase assays and RT-PCR analysis. These results indicate that an electrophilic functional group by itself is not sufficient to inhibit pre-mRNA splicing.

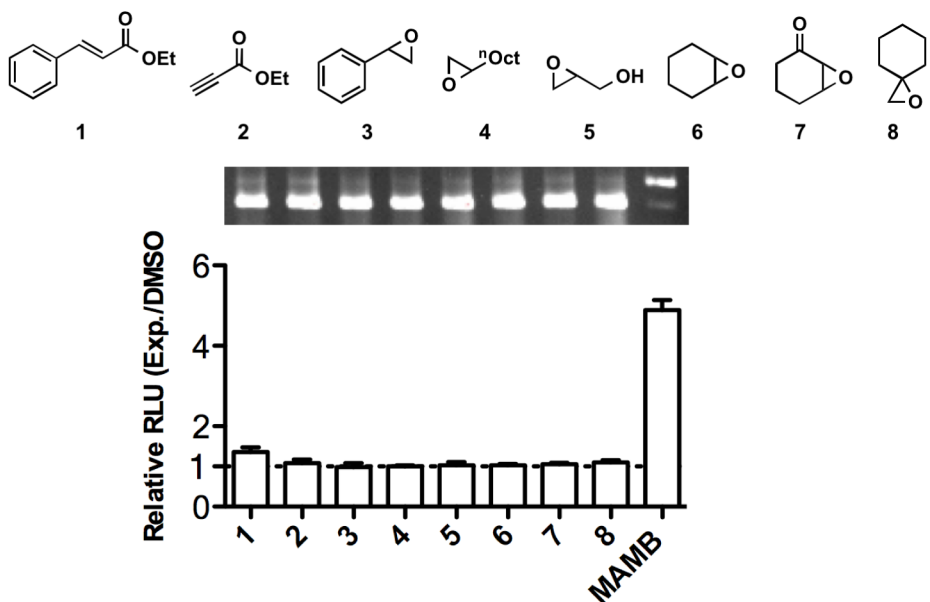


Figure 2-8 Epoxides and Michael acceptors do not inhibit splicing

2.1.3 Conclusion

We implemented a previously reported cell-based splicing assay system in a 96-well format using meayamycin B as a positive control. The validated assay permitted a direct, quantitative, and comparative evaluation of the currently available analogs of FR901464 and herboxidiene for an inhibition of constitutive splicing activity. The assay delivered graded responses and ED₅₀ values for all agents; meayamycin B was the most potent, while meayamycin, spliceostatin A, and FR901464 were equipotent, and herboxidiene was the least potent. Meayamycins inhibited pre-mRNA splicing for longer periods than spliceostatin A, FR901464, and herboxidiene. Antiproliferative activity and splicing inhibition by meayamycin B were strongly correlated. Moreover, we found that simple electrophilic functional groups did not suffice for splicing inhibition in HEK293-II cells. Our data validate meayamycin B as the most potent spliceosome

inhibitor to date, whose cytotoxic effects may directly result from splicing inhibition. We posit that meayamycin B is a useful chemical probe to further validate the spliceosome as an anticancer target, and a starting point for development of novel antineoplastic agents.

2.1.4 Experimental

Preparation of compound solutions. All small molecules tested were dissolved in DMSO as stock solutions (10 mM) and stored at -20 °C. For the experiments, diluted solutions were prepared in DMSO immediately before use. Unless mentioned otherwise, stock solutions (1.0 μL) at appropriate concentrations were directly added into cell culture media (200 μL) to afford a final 0.5% (v/v) DMSO concentration. This vehicle concentration was previously demonstrated to be nontoxic for the cells.¹²⁹

Cell Culture. The transformed HEK293 cell lines were gifts from Professor Melissa Moore (University of Massachusetts Medical School). The cells were cultured in Dulbecco's Modified Eagle Medium supplemented with 10% (v/v) fetal bovine serum, 4.5 g/L D-glucose, 2.0 mM L-glutamine, 100 units mL⁻¹ penicillin and 100 μg/mL streptomycin. The cells were all maintained at 37 °C in a humidified atmosphere containing 5% carbon dioxide. Once the cells reached 70–80% confluency, they were either subcultured by being diluted at 1:10 to a new flask or used for experiments. Cells were discarded after 20 passages.

Luciferase assay. Luciferase activity was evaluated by measuring the intensity of luminescence produced from luciferin oxidation using luciferase assay system kit (Promega). For the luciferase assay performed in a 96-well format, culture medium was removed by aspiration, and cells were rinsed once with phosphate-buffered saline (200 μL, 137 mM NaCl, 2.7 mM KCl, 10 mM Na₂HPO₄, and 2 mM KH₂PO₄). 1x Cell Culture Lysis Reagent (25 mM Tris-phosphate

pH 7.8, 2 mM DTT, 2 mM 1,2-diaminocyclohexane-*N,N,N',N'*-tetraacetic acid, 10% (v/v) glycerol, 1% (v/v) Triton X-100; 20 μ L) was then added to release the luciferase from the cells. After 10 min of incubation at 25 °C, the luciferase assay reagent (100 μ L) (reconstituted by combining the luciferin substrate and luciferase assay buffer provided in the Promega Luciferase Assay Kit) was added to each well. Luminescence was measured immediately on a Spectromax M5 plate reader (Molecular Devices) or a Modulus II Microplate Multimode Reader (Turner BioSystems). With the M5 plate reader, white 96-well plates with clear bottoms were used. With the Modulus II, white solid-bottomed 96-well plates were used.

BCA total protein assay. For luciferase assays (in a 96-well format) with which BCA protein assays were performed simultaneously in the same samples, Cell Culture Lysis Reagent (25 μ L) was added to each well of cells. Aliquots (5 μ L) of cell lysate from each well were transferred to a clear 96-well microtiter plate. Another 1x Cell Culture Lysis Reagent (20 μ L) was then added to each aliquot (5 μ L) to make a total volume of 25 μ L, which was subsequently combined with the BCA assay reagent (200 μ L). The samples were incubated at 37 °C for 30 min before absorbance at 562 nm was measured. The total protein concentration (proportional to the absorbance at 562 nm) from each sample was measured based on a standard curve developed with pure BSA. The standard curve was obtained by diluting BSA by the same Cell Culture Lysis Reagent, and the dose-dependent increasing absorbance at 562 nm was then collected and fit into a built-in linear regression model in GraphPad Prism.

Cell proliferation assay. Cell proliferation was evaluated using the MTS dye reduction assay with PMS as the electron acceptor assay performed in triplicate. To this end, cells were seeded in 96-well plates at 1.6×10^4 cells per well and incubated for 24 h at 37 °C. Cells were then exposed to various concentrations (serial three-fold dilutions) of the indicated compounds

for 72 h at 37 °C. An MTS solution (20 µL of MTS: PMS at 20:1) was added, and cells were incubated for 2 h at 37 °C before the absorption signals were measured at 490 and 650 nm. Growth inhibition was calculated as defined by the National Cancer Institute [$GI_{50} = 100 \times (T - T_0)/(C - T_0)$; T_0 = cell density at time zero; T = cell density of the test well after period of exposure to test compound; C = cell density of the vehicle treated].

Optimization of the length of exposure. To optimize length of exposure to meayamycin B, the HEK293-II cells were plated at 1.0×10^4 cells per well in 96-well white solid-bottomed polystyrene microplates and were incubated for 24 h. The cells were then subjected to 10 nM meayamycin B or DMSO (0.5 % v/v) as a vehicle control in duplicates for 3 d, and luciferase activity was measured at the indicated time points with a luciferase assay system (Promega). Data analysis and graphing were performed by using a GraphPad Prism software, version 5.0a for Mac OS X.

Optimization of cell density. For a 16-h assay in a 96-well format, HEK293-II cells were seeded at 4.0×10^3 – 2.0×10^4 cells per well in duplicates with a 2.0×10^3 cell increment per well. After 40 h (mimicking 24 h cell-seeding plus 16 h compound treatment) of incubation, luciferase activity was measured.

Evaluation of meayamycin B as a positive control. HEK293-II cells were plated at 1.6×10^4 cells per well in 96-well plates and cultured for 24 h. Thereafter, cells were exposed in duplicates to either meayamycin B at various concentrations or DMSO for 16 h before luciferase activity was assessed. We subsequently calculated the ED_{50} value of splicing inhibition by meayamycin B to HEK293-II by plotting dose-response curves using a nonlinear regression model in GraphPad Prism. A BCA protein assay was adopted as an evaluation of cell density for each well that was measured for luciferase activity. Each experiment was repeated on three

separate days to confirm the reproducibility, and the luciferase assay and BCA assay were carried out simultaneously.

Z-factor. The HEK293-II cells were seeded at 1.6×10^4 per well in a white 96-well plate. After 24 h of incubation, 48 wells were treated with 10 nM meayamycin B for 16 h and the other 48 wells were treated with DMSO. This experiment was repeated on three separate days. Dosing solutions were added manually with an Eppendorf Research® Plus pipette carrying 0.1–2.5 μ L adjustable range of volumes. The random error limits of this pipette are $\pm 6.0\%$ ($\pm 0.075 \mu$ L) when a volume of 1 μ L is delivered. Our calculated Z-factor values did not factor in these potential errors. The Z-factor was calculated using the equation shown below.¹⁴⁰ σ and μ stand for standard deviation and mean, respectively; P and N stand for positive and negative controls, respectively.

$$Z - factors = \frac{|\mu_P - \mu_N| - 3 \times (\sigma_P + \sigma_N)}{|\mu_P - \mu_N|} = 1 - \frac{3 \times (\sigma_P + \sigma_N)}{|\mu_P - \mu_N|}$$

RT-PCR. Cells were seeded at 3.5×10^5 per dish in 35-mm dishes for 24 h and were treated with DMSO or compounds dissolved in DMSO for 16 h. After aspirating the media, the total RNA was extracted with TRIzol® (Invitrogen). The RNA was dissolved in diethylpyrocarbonate-treated water and quantified in a UV-compatible 96-well plate by a Modulus II Microplate Multimode Reader at wavelengths of 260 and 280 nm (Abs_{260}/Abs_{280}). The RNA was free of degradation as determined by gel electrophoresis. Reverse transcription was carried out by using 200 U SuperScript® III reverse transcriptase (Invitrogen), each primer (2 pmol), ribonucleotide (10 nM each), 0.1 μ M DTT, and RNase inhibitor (20 U) for total RNA

(1 µg). The reaction conditions were as follows: 65 °C for 5 min, 0 °C for 1 min, 55 °C for 45 min, and 70 °C for 15 min. Afterwards, the reaction mixture (2 µL) was used as the template for PCRs. The PCR program involves the initial denaturation at 94 °C for 5 min, 30 cycles at 94 °C for 30 s, 55 °C for 45 s, 72 °C for 45 s, and final elongation at 72 °C for 7 min. The primers for TPI minigene were EX1F 5'-TAA ACT TAA GCT TCA GCG CCT CGG-3' and EX2R 5'-TAG CGC TTC ATG GCT TTG TGC AG-3'; the primers for luciferase gene were Luc_F 5'- TCA AAG AGG CGA ACT GTG TG-3' and Luc_R 5'-GGT GTT GGA GCA AGA TGG AT-3'. PCR products and a MassRuler DNA ladder (MBI Fermentus) were resolved on 1.5% (w/v) agarose gels. The DNA in the gels stained with ethidium bromide was visualized by a UV-Vis digital camera system (Eagle Eye II, Stratagene).

Preparation of spliceostatin A. Spliceostatin A was prepared from FR901464 in our laboratory according to the literature.⁹² There is a lack of evidence for the purity of spliceostatin A in the original literature⁹² or any other published work involving the use of this agent. Multiple rounds of HPLC purification yielded ~90% pure spliceostatin A.

Correlation assay. HEK293-II cells were treated with meayamycin B or herboxidiene at various concentrations and assayed under optimized screening conditions as described above. Cells for antiproliferation assays were treated simultaneously in the same manner. The antiproliferation was evaluated with the standard MTS method described above. Correlation analyses between luminescence intensity and relative viability data were performed using GraphPad Prism that calculated the Pearson's correlation coefficient (r).¹⁴⁴

$$r = \frac{\sum_{i=1}^n ((x_i - \bar{x})(y_i - \bar{y}))}{\sqrt{\sum_{i=1}^n (x_i - \bar{x})^2 \sum_{i=1}^n (y_i - \bar{y})^2}}$$

2.2 MEAYAMYCIN B SENSITIZES NON-SMALL CELL LUNG CARCINOMA TO BCL-X_L/BCL-2 INHIBITOR

This section is in part taken from “Gao, Y. and Koide, K. (2013) Chemical perturbation of Mcl-1 pre-mRNA splicing to induce apoptosis in cancer cells, *ACS Chem. Biol.* **8**, 895–900.”

2.2.1 Research design

In this study, we aim to investigate the feasibility of manipulating anti-apoptotic Bcl-2 family members by small-molecule SF3b modulators, to the end of triggering apoptosis in cancer cells. The rationale is that many Bcl-2 family genes undergo alternative pre-mRNA splicing and produce both proapoptotic and antiapoptotic protein isoforms. For example, *BCL2L1* and myeloid cell leukemia-1 (*MCL1*) genes are alternatively spliced into proapoptotic Bcl-x_S and Mcl-1_S, antiapoptotic Bcl-x_L and Mcl-1_L, and the unannotated Mcl-1_{ES}, respectively.¹⁴⁵⁻¹⁴⁷ In cancer, antiapoptotic isoforms are predominant.¹⁴⁸ Although other antiapoptotic Bcl-2 family proteins such as Bcl-2 and Bcl-w are present in cancer cells, inhibition of both Bcl-x_L and Mcl-1_L is necessary and sufficient to trigger massive cell death.¹⁴⁹ In support of this notion, ABT-737 (Figure 2-9), a small molecule that selectively binds to and antagonizes Bcl-2, Bcl-x_L and Bcl-w, but not Mcl-1_L,¹⁵⁰⁻¹⁵¹ encountered resistance in cancer cells that overexpressed Mcl-1_L.¹⁵²⁻¹⁵⁶ To circumvent the drug resistance, Mcl-1 expression was inhibited by biological or pharmacological means, which restored the anticancer activity of ABT-737.^{152, 157-158} However, the only endeavor successfully sequestering Mcl-1_L by perturbing the alternative splicing of Mcl-1 pre-mRNA was antisense morpholino oligonucleotides.¹⁵⁹ So far, there is no small molecule reported to have such activity.

The expression of Mcl-1_S and Bcl-x_S mRNAs was upregulated when splicing factor 3B 1 (SF3B1; a.k.a. SAP155) was knocked down, indicating that SF3B1 is involved in the alternative splicing of these apoptosis-related genes.¹²³ SF3B1 has also been identified as a *trans*-acting splicing factor that enhances the production of Bcl-x_L in A549 cells.⁶⁴ Having demonstrated that meayamycin B (Figure 2-9) as the most potent SF3B1 inhibitor,¹⁶⁰ here, we hypothesized that meayamycin B could switch the alternative splicing of Bcl-x and/or Mcl-1 pre-mRNAs towards the overexpression of Bcl-x_S and Mcl-1_S, which might overcome ABT-737 resistance. We choose non-small cell lung carcinoma (NSCLC) because they commonly overexpress anti-apoptotic Bcl-2 proteins.¹⁶¹

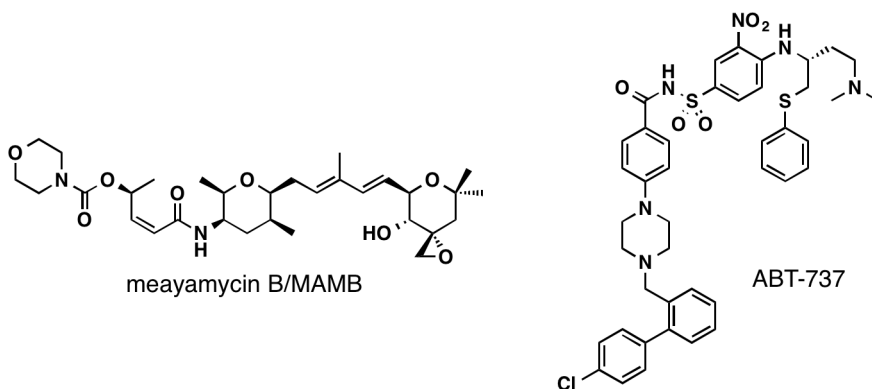


Figure 2-9 Structures of meayamycin B and ABT-737

2.2.2 Results and Discussion

2.2.2.1 Dose-dependent modulation of alternative splicing of Mcl-1

Mcl-1_L is generally overexpressed in non-small cell lung cancer cells including A549 and H1299 cells.¹⁶²⁻¹⁶³ To test the aforementioned hypothesis about meayamycin B, A549 and H1299 cell

lines were exposed to meayamycin B at various concentrations. The exposure time was only 9 h, which was sufficient to generate clear-cut data because the half-life of Mcl-1 mRNA is approximately 40 min.¹⁶⁴⁻¹⁶⁵ The short assay also minimizes the downstream secondary effects of meayamycin B. After the 9-h exposure, the relative mRNA levels of Mcl-1 splicing variants including Mcl-1_L and Mcl-1_S were evaluated by means of semi-quantitative RT-PCR (Figure 2-10A). For the RT-PCR experiment, we used primers (see Table 2-1 and arrows in Figure 2-10A) that were designed to reverse-transcribe multiple sites of the gene. As shown in Figure 2-10B, meayamycin B dose-dependently downregulated and upregulated Mcl-1_L and Mcl-1_S, respectively (NCBI GenBank accession number NM_021960 and NM_182763).¹⁴⁶ Specially, the ratio of Mcl-1_S/Mcl-1_L increased from 0.0065 (H1299 cells) and 0.035 (A549 cells) with DMSO to 69 (H1299 cells) and 5.9 (A549 cells) with 100 nM meayamycin B. In accordance with the change at the mRNA level, immunoblotting showed that meayamycin B abrogated the expression of the full length Mcl-1 protein isomer Mcl-1_L (40 kDa) and simultaneously increased Mcl-1_S (35 kDa) (Figure 2-10C). Mcl-1_L protein was more prevalent in H1299 than in A549, which might explain why 10 nM meayamycin B was required to completely remove Mcl-1_L in H1299 cells. Mcl-1_S protein became the dominant Mcl-1 isoform in A549 cells with only 0.1 nM meayamycin B.

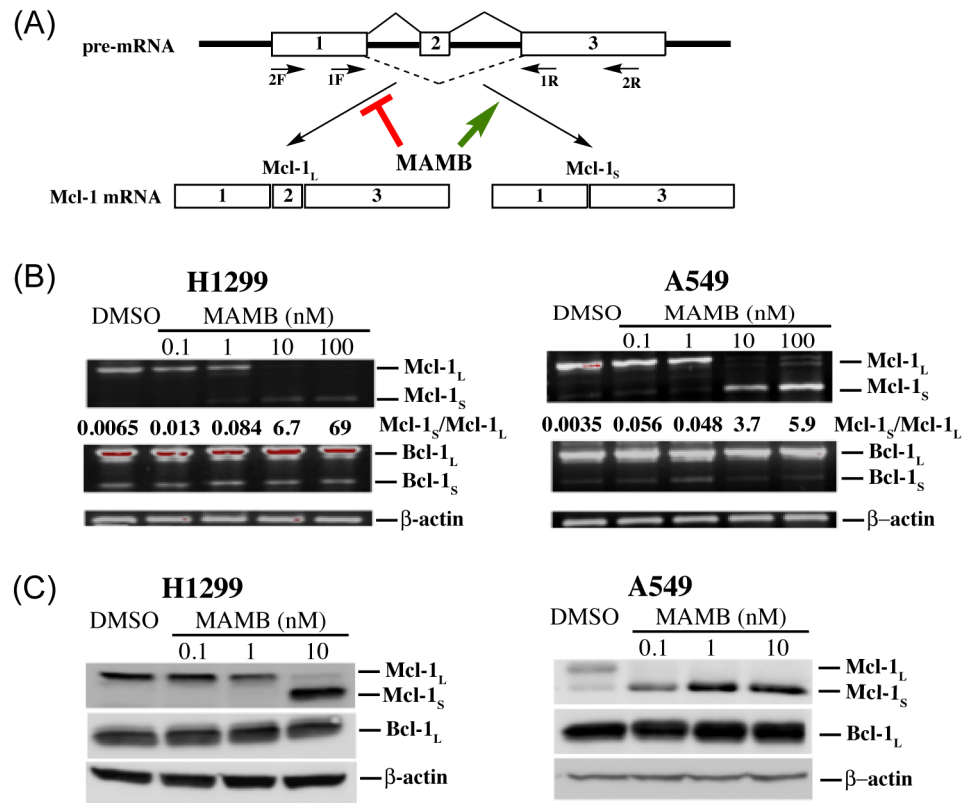


Figure 2-10 Dose-dependent regulation of Mcl-1 alternative splicing

2.2.2.2 Time-dependent modulation of alternative splicing of Mcl-1

Mcl-1 has a very short half-life at the mRNA and protein levels.¹⁶⁴⁻¹⁶⁵ Therefore, we thought it would be possible to observe changes in the expression of *MCL1* soon after the addition of meayamycin B to the aforementioned cells. Thus, H1299 and A549 cells were exposed to 10 nM meayamycin B for 1, 3, 9, and 24 h before relative expression of Mcl-1 splicing variants were determined at the mRNA and protein levels. The semi-quantitative RT-PCR analysis revealed that the increase of the Mcl-1_S mRNA was detectable after 1 h of treatment (Figure 2-11A). In addition, the suppression of the Mcl-1_L mRNA by meayamycin B was complete in 9 h and

remained as such for the next 15 h. At the protein level (Figure 2-11B), Mcl-1_s was the dominant Mcl-1 isoform in both A549 and H1299 cell lines after 9 h of exposure to meayamycin B.

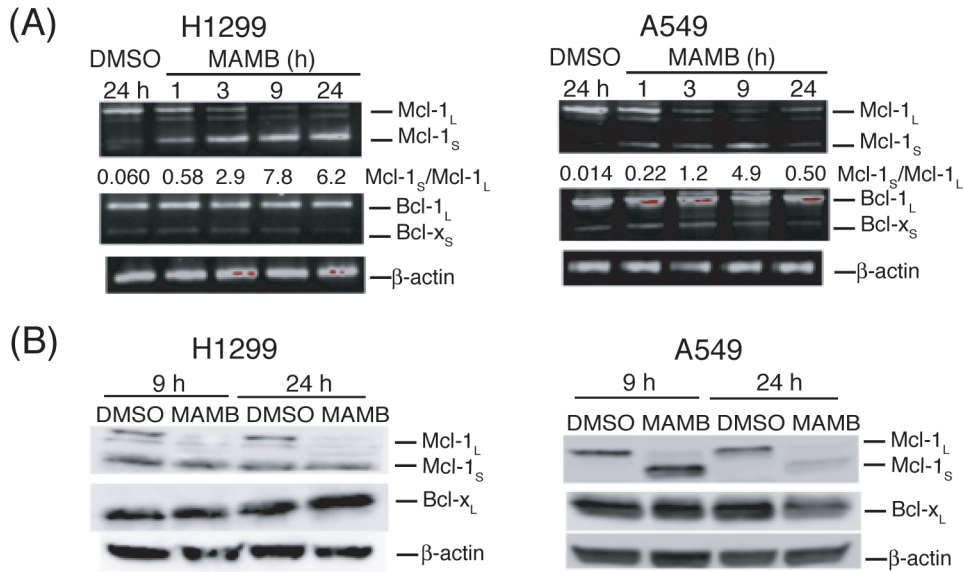


Figure 2-11 Time-dependent regulation of Mcl-1 alternative splicing

We also observed larger RT-PCR products that increased over time. These products were partially spliced Mcl-1 pre-mRNA retaining both intron 1 and intron 2 (Figure 2-12), indicating that meayamycin B acted as both a constitutive splicing inhibitor and an alternative splicing modulator for Mcl-1 pre-mRNA.

Of note, we did not detect the full-length pre-mRNA in the cytoplasm of the cells exposed to meayamycin B. This is consistent with the recent evidence showing SF3B1 inhibition can affect mRNA surveillance NMD pathways, causing the leakage of partially spliced pre-mRNA into cytoplasm for translation. In addition, full-length pre-mRNA could not be efficiently exported in to cytoplasm since this species was absent in the RT-PCR products.¹⁰⁰

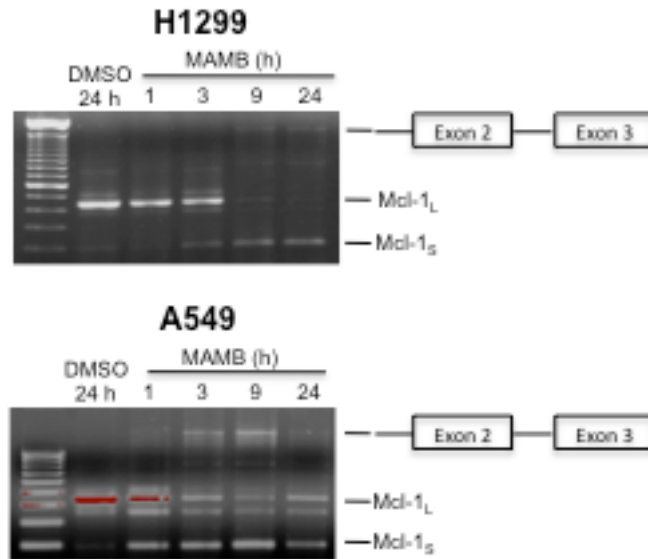


Figure 2-12 Meayamycin B inhibits the constitutive splicing of Mcl-1

2.2.2.3 Meayamycin B does not regulate alternative splicing of Bcl-x

SF3B1 is also a *trans*-acting splicing factor for the Bcl-x gene in A549 cells.⁶⁴ In neither dose- nor time-dependent treatments did meayamycin B significantly increase Bcl-x_S (Figure 2-12). This is in agreement with the results from the Webb group using sudemycins (analogs of FR901464) in pediatric rhabdomyosarcoma cell line Rh18 for 24 h.⁸¹ We reasoned that since SF3B1 might regulate Bcl-x_L alternative splicing only in response to ceramide. Interestingly, RNAi knockdown of SF3B1 resulted in alteration of the alternative splicing of both Mcl-1 and Bcl-x. In our model system, the different responses between the Mcl-1 system and the Bcl-x system toward meayamycin B indicate the complexity of the regulatory pathways of these two anti-apoptotic Bcl-2 proteins. Besides, the effect of RNAi and small-molecule inhibitor again protein targets could be strikingly different when the target proteins are heavily involved in protein-protein and protein-RNA/DNA interactions.¹⁶⁶ SF3B1 fits in this category of protein

targets. While biological means eliminates physical SF3B1, which might inevitably affects the actions of all binding partners of SF3B1, chemical approach such as meayamycin B disables SF3B1, whose physical scaffold might still serve its due functions that rely on interactions with other proteins and RNA molecules. Given the fact that there is no proof showing that SF3B1 directly binds to a cis-regulatory element on Mcl-1 pre-mRNA, like CRCE-1 on Bcl-x in response to ceramide, this incongruent observation about Bcl-x alternative splicing calls for further investigation of the role of SF3b (possibly SF3B1) at global alternative splicing level.

2.2.2.4 Meayamycin B sensitizes A549 and H1299 cells to ABT-737

Mcl-1_L expression has been recognized as the culprit for ABT-737 resistance in various cancers, including lung cancer cell monolayer cultures and spheroids.^{154, 157, 167} Therefore, we hypothesized that meayamycin B could overcome the ABT-737 resistance in cancer cells that rely on Mcl-1_L to survive. To test this hypothesis, A549 and H1299 cells were exposed to serial dilutions of meayamycin B and ABT-737 as single agents or in simultaneous combination at a constant ratio (meayamycin B:ABT-737 = 1:500) based on the Chou and Talalay method for 72 h.¹⁶⁸ Post-treatment cell viability was evaluated using 3-(4,5-dimethylthiazol-2-yl)-5-(3-carboxymethoxyphenyl)-2-(4-sulfophenyl)-2H-tetrazolium inner salt (MTS) method. ABT-737 did not affect cell viability as a single agent even at a 100 μM concentration that is the upper limit due to its solubility in a cell culture medium (Figure 2-13A and B). Meayamycin B inhibited cell growth as a single agent with GI₅₀ values of 0.14 ± 0.008 nM and 0.15 ± 0.008 nM (*n* = 3) in A549 and H1299 cells, respectively. With meayamycin B by itself, the treated cells did not undergo cell death. In sharp contrast, a combination of meayamycin B and ABT-737 induced cell death at doses (≥ 10 nM and ≥ 2.5 μM, respectively) that were not cytotoxic with either of

the two compounds as single agents. When the treated cells were examined under a microscope, only the combination treatment caused apoptosis-like cell shrinkage (data not shown). Although full cell-killing curves from each compound as a single agent could not be generated due to the poor solubility of ABT-737, preventing us from calculating the combination index values,¹⁶⁸ the remarkable cytotoxic effect from the meayamycin B–ABT-737 combination indicated a strong synergism. Interestingly, under a microscope, H1299 cells displayed more prominent apoptotic morphology than A549 cells upon meayamycin B treatment. This might be related to the different p53 gene status: A549 expresses wild-type p53 protein while H1299 is p53-deficient.¹⁶⁹ Further studies are warranted since generally the p53-null genotype in H1299 affords them stronger resistance to apoptotic stimuli.¹⁷⁰ Nonetheless, the sensitivity of H1299 cells indicated that the apoptosis triggered by the combination of meayamycin B and ABT-737 does not require the expression of wild-type p53.

2.2.2.5 Mcl-1 abundance correlates with meayamycin B-sensitivity

After examining the potency of meayamycin B in H1299 and A549, we used immunoblotting to assess the basal expression of antiapoptotic Bcl-2 family proteins in these cell lines. It was demonstrated that H1299, expressing higher level of Mcl-1_L, was also more responsive to single-agent meayamycin B. The basal Mcl-1_L level (Mcl-1_L/β-actin) was 1.32 in H1299 versus 0.41 in A549 (Figure 2-13C) and meayamycin B dropped the cell viability to approximately 50% and 75% in H1299 and A549, respectively. The same pattern was also observed in head-and-neck squamous cell carcinoma (HNSCC) cell lines. As an example, the data from PCI-13 and 93-UV-147T showed Mcl-1_L expression levels at 1.24 and 0.07 (Figure 2-13D). In consistence, meayamycin B reduced the cell viability to 0% in PCI-13 but was inactive in 93-UV-147T

(Figure 2-13E and 2-13F). These data indicate the potential use of meayamycin B for cancer types that overexpress Mcl-1_L.

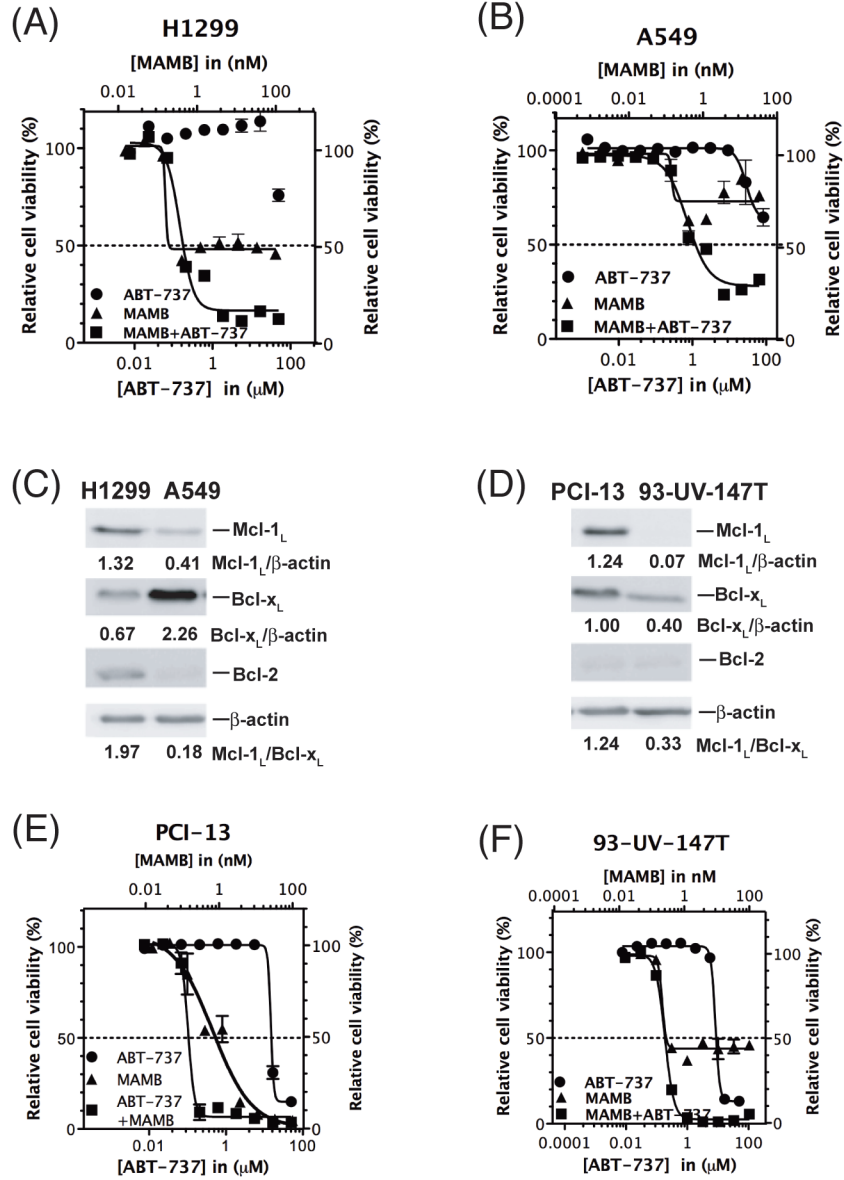


Figure 2-13 Mcl-1 abundance correlates with meayamycin B-sensitivity

2.2.2.6 Meayamycin B and ABT-737 combination synergistically causes apoptosis

To determine whether the combination induced apoptosis, we measured the caspase 3/7 activity of the treated H1299 and A549 cells. The cells were exposed to the combination of meayamycin B and ABT-737, as single agent or in combination, at 1 nM and 500 nM (their GI_{50} values when used in combination), respectively. After 9 h exposure, although single-agent ABT-737 caused an increase of caspase 3/7 activity in a dose-dependent manner, the combination treatment induced a significantly higher level of caspase 3/7 activity (Figure 2-14). The major cell death in 24-h combination treatment led to a relatively low caspase 3/7 readout. Meayamycin B by itself was a weak apoptosis inducer. The rapid activation of caspase 3/7 observed in the combination-treated cells indicated a strong synergism between meayamycin B and ABT-737 in inducing apoptosis.

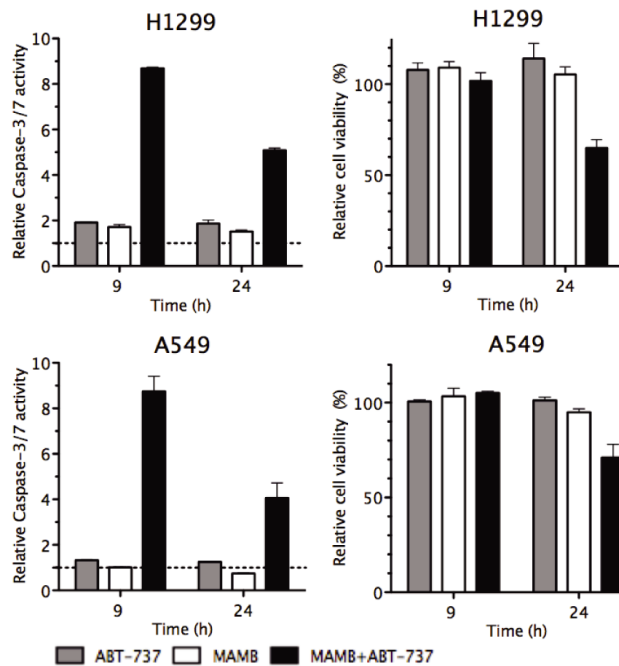


Figure 2-14 Rapid onset of apoptosis triggered by the combination in NSCLC cells

To better understand the stages of apoptosis in the cells exposed to the combination of meayamycin B and ABT-737, we stained the cells with fluorescein isothiocyanate (FITC), annexin V, and 7-aminoactinomycin D (7-AAD) and monitored the fluorescence with flow cytometry. Annexin-V stains early apoptotic cells by detecting the externalization of phosphatidylserine,¹⁷¹ and 7-AAD intercalates double-stranded DNA to detect dead or late-stage apoptotic cells.¹⁷² The cells treated with both meayamycin B and ABT-737 displayed a significantly higher population of annexin V⁺/7-AAD⁻, indicating that these cells were in an early stage of apoptosis (Figure 2-15, lower right quadrants) and annexin V⁺/7-AAD⁺ (late apoptotic/necrotic; Figure 2-15 upper right quadrants), indicating synergistic apoptosis stimulation.

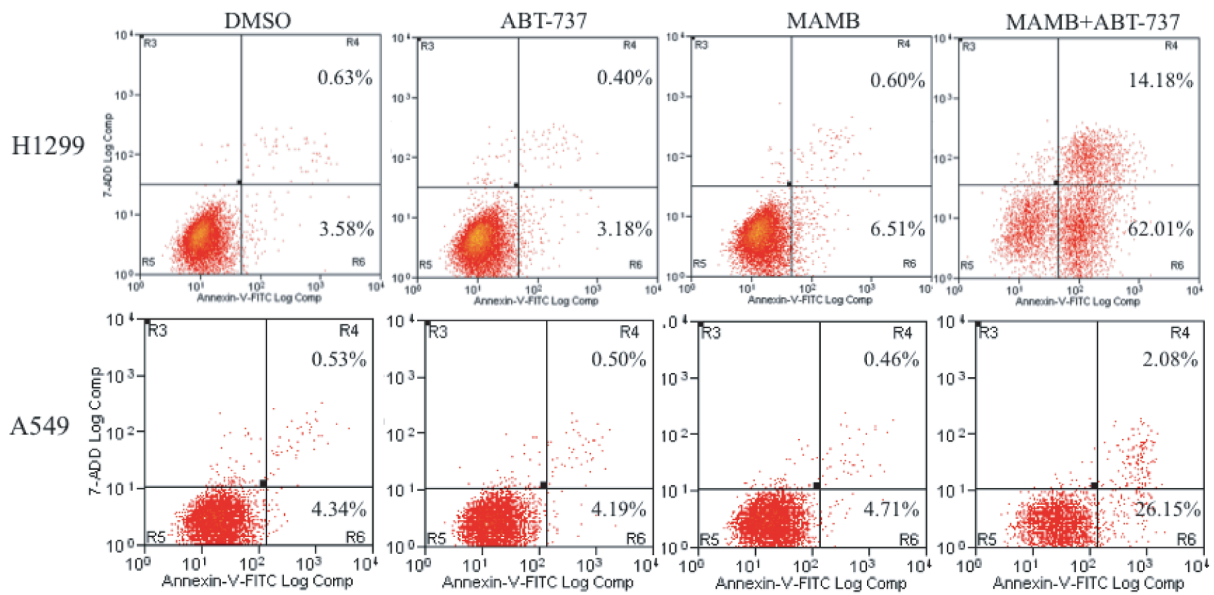


Figure 2-15 Apoptosis activation monitored with Annexin V-FITC and PI staining

2.2.3 Conclusion

In conclusion, meayamycin B inhibits the constitutive splicing and switches the alternative splicing of Mcl-1 in a dose- and time-dependent manner in non-small cell lung cancer A549 and H1299 cell lines. The alteration of Mcl-1 alternative splicing increased pro-apoptotic Mcl-1_S with a concomitant decrease of anti-apoptotic Mcl-1_L. This is, to the best of our knowledge, the first report of the modulation of Mcl-1 alternative splicing by a single small molecule. Although both A549 and A1299 cells were resistant to cell death in the presence of either meayamycin B or ABT-737, treatment of these cells with both meayamycin B and ABT-737 induced cell death, presumably through the meayamycin B-mediated modulation of Mcl-1 pre-mRNA splicing. These results support the feasibility of using the combinations of Mcl-1_L and Bcl-x_L inhibitors for both research and therapeutic purposes.

2.2.4 Experimental

Cell lines. A549 and H1299 cells were obtained from the American Type Culture Collection (ATCC). PCI-13 and 93-UV-147T cell lines are kind gifts from Dr. Robert Ferris (University of Pittsburgh). The A549 and H1299 cells were maintained in Roswell Park Memorial Institute-1640 (RPMI-1640) medium, PCI-13 were grown in Dulbecco's Modified Eagle's Medium and 93-VU-147T cell line was grown in DMEM/F12 medium. All media were supplemented with 10% (v/v) fetal bovine serum, 4.5 g/L D-glucose, 2.0 mM L-glutamine, 100 units/mL penicillin, and 100 µg/mL streptomycin. The cells were cultured at 37 °C in a humidified incubator with 5% CO₂.

Compound treatment. ABT-737 was purchased from Selleck. Meayamycin B was synthesized in our laboratory.⁹⁴ The compounds were dissolved in dimethyl sulfoxide (DMSO) to make 10 mM stock solutions and stored at $-20\text{ }^{\circ}\text{C}$. For 96-well format assays, we diluted the compounds with cell culture medium and transferred each dilution (100 μL) to cell cultures (100 μL) in triplicate. For 35-mm dish-format assays, cells were seeded in 35-mm dishes and cultured for 24 h ($\sim 70\%$ confluence) before vehicle or test compounds were added directly from stock at appropriate concentrations. In both cases, the final vehicle% was controlled at 0.5% for all of the treatments. After incubation for the indicated periods of time (1, 3, 9 and 24 h for time-dependence experiments, 9 or 72 h for dose-dependence experiments), the cells in 96-well plates were lysed and subjected to luciferase assays or caspase-3/7 assays and the cells from 35-mm dishes were subjected to total RNA extraction and the RT-PCR experiments.

Apoptosis detection: (1) FITC Annexin V and 7-aminoactinomycin D (7-AAD) staining. Cells (1×10^6 cells) were treated for 9 h with 10 nM meayamycin B, 5 μM ABT-737, a combination of these compounds, or an equal volume of DMSO as a negative control. After treatment, the cells were harvested, washed in ice-cold PBS, and directly stained with 5 $\mu\text{g mL}^{-1}$ FITC Annexin V (BD Pharmingen, cat. no. 556420) and 2.5 $\mu\text{g mL}^{-1}$ 7-AAD (BD Pharmingen, cat. no. 559925). After 20 min of incubation at room temperature in the dark, cells were analyzed by flow cytometry using a Beckman Coulter Epics XL-MCL. Data were analyzed using Summit V4.3 software. (2) Caspase 3/7 activity assays. The cells were seeded at $10,000\text{ well}^{-1}$ in medium (100 μL) in white solid-bottom 96-well plates and cultured for 24 h. Meayamycin B (0.1, 1, 10 and 100 nM) and ABT-737 (0.05, 0.5, 5 and 50 μM), either separately or in combination (constant ratio of 1:500), were added in duplicate into the cells for 9 h. Caspase-3/7 activity was quantified using a Caspase-Glo[®] 3/7 reagent (Promega, cat. no. G8091) following the

manufacturer's optimized protocol. Specifically, the Caspase-Glo® 3/7 buffer and the substrate were equilibrated to room temperature and mixed immediately before assays. This conjugated assay buffer (100 µL) was added to a cell culture (100 µL) that was equilibrated to room temperature and the mixture was incubated at room temperature for 1 h. Luminescence was directly measured with a Modulus II Microplate Multimode Reader. The caspase-3/7 activity was expressed as the mean luminescence of compound-treated wells divided by that of vehicle-treated wells.

Semi-quantitative reverse transcription-Polymerase Chain Reaction (RT-PCR). The total RNA was extracted using a Trizol reagent (Invitrogen, cat. no. 15596-026) and cDNA generated by reverse transcription using 1 µg of total RNA and SuperScript® II reverse transcriptase (Invitrogen, cat. no. 18064-014). The primer sequences are shown in Table 2-1. For semi-quantitative RT-PCR, the thermocycler program for Bcl-x, Mcl-1 and β-actin involved an initial denaturation at 94 °C for 5 min, 35 cycles at 94 °C for 30 sec, 58 °C for 30 sec, 72 °C for 50 sec, and a final elongation at 72 °C for 7 min. The PCR products were examined on 1.5% agarose gels containing 0.5 µg/mL ethidium bromide and imaged by a Molecular Imager Gel Doc™ XR+ (BioRad). The intensity of the bands was quantified with the Lab Imager software (BioRad).

Table 2-1 Primer sequences for RT-PCR experiments in NSCLC system

Genes	Sequences
Bcl-x	Bcl-xF: 5'- GAG GCA GGC GAC GAG TTT GAA -3'
	Bcl-xR: 5'- TGG GAG TTG AGA GTG GAT GGT -3'
Mcl-1	Mcl-1F: 5'- ATC TCT CGG TAC CTT CGG GAG C -3'
	Mcl-1R: 5'- CCT GAT GCC ACC TTC TAG GTC C -3'
	Mcl-2F: 5'- AGG AAT TCG ATG TTT GGC CTC AAA AGA AAC GCG GTA -3'
	Mcl-2R: 5'- GAA TTC GGA AGT TAC AGC TTG GAG GAG TCC AAC TGC -3'
β -actin	Forward: 5'- GCA CCA CAC CTT CTA CAT GAG C -3'
	Reverse: 5'- TAG CAC AGC CTG GAT AGC AAC G -3'

Western blotting. Cells were harvested in a cell lysis buffer (50 mM Tris-HCl, 150 mM NaCl, 1% Triton X-100, 0.1% SDS, and 1 mM PMSF) and a mixture of protease inhibitors (Roche, cat. no. 05 892 791 001). Total protein (100 μ g) was electrophoresed on a 12% SDS-polyacrylamide gel and electrotransferred to a polyvinylidene difluoride membrane (Millipore, cat. no. IPVH10100). Membranes were blocked at room temperature for 1 h with a blocking buffer (5% non-fat dry milk in 10 mM Tris-HCl pH7.6, 150 mM NaCl, 0.1% Tween-20) and then incubated at 4 °C overnight with rabbit anti-Mcl-1 monoclonal antibody (1:1000 dilution; Cell signaling technology, cat. no. 5453S), rabbit anti-Bcl-x_{L/S} monoclonal antibody (1:1000 dilution; Santa Cruz, cat. no. sc-634) or rabbit anti- β -actin monoclonal antibody (1:1000 dilution; Cell signaling technology, cat. no. 4970S), followed by 1 h of incubation with horseradish peroxidase-conjugated anti-rabbit (1:1000 dilution; Cell signaling technology, cat. no. 7074S) secondary antibody. Blots were developed with ECL Plus reagents (PerkinElmer Life and Analytical Science, cat. no. NEL103001EA). Mcl-1_L, Mcl-1_S, Bcl-x_L, Bcl-x_S, and β -actin

proteins migrated at 40, 35, 30, 26, and 45 kDa, respectively. The densities of the resulting bands were quantified using Image Gauge Ver. 4.0 (FUJIFILM).

Statistics. Data analysis and graph plotting were carried out using a GraphPad Prism 5.0c for Mac (GraphPad Software). All the data were presented as mean \pm standard deviation. The significance level for all analyses was 5%.

2.3 MEAYAMYICN B SENSITIZES HEAD AND NECK SQUAMOUS CELL CARCINOMA TO BCL-X_L/BCL-2 INHIBITOR

This section is in part taken from the manuscript entitled “Gao, Y., Trivedi, S., Ferris, R., and Koide, K. SF3B1 inhibitor perturbs the splicing of HPV16 E6 and MCL1 and synergistically induces apoptosis in combination with a BCL-X_L/BCL-2 inhibitor in head and neck squamous cell carcinoma”.

2.3.1 Introduction

HNSCC is the sixth most common cancer worldwide.¹⁷³ HNSCC mostly occurs by cigarette/alcohol consumption; however, a subgroup of HNSCC (26%) is caused by the integration of high-risk human papillomavirus (HPV), especially HPV16.¹⁷⁴ It has been perplexing that only ~10% of those who were exposed to high-risk HPV16 or 18 develop cancer.¹⁷⁵ In oropharyngeal carcinoma particularly, HPV16 is detected in over 60% of the cancer tissues.¹⁷⁶ Due to their distinct mechanisms of tumorigenesis, HPV-positive and HPV-negative HNSCC should be treated separately.¹⁷⁷⁻¹⁷⁸ Platinum-based chemotherapy, the most commonly

used drug regardless of HPV status, is far less effective against HPV-negative HNSCC.¹⁷⁹⁻¹⁸⁰ Moreover, in the past thirty years, the five-year overall survival rate of HNSCC has not improved,¹⁸¹ warranting the discovery of new pharmacological interventions.

The discovery of novel therapeutics requires a comprehensive understanding of the disease biology. Since HPV16 is present in nearly 60% of all cervical cancers,¹⁸² its expression is most widely studied in cervical cancer models. The HPV16 genome encodes six early (E) viral proteins (E1, E2, E4, E5, E6, and E7) and two late (L) viral capsid proteins (L1 and L2), accompanying the differentiation stages of the host keratinocytes.¹⁸³ Among these proteins, only the overexpression of E6 and E7 was correlated with malignant transformation.¹⁸⁴ At the transcription level, *E6* and *E7* share a mutual early p97 promoter. Because the open reading frames of *E6* and *E7* are only 2 nucleotides apart, the transcription of full-length *E6* prohibits the translation of *E7* protein. Otherwise, when intron 1 (Figure 2-16) is excised, splicing variant *E6** is generated, which in turn allows the translation of *E7*.¹⁸⁵⁻¹⁸⁶ In response to epidermal growth factor (EGF), the activation of ERK1/2 pathway facilitates the production of *E6*. SiRNA knockdown experiments demonstrated that hnRNP A1 and hnRNP A2/B1 favored *E6*, while splicing factor Sam68 and transcription factor Brm favored *E6**.¹⁸⁷ This report indicated that splicing and transcription are coupled in HPV16 *E6/E7* expression.

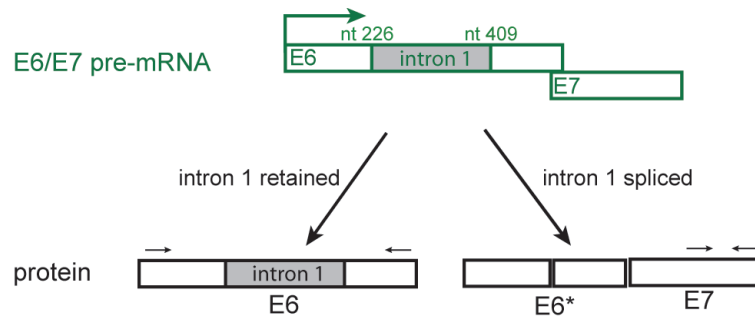


Figure 2-16 Generation of HPV16 E6 and E7 oncoproteins

Functionally, E6 inhibits apoptosis by triggering the degradation of p53, and E7 enhances cell proliferation by binding to another tumor suppressor protein retinoblastoma-associated protein (pRb).¹⁸⁸⁻¹⁸⁹ Whereas the function of full-length E6 is relatively well understood, the function of E6* is still elusive, and available data lend controversial conclusions; through RT-PCR analysis, E6* expression was found to be significantly higher in late stage cervical lesion than early stage counterparts.¹⁹⁰⁻¹⁹¹ In contrast, E6* counteract the anti-apoptotic action of E6 in the degradation of p53 and precaspase 8.¹⁹²⁻¹⁹³ Additionally, the overexpression of E6* is cytotoxic when expressed in immortalized monkey fibroblasts CV-1 cells.¹⁹⁴ In sum, these unconnected pieces of data argue that both basic and translational studies of E6 splicing are lagging behind, calling for further studies advanced by novel strategies.

Meayamycin B (Figure 2-9), the most potent inhibitor of SF3b, sensitized NSCLC cells (A549 and H1299) to ABT-737 (Figure 2-9) by modulating the splicing of Mcl-1.¹⁹⁵ Similar observations were reported for the combination of spliceostatin A (structurally similar to meayamycin B) and ABT-737 in neuroblastoma.¹⁹⁶ Given the mutual risk factors, such as alcohol and cigarette consumption, shared between NSCLC and HNSCC,¹⁹⁷⁻¹⁹⁸ we reasoned that meayamycin B might also prime HNSCC cells for ABT-737. Therefore, we wished to examine

the anticancer activity of meayamycin B, as a single-agent or in combination with ABT-737. In addition, we used meayamycin B to examine the role that SF3B1 plays in the splicing of Mcl-1 and more importantly, HPV16 E6.

2.3.2 Results and Discussion

2.3.2.1 Meayamycin B and ABT-737 combination causes apoptosis

We investigated the apoptotic response of a panel of HNSCC cells to meayamycin B and ABT-737. There are two methods in common use for calculating the dose-response relationship expected from combination therapy when two drugs are assumed to have no interactions: Loewe additivity¹⁹⁹ and Bliss independence.²⁰⁰ Loewe additivity assumes that two inhibitors act on a target through a similar mechanism, as shown by Chou and Talalay for mutually exclusive enzyme inhibitors.¹⁶⁸ Bliss independence assumes that inhibitors can bind mutually and nonexclusively through distinct mechanisms. Unfortunately, the insufficient water solubility of ABT-737 prohibited the generation of dose response curves required for the Loewe method. Therefore, Bliss independence was used to determine drug interactions. To this end, we performed 72-h MTS-based antiproliferation assays in a panel of seven cell lines including PCI-13, PCI-15B, UM-SCC22B, UPCI:SCC90, 93-VU-147T, UM-SCC47, and UD-SCC2. The GI₅₀ values (n = 3) are shown in Table 2-2.

Table 2-2 GI50 values for 72-h antiproliferation assays in HNSCC cells

Cell lines		GI ₅₀		
		Single agent		ABT-737 (μM) in combination
		Meayamycin B (nM)	ABT-737 (μM)	
PCI-13	HPV16-negative	0.19±0.07	15±1.8	0.59±0.83
PCI-15B		0.14±0.06	11±4.5	0.19±0.19
UM-SCC22B		0.60±0.12	19±2.9	0.84±0.86
UM-SCC47	HPV16-positive	0.038±0.006	19±12.3	0.20±0.11
93-VU-147T		0.074±0.039	4.3±3.5	0.50±0.70
UD-SCC2		0.025±0.009	28±2.9	0.15±0.02
UPCI:SCC90		0.074±0.022	6.6±1.5	0.14±0.082

Meayamycin B only arrested the growth of 93-VU-147T, UM-SCC47, and UD-SCC2 cells, while the combination of meayamycin B and ABT-737 eradicated these cells (Figure 2-17). In the other four cell lines, especially UM-SCC22B and UPCI:SCC90, single-agent meayamycin B induced substantial cell death, nearly the same level caused by the combination with ABT-737.

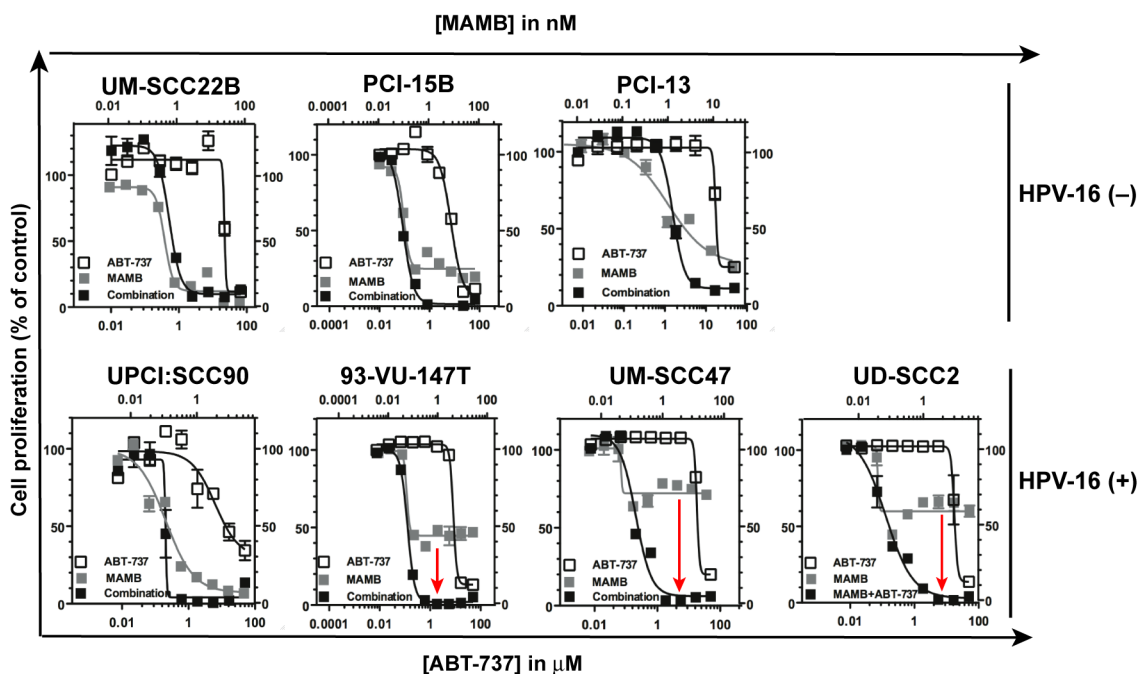


Figure 2-17 Antiproliferation assays of meayamycin B and ABT-737 in HNSCC cells

As an evaluation of drug interaction with Bliss independence, we calculated ΔE values for the combination treatment in each cell line. Assuming the two test compounds have additive interactions, ΔE is expressed as the difference between the expected and the observed cell viabilities. As shown in Figure 2-18A, the combination caused significantly higher levels of cell death than expected. Accordingly, Bliss sums clustered in the range of 400–600 (Figure 2-18B), indicating strong synergism. Meayamycin B dropped ABT-737's GI_{50} values by 1–2 orders of magnitude. These data underscore the scope and generality of the efficacy from the combination of meayamycin B and ABT-737 in HNSCC cell lines.

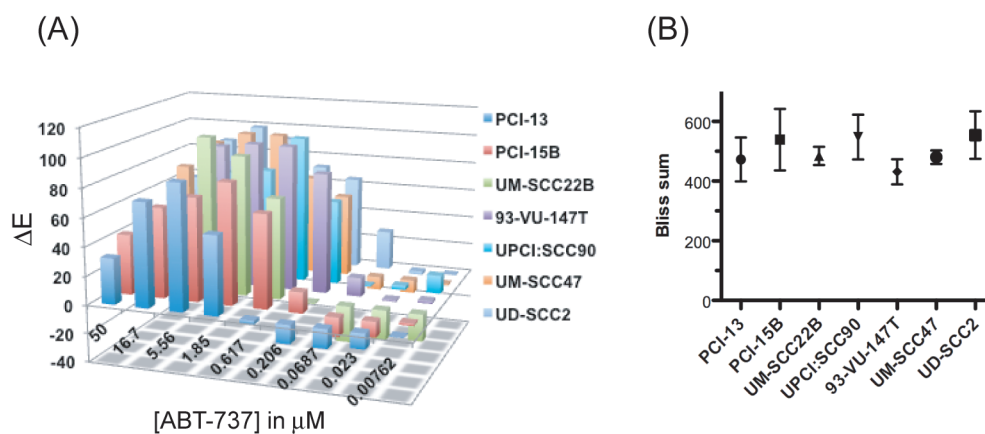


Figure 2-18 Bliss Independence evaluation of meayamycin B and ABT-737 combination

To confirm that the meayamycin B and ABT-737 combination causes apoptosis, we stained treated cells with Annexin V-FITC and PI and monitored the rates of apoptosis using flow cytometry. To demonstrate an early onset of apoptosis triggered by the combination, we chose 4-h exposure for four HNSCC cell lines (PCI-15B and PCI-13 as HPV16-negative, and UM-SCC47 and UPCI:SCC90 as HPV16-positive). After 4-h exposure, we observed 5–10% more Annexin V-positive population (Figure 2-19, right quadrants) in the combination-treated than in the cisplatin-treated (20 $\mu\text{g}/\text{mL}$, positive control) cells, indicating the rapid apoptosis by the combination. Necrosis (Figure 2-19, upper left quadrants) was also induced as a secondary event in the apoptotic pathway.²⁰¹

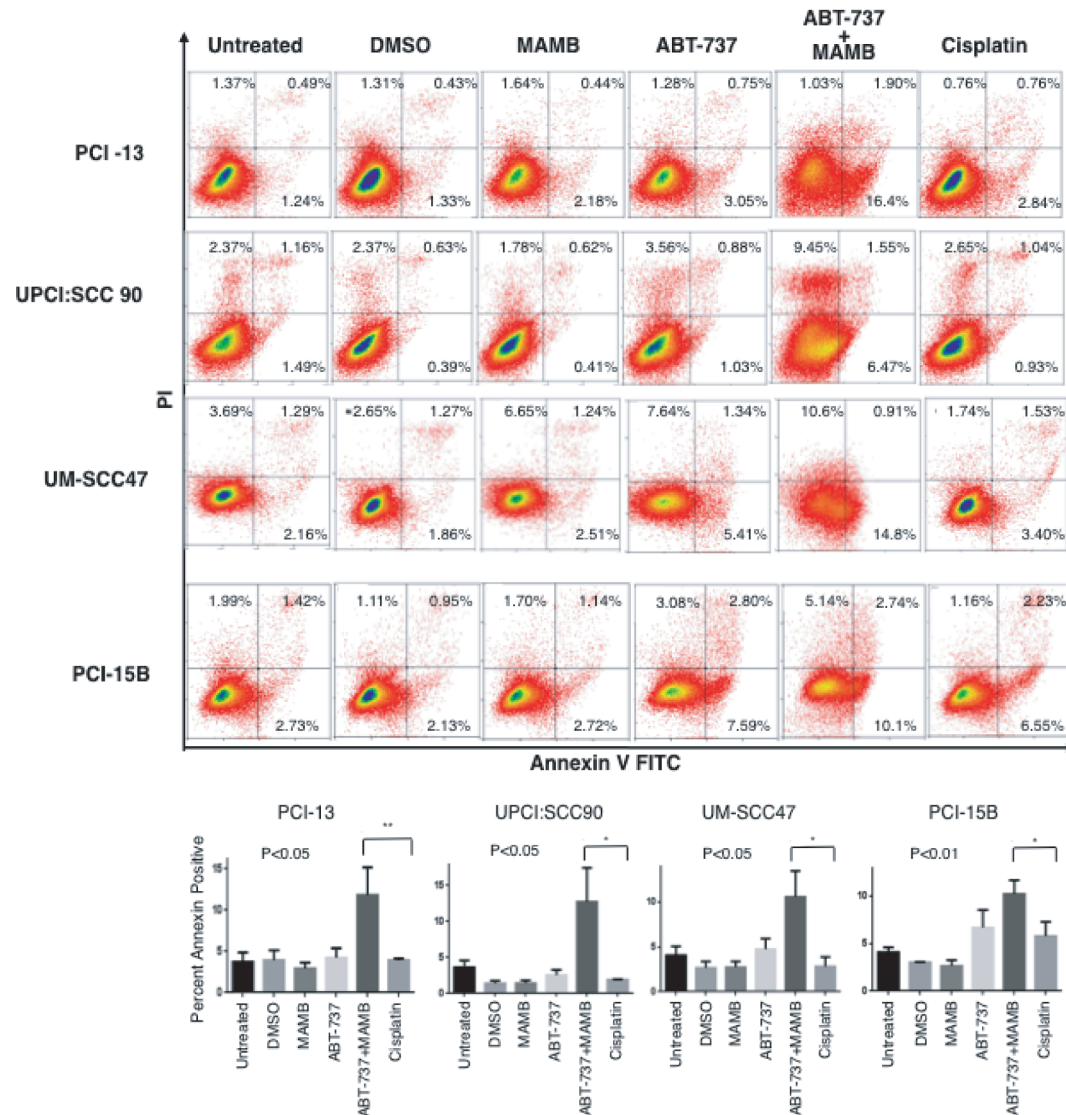


Figure 2-19 Apoptosis activation monitored with Annexin V-FITC and PI staining

As a downstream apoptotic event, caspase 3/7 (9-h exposure) experienced 7- to 15-fold increases almost exclusively in combination-treated cells (Figure 2-19A upper panel). Single-agent ABT-7373 more strongly activated caspase 3/7 in HPV16 negative and UPCI:SCC90 cells. Meayamycin B, on the other hand, was not a strong apoptosis inducer. The combination also led to higher growth inhibition in HPV16 negative cell lines (Figure 2-19A lower panel). Taken

together, the Annexin V-FITC/PI staining and the caspase 3/7 activity assays both suggest rapid induction of synergistic apoptosis by the combination of meayamycin B and ABT-737.

To determine whether the onset of apoptosis is mediated by Bax/Bak, we exposed *Bax*^{-/-}/*Bak*^{-/-} mouse embryonic fibroblasts (MEFs) and SV40-immortalized wild-type MEFs to the combinations of meayamycin B and ABT-737. We chose 9-h exposure for caspase 3/7 activity assays because it should take more than 4 h to observe the downstream effects of meayamycin B. Similarly to HNSCC, the wild-type, but not *Bax*^{-/-}/*Bak*^{-/-} MEFs, showed dose-dependent caspase 3/7-activation upon the combination treatments (Figure 2-20B upper panel). Accordingly, *Bax*^{-/-}/*Bak*^{-/-} MEFs were significantly more resistant to the combination treatments (Figure 2-20B lower panel), suggesting that Bax/Bak-mediated apoptosis is a mechanism of cell killing by the combination of meayamycin B and ABT-737. Of note, other cell death pathways such as autophagy might have contributed to a ~15% decrease of proliferation in *Bax*^{-/-}/*Bak*^{-/-} MEFs caused by the combination, since Mcl-1-elimination triggers autophagic cell death when Bax is defected.²⁰¹⁻²⁰² This hypothesis needs to be tested through more experiments.

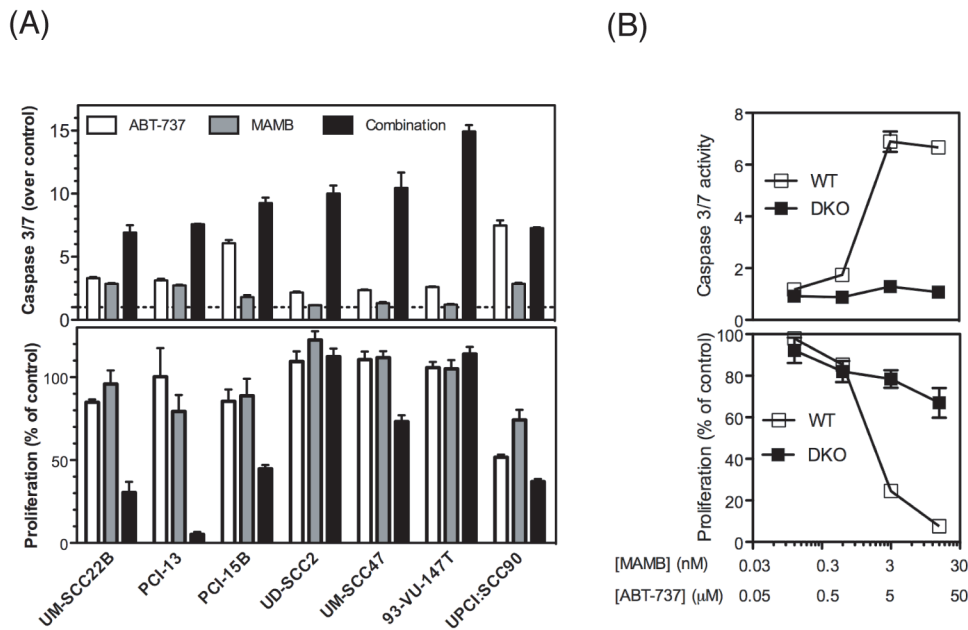


Figure 2-20 Bak/Bax-mediated apoptosis

2.3.2.2 Basal level of MCL-1 correlates with meayamycin B sensitivity

In PCI-13 and 93-VU-147T cells, we previously observed a correlation between the Mcl-1_L level and the cellular response to meayamycin B.¹⁹⁵ To determine whether basal Mcl-1_L expression more broadly correlates with meayamycin B sensitivity, we assessed the basal expression of Mcl-1_L, Bcl-x, and Bcl-2 using Western blotting (Figure 2-21). Mcl-1_L was the dominant Mcl-1 isoform in all the cell lines except UM-SCC22B, which exclusively expressed Mcl-1_S. In addition, the total levels of Mcl-1 in PCI-13, PCI-15B, UM-SCC22B and UPCI:SCC90 were consistently higher than those in the other cell lines (Mcl-1/β-actin ≥ ~1.5 versus ≤ 0.8). Interestingly, three out of the four Mcl-1-abundant cell lines were HPV16-negative. Conversely, Bcl-X_L was expressed in all the cell lines at levels statistically unrelated to meayamycin B response; Bcl-2 was only detected in UPCI:SCC90.

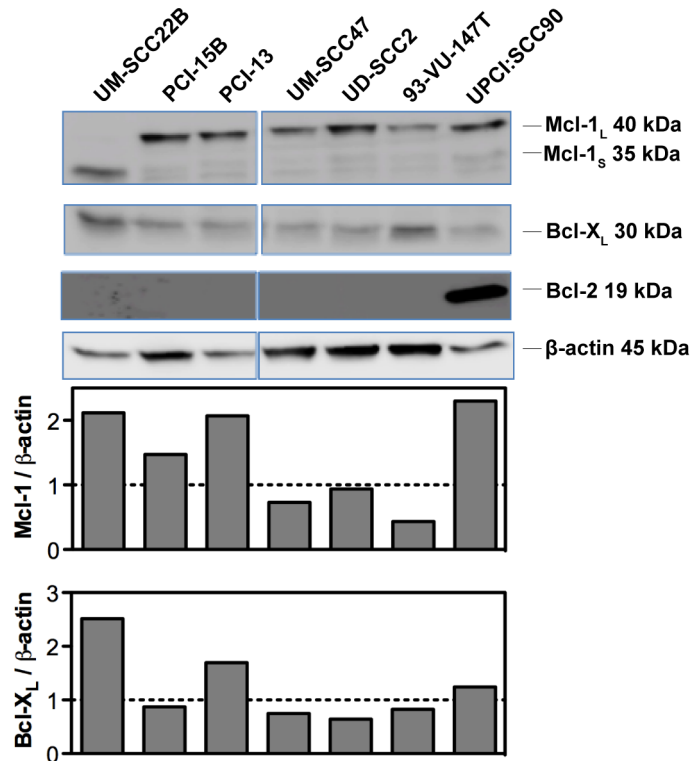


Figure 2-21 Basal expression of anti-apoptotic Bcl-2 proteins at the protein level

In the meantime, the efficacy of meayamycin B against the seven HNSCC cell lines was revisited. Based on their responses to the compound, they fell into two sub-groups; PCI-13, PCI-15B, UM-SCC22B and UPCI:SCC90 were nearly eradicated, while UM-SCC47, UD-SCC2, and 93-VU-147T stopped growing upon meayamycin B exposure at sub- to low-nanomolar concentrations (Figure 2-22). With the exception of UPCI:SCC90, all meayamycin B-responsive cell lines were HPV16-negative, indicating that HPV16 might desensitize cells to meayamycin B. In summary, HPV16-negative, Mcl-1-abundant HNSCC cells were more responsive to meayamycin B.

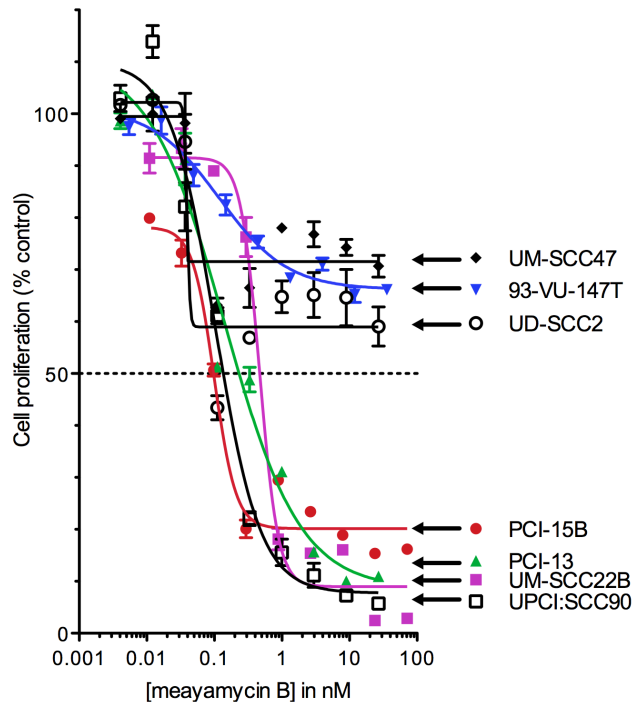


Figure 2-22 Anti-proliferative activity of meayamycin B in HNSCC cell lines

2.3.2.3 Regulation of the splicing of Mcl-1 pre-mRNA

Mcl-1 pre-mRNA is spliced into antiapoptotic Mcl-1_L (solid line; Figure 2-10A) and proapoptotic Mcl-1_S (dotted line). We exposed the cells to meayamycin B either at 3 nM for various periods (1, 9, and 24 h) or for 9 h at various doses (0.03, 0.3, and 3 nM). At the mRNA level, meayamycin B up-regulated Mcl-1_S and down-regulated Mcl-1_L in a dose- and time-dependent manner in all tested HNSCC cell lines (Figure 2-23A and B). This reciprocal change of the two isoforms was detectable at 9 h with 0.3 nM or 1 h with 3 nM meayamycin B treatments and peaked within 9 h of 3 nM meayamycin B exposure. Meayamycin B did not generate other splicing variants of *MCL1* as evidenced by results from the RT-PCR for an amplicon (see Table 2-3 for sequences) spanning all three exons of *MCL1*.

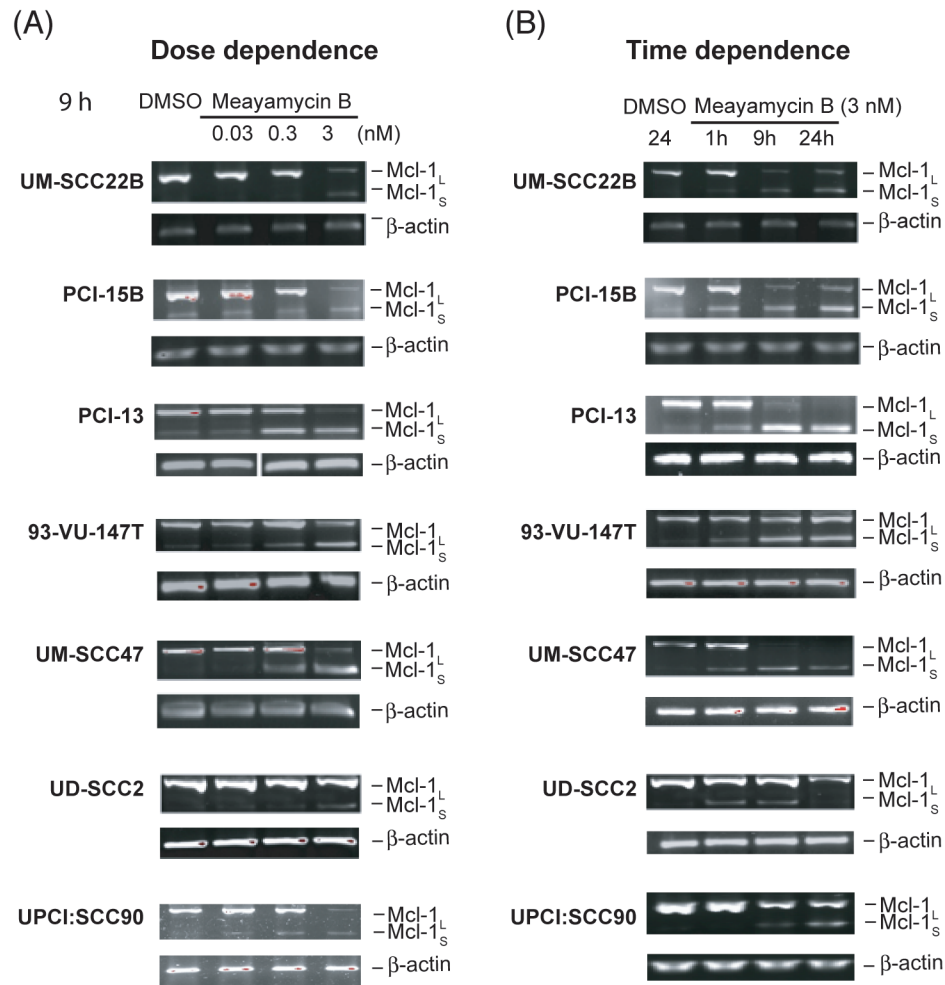


Figure 2-23 RT-PCR analysis of the alteration of Mcl-1 alternative splicing

At the protein level, we observed the same alteration of Mcl-1 splicing by meayamycin B in six of the seven HNSCC cell lines (Figure 2-24); in UM-SCC22B, RT-PCR showed a switch of Mcl-1 alternative splicing, but Western blotting showed only a dominant Mcl-1_S regardless the meayamycin B exposure. This observation indicates that Mcl-1 expression may be regulated at other levels, such as post-translational modifications, that are specific for this cell line.

Also, in comparison to a partial obliteration of Mcl-1_L caused by single-agent meayamycin B, the cells exposed to the combination for the same period (9 h in PCI-15B) completely lost both variants of Mcl-1, demonstrating the onset of apoptotic cell death (Figure 2-25).

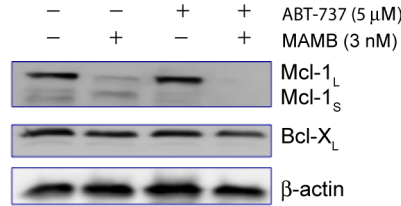


Figure 2-25 Enhanced Mcl-1 elimination by meayamycin B and ABT-737 combination

Meayamycin B also inhibited the constitutive splicing of Mcl-1 in UM-SCC22B, PCI-15B, PCI-13, and UM-SCC47 cell lines, as manifested by the accumulation of transcripts without exon 1 (Figure 2-26) in cytoplasm. These are partially spliced pre-mRNA containing the two introns. This observation is consistent with previous report in other cancer cell models.^{100, 195} The full-length pre-mRNA was not detected in any of these cell lines, indicating the incapability of this RNA species to be transported out of nucleus.

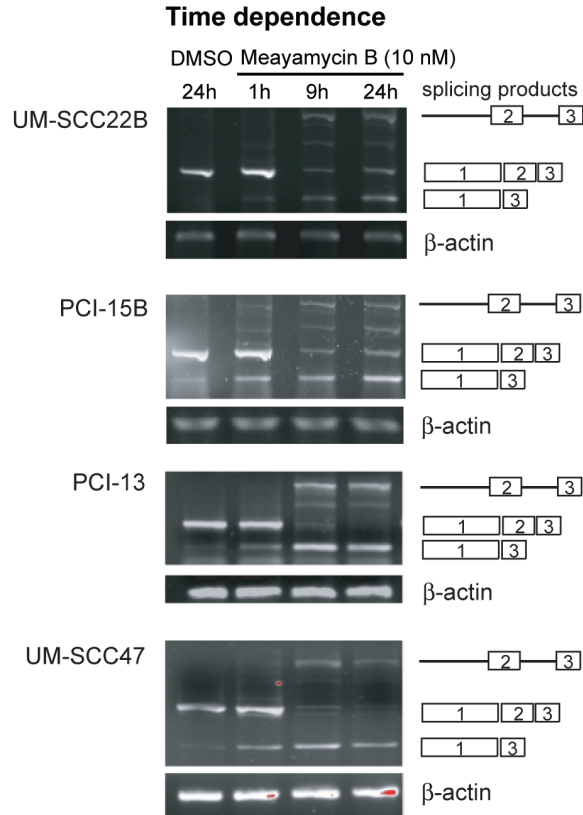


Figure 2-26 Meayamycin B inhibits constitutive splicing Mcl-1

In parallel, we also examined *BCL-X*, which is also prone to regulation at the pre-mRNA splicing level in response to anticancer drugs, producing enhanced levels of the proapoptotic Bcl-X_s.²⁰³ As shown in Figure 2-27, the splicing of *BCL-X* did not change when the cells were incubated with 3 nM meayamycin B for up to 24 h, in agreement with our observation in NSCLC.¹⁹⁵

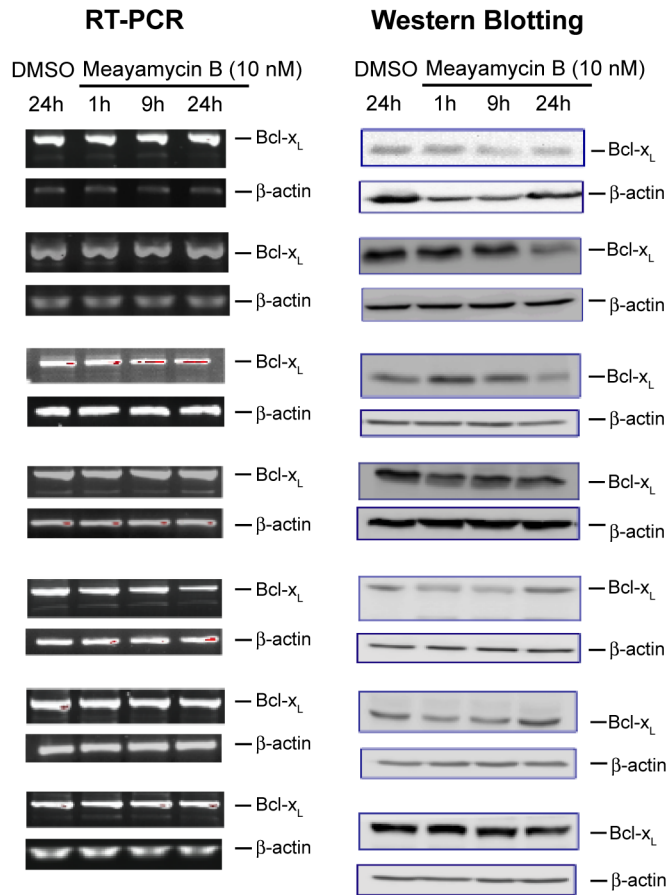


Figure 2-27 Meayamycin B does not regulate Bcl-x alternative splicing

2.3.2.4 Cell type-dependent inhibition of HPV-16 E6 splicing

During the splicing process, inclusion or exclusion of intron 1 of *E6* produces E6 or E6* splicing variant, respectively (Figure 2-16). We assessed the levels of E6 and E7 mRNA in meayamycin B- or DMSO-treated HPV16-positive HNSCC cell lines. Figures 2-28A and B show that the full-length transcript was dominant for *E6* in the DMSO-treated cells. In meayamycin B-treated UM-SCC47, 93-VU-147T, and UPCI:SCC90 cells, E6 mRNA increased and E6* mRNA decreased in a dose- and time-dependent manner. The inhibition was observed as early as 1 h of meayamycin B-exposure as demonstrated in UPCI:SCC90 cells (Figure 2-28C). However, this alteration was not as prominent in cell lines constitutively expressing lower levels of E6*, such

as UD-SCC2 cells. Due to the unavailability of HPV16 E6 antibody, we did not examine the changes of splicing of E6 at the protein level. In all HPV16-positive cell lines, the E7 mRNA level was unaffected, although E6 and E7 genes are co-transcribed.²⁰⁴

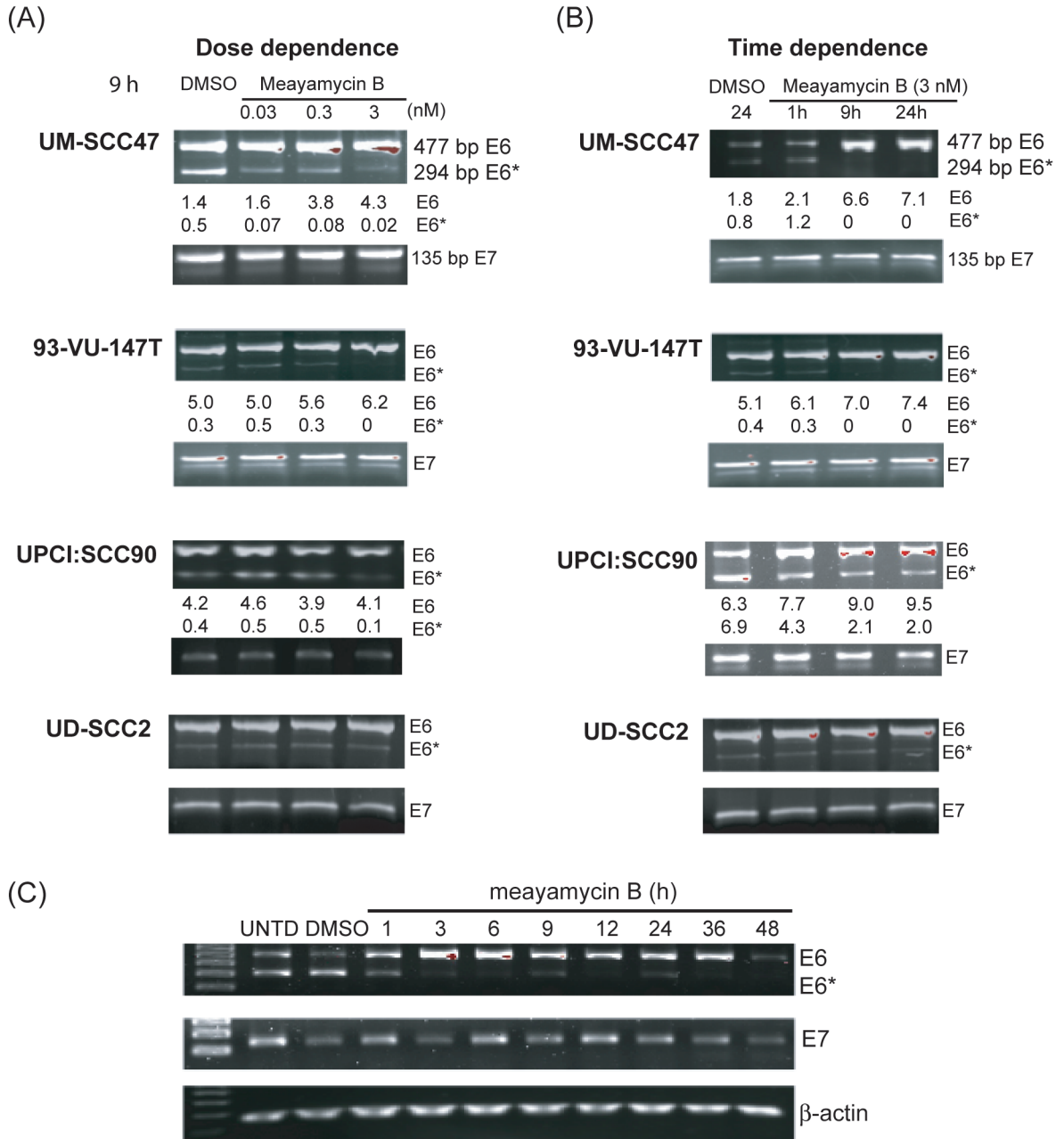


Figure 2-28 Meayamycin B regulates HPV16 E6/E7 splicing

2.3.2.5 SF3B1 inhibition by siRNA and meayamycin B

Subsequently, we asked whether SF3B1 regulates the splicing of HPV16 E6 and Mcl-1. To answer this question, we decided to examine the splicing regulation of HPV16 E6 and Mcl-1 by SF3B1 knockdown and meayamycin B treatment, individually or in combination. Since none of these patient-derived HNSCC cell lines had been subjected to gene delivery, we used HeLa cells to test the RNAi protocol. At 48 h and 72 h post siRNA transfection, HeLa cells were directly subjected to RNA extraction for the detection of Mcl-1 alternative splicing pattern using RT-PCR. As shown in Figure 2-29, SF3B1-siRNA delivery remarkably switched the dominant Mcl-1 variant from Mcl-1_L to Mcl-1_S, indicating SF3B1 is involved in the alternative splicing of Mcl-1 in HeLa cells. This initial observation, in consistent with the literature, indicated the efficiency of the transfection system.¹²³

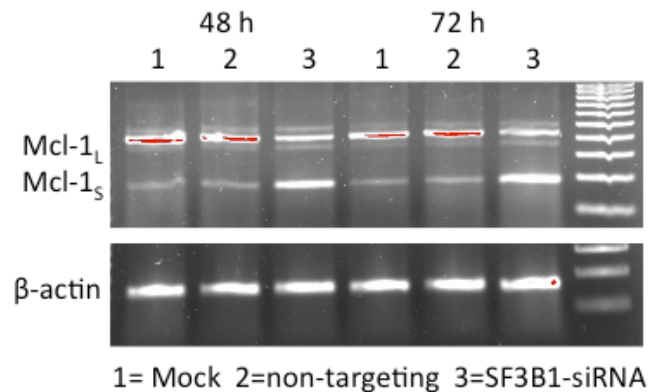


Figure 2-29 SF3B1 knockdown switches the pattern of Mcl-1 alternative splicing

Then, we knocked down SF3B1 in HPV16-positive UM-SCC47 and 93-VU-147T cell lines. These two cell lines bear distinct splicing patterns of E6; UM-SCC47 expresses comparable levels of E6 and E6* while 93-VU-147T cells mainly express E6 (Figure 2-28). In

all cases, cells were collected at 48 h post transfection because Mcl-1 was regulated similarly at 48 h and 72 h of SF3B1 knockdown in HeLa cells (Figure 2-29). In addition, the deletion of SF3B1 caused significant cell death at 48 h post transfection, indicating an effective SF3B1 knockdown. Figure 2-30 shows that SF3B1-siRNA effectively eliminated a majority of SF3B1 protein in both cell lines.

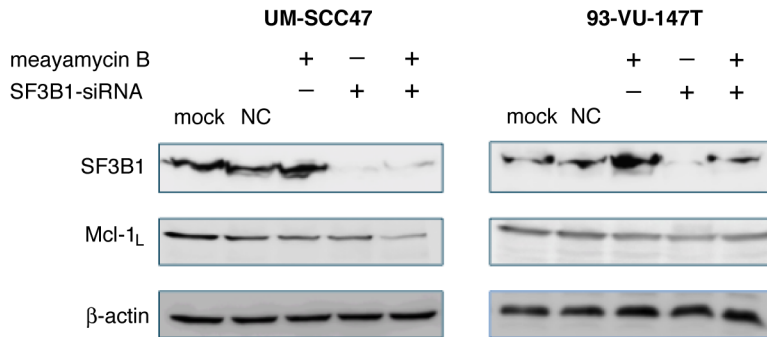


Figure 2-30 SF3B1 knockdown in UM-SCC47 and 93-VU-147T

Figure 2-31 displays the effect of SF3B1 knockdown and meayamycin B, as single treatment or in combination, on the splicing of E6 and Mcl-1. RT-PCR was used to examine the relative abundance of each splice variant of E6 and Mcl-1. Without SF3B1 deletion, the E6/E6* ratios were 47/53 and 92/8 in UM-SCC47 and 93-VU-147T, respectively. In UM-SCC47, SF3B1 knockdown increased the E6/E6* ratio to 82/18, while non-targeting siRNAs did not alter the ratio. The difference between the two treatments was less evident in 93-VU-147T, probably because of the low basal level of E6*. Analogous to the E6 system, the Mcl-1_L/Mcl-1_S ratios in UM-SCC47 and 93-VU-147T cell lines were decreased by SF3B1 knockdown from 86/14 and 81/19 to 65/35 and 48/52, respectively. These data indicate that SF3B1 is involved in the regulation of the splicing of HPV16 E6 and Mcl-1 in HNSCC cells.

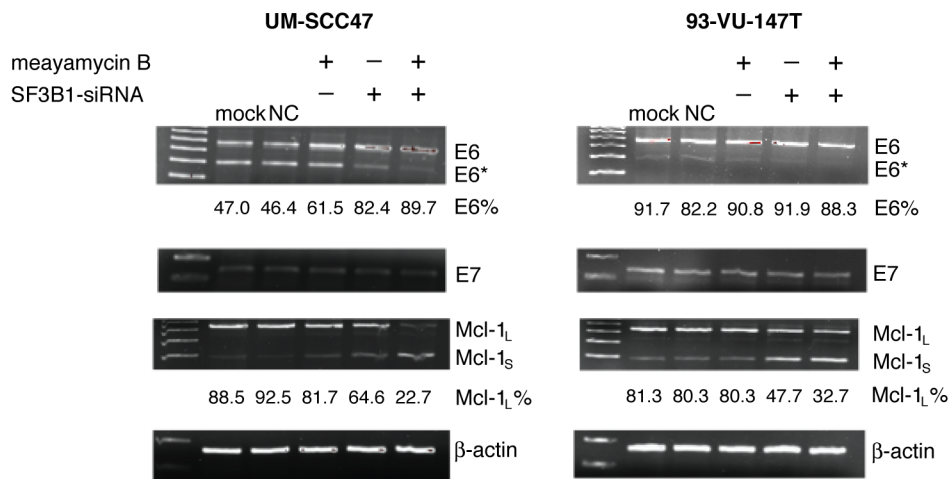


Figure 2-31 SF3B1 controls splicing patterns of HPV16 E6 and Mcl-1

Single-agent meayamycin B caused the splicing alterations to the E6 and Mcl-1 in HPV16-positive HNSCC cells. Hence we asked whether such effect from meayamycin B (Figure 2-22 and 2-28) was solely via SF3B1 inhibition. We exposed UM-SCC47 and 93-VU-147T cells treated with SF3B1 siRNA or non-targeting siRNAs to 1 nM meayamycin B for 3 h. Interestingly, although meayamycin B-exposure alone altered the splicing patterns of E6 and Mcl-1, this combination treatment significantly enhanced the levels of changes caused by SF3B1 knockdown (Figure 2-31). This was especially prominent in UM-SCC47 cells, with the E6/E6* ratios increased from 82/18 to 90/10, and Mcl-1_L/ Mcl-1_S ratios increased from 65/35 to 23/77. The fact that short-term, low-dose meayamycin B-exposure could change the splicing pattern beyond knocking down SF3B1 indicates other unknown mechanisms of meayamycin B exist, besides SF3B1-inhibition. In addition, effective siRNA knockdown requires 24–48 h depending on the targets, while small-molecule inhibitors quickly hits the proteins. Furthermore, for protein targets such as SF3B1 that extensively interact with RNAs and proteins, the differential effects

of siRNA knockdown and small-molecule inhibitors must be considered when examining the results. An siRNA eliminates the entire entity of the target, which in turn abruptly any interactions the target participates in. In contrast, a small-molecule inhibitor might inhibit a subset of the functions of the target with minimum disturbance to the protein scaffold crucial for RNA-protein and protein-protein interactions.¹⁶⁶

2.3.3 Discussion

More than 90% of human genes undergo alternative splicing to generate multiple mRNA variants in a tissue-specific manner.¹⁷ The corresponding protein isoforms have different, even antagonistic, properties. Their deregulation has been implicated in various disease states, including cancer.¹⁸ Therefore, alternative splicing represents a promising molecular therapeutic target. This study in seven HNSCC cell lines revealed that meayamycin B synergized with ABT-737 to quickly trigger Bax/Bak-mediated apoptosis. Meayamycin B regulated alternative splicing of Mcl-1, increasing proapoptotic Mcl-1_S and decreasing antiapoptotic Mcl-1_L. The data from certain cell lines also indicated meayamycin B also inhibited constitutive splicing of Mcl-1 and E6, with partially spliced Mcl-1 leaked into cytoplasm. Interestingly, meayamycin B treatment can further enhance the extent of splicing regulation of E6 and Mcl-1 caused by SF3B1 knockdown, demonstrating the existence of other splicing regulatory mechanisms by meayamycin B.

The regulation of E6 splicing awaits full characterization. U1-binding *cis*-acting elements have been identified in the HPV16 genome.²⁰⁵ Our data demonstrate that U2 snRNP binds to HPV16 genome as well, possibly mediated by subcomplex SF3b. In addition, viruses can modify the expression of splicing factors in the host cells to meet their needs,²⁰⁶ calling for further

studies on the splicing regulations of these tumorigenic viruses in host cells. Distinct responses of HNSCC cell lines against meayamycin B also support the emerging needs to treat HPV16-positive and HPV16-negative HNSCC as two separate diseases.

In HNSCC, SF3B1 inhibitor meayamycin B and SF3B1 knockdown each could switch the splicing of HPV16 E6 and Mcl-1 towards E6 and Mcl-1_s, respectively. These demonstrated that the biogenesis of E6* and Mcl-1_s requires SF3B1 in HNSCC cells. Interestingly, 3-h treatment of meayamycin B significantly enhanced the effect of SF3B1 knockdown. Concerning the short-term effect of meayamycin B exposure, the enhancement of splicing regulation likely resulted from a direct interaction between meayamycin B and its binding targets. Possible explanations include the following: (1) meayamycin B might fit into an interface where SF3B1 interact with its binding partners including SF3B3;¹⁰⁰ (2) meayamycin B has other unknown, independent binding targets. This should not be surprising since FR901464 was suggested to target transmembrane thioredoxin-related protein.⁹⁹

In general, HPV16-positive cells showed higher resistance to meayamycin B or ABT-737. This resistance was completely overcome when the compounds were combined. The resistance might stem from the oncogenic HPV16 proteins such as E6, E7 and E2 that negatively regulate the pro-apoptotic proteins in the host cells,^{188, 207-208} although this needs to be carefully examined in our experimental context.

In four out of seven HNSCC cell lines, partially spliced, but not full-length unspliced, Mcl-1 pre-mRNA detected in RT-PCR using cytoplasmic RNA extracts. Mammalian cells possess stringent RNA surveillance system, with non-sense-mediated RNA decay (NMD) as the main pathway. NMD prohibits the export and translation of such misprocessed RNA species. It remains unknown why these partially spliced pre-mRNAs were only detected in certain cell

lines. Since pre-mRNA alternative splicing and NMD pathway are closely coordinated,¹⁰⁴ it would be interesting to investigate how SF3b inhibitors might impact the NMD machinery-mediated RNA surveillance at a global scope.

A myriad of strategies employ genetic and pharmacologic approaches for targeting Mcl-1.²⁰⁹ Since Mcl-1 is alternatively spliced into isoforms with antagonistic functions, targeting alternative splicing is advantageous; with the obliteration of antiapoptotic Mcl-1_L, proapoptotic Mcl-1_S increases and selectively neutralizes existing Mcl-1_L. Here we report the first small molecule that modulates the splicing of Mcl-1 in HNSCC. Combined with our previous report in NSCLC, these studies demonstrate a positive correlation between the Mcl-1 level and the efficacy of SF3b inhibitors, highlighting their potential usage for cancers overexpressing Mcl-1.

Meayamycin B and other FR901464 analogs presumably target SF3B1, which was recently reported to regulate Bcl-x alternative splicing in response to ceramide signaling.⁶⁴ Interestingly, Bcl-x, also abundantly expressed in HNSCC, was not altered by meayamycin B. This was consistent with our previous finding in NSCLC and Webb's finding in pediatric rhabdomyosarcoma Rh18 cells.^{81, 195} The lack of changes in the Bcl-x system implies that SF3B1 might be a splicing factor for Bcl-x that is exclusively involved in the ceramide-mediated splicing regulation. Importantly, the unresponsiveness of Bcl-x with extended exposure (48-h data not shown) indicates that the rapid modulation of Mcl-1 splicing was the main contributor to the rapid apoptosis we observed from the meayamycin B and ABT-737 combination.

2.3.4 Conclusion

In summary, we demonstrated that the combination of SF3B1 inhibitor meayamycin B and Bcl-x/Bcl-2 inhibitor ABT-737 triggered apoptosis in HNSCC cell lines. Single-agent meayamycin B

elicited stronger toxicity in Mcl-1-abundant than in Mcl-1-deficient HNSCC, representing a potential therapy for Mcl-1-addicted cancer. In addition, we showed that *HPV E6* as the first viral gene known to be regulated by SF3b inhibitors at the splicing level.

2.3.5 Experimental

Cell lines. Four HPV16-positive HNSCC cell lines, UD-SSC2 (gift from Professor Henning Bier, University of Dusseldorf, Germany),²¹⁰ UM-SCC47 (gift from Professor Thomas Carey, University of Michigan),²¹¹⁻²¹² 93-VU-147T (gift from Professor Hans Joenje, VU Medical Center, The Netherlands),²¹³ UPCI:SCC90,²¹⁴ and the HPV16-negative HNSCC cell lines PCI-13 and PCI-15B (gifts from Professor Theresa Whiteside, University of Pittsburgh Cancer Institute)²¹⁵ and UM-SCC22B (gift from Professor Thomas Carey, University of Michigan)²¹⁶ were used throughout the study. *Bax*^{-/-}/*Bak*^{-/-} and wild-type mouse embryonic fibroblasts (MEFs) were gifts from the late Professor Korsmeyer (Harvard Medical School) through Professor Scott Oakes (University of California, San Francisco).²¹⁷ 93-VU-147T cell line was cultured in Dulbecco's Modified Eagle's Medium /F12 medium (Gibco, New York), and other cell lines were cultured in DMEM (Gibco, New York). All cell culture media were supplemented with 10% fetal bovine serum, 1% penicillin/ streptomycin, and 2% L-glutamine. Cells were maintained at 37 °C in air containing 5% CO₂.

Pharmacodynamic interaction analysis. The cells were exposed to meayamycin B and ABT-737 at various concentrations, either as single agents or in concomitant combinations (at a constant 3:5000 ratio) for 72 h until cell viability was monitored using the MTS (([3-(4,5-dimethylthiazol-2-yl)-5-(3-carboxymethoxyphenyl)-2-(4-sulfophenyl)-2H-tetrazolium, inner salt])) method. Bliss expected effect (E_{EXP} , expressed as cell viability) from the combination of

meayamycin B and ABT-737 were calculated using $E_{EXP}=E_A+E_B-E_A * E_B$, where E_A and E_B are effects from each single-agent treatment at a given dose. The difference between the Bliss expected and the observed effect (E_{OBS}) of the combination is $\Delta E = E_{EXP} - E_{OBS}$. ΔE scores were summed across the dose range to generate a Bliss sum. Bliss sum = 0 indicates that the combination treatment is additive (as expected for independent pathway effects); Bliss sum > 0 indicates an activity greater than additive (synergy); and Bliss sum < 0 indicates the combination is less than additive (antagonism).

Annexin V - fluorescein isothiocyanate (FITC) and propidium iodide (PI) staining.

In all cases, cells were treated with 3 nM meayamycin B and 5 μ M ABT-737 (alone or in combination), an equal volume of DMSO as a negative control, or 133 μ M cisplatin as a positive control. Cells were treated for 5 h and stained with Annexin V-FITC (BD Pharmingen, CA) and PI (BD Pharmingen, CA) following the manufacturer's protocol. The cells were then analyzed by flow cytometry using a CyAn cytometer (Beckman Coulter, CA). Data were analyzed using Summit V4.3 software.

Caspase 3/7 activity assays. The cells, seeded at 1.0×10^4 per well in triplicate in white solid-bottom 96-well plates, were treated with 3 nM meayamycin B and 5 μ M ABT-737 (alone or in combination) or an equal volume of DMSO as a negative control for 9 h. Then, caspase 3/7 activity was monitored using Caspase-Glo® 3/7 reagent (Promega, WI) with a Modulus II Microplate Reader (Promega, WI) following the manufacturers' protocols. The caspase 3/7 activity was expressed as the mean luminescence signal from the compound-treated wells divided by that from vehicle-treated wells.

RNA isolation and RT-PCR. Total RNA was isolated using RNeasy mini kit (QIAGEN, Maryland) and subjected to RT-PCR analysis (1 μ g per reaction) using the SuperScript® II

reverse transcriptase (Invitrogen, New York). The thermocycler program for the HPV-16 E6 and E7, Bcl-x, Mcl-1, and β -actin involved an initial denaturation at 94 °C for 5 min, 30 cycles at 94 °C for 30 sec, 58 °C for 30 sec, 72 °C for 50 sec, and a final elongation at 72 °C for 7 min. The primer sequences are included in Table 2-3. The PCR products were examined on 1.5% agarose gels and imaged by a Molecular Imager Gel Doc™ XR+ (Bio-Rad, CA). For each gel, the relative intensity of the bands was quantified with the Lab Imager software (Bio-Rad, CA).

siRNA transfection. The pre-designed ON-TARGETplus modified siRNA duplexes targeting SF3B1 (020061-13) was obtained from Dharmacon (Dharmacon, MA). HeLa, UM-SCC47 and 93-VU-147T cells were seeded (2.5×10^5) into 35-mm dishes and transfected with 100 nM siRNA using lipofectamine 2000 (Invitrogen, NY) for 48 h before usage. siGENOME Non-Targeting siRNA Pool #2 (Dharmacon, MA) was used as a negative control. Transfection efficiency was evaluated by RT-PCR amplification of the HPV-16 E6, Mcl-1, and β -actin genes as described above.

Western blotting. Cells were harvested in a cell lysis buffer (50 mM Tris-HCl, 150 mM NaCl, 1% Triton X-100, 0.1% SDS, and 1 mM PhCH₂SO₂F) and a cocktail of protease inhibitors (Roche, IN). Total protein (50 μ g) was electrophoresed on a 12% SDS-polyacrylamide gel and transferred to polyvinylidene difluoride membranes (Millipore, MA). Membranes were blocked at room temperature for 1 h with a blocking buffer (5% non-fat dry milk in 10 mM Tris-HCl pH 7.6, 150 mM NaCl, 0.1% Tween-20) and then incubated at 4 °C overnight with anti-SF3B1 (D221-3, MBL), anti-Mcl-1 (5453S), anti-Bcl-2 (2870S), anti- β -actin (4970S) (Cell signaling technology, MA), or anti-Bcl-x_L/Bcl-x_S (sc-634) (Santa Cruz, CA) followed by 1-h incubation with a horseradish peroxidase (HRP)-conjugated anti-rabbit IgG (7074S) (Cell signaling technology, MA) secondary antibody. Blots were developed with ECL Plus reagents

(PerkinElmer Life and Analytical Science, MA) and quantified using an Image Gauge Version 4.0 (FUJIFILM, NJ).

Statistics. Data analysis and graph plotting were carried out using a GraphPad Prism 5.0c for Mac (GraphPad Software). All of the data were presented as mean \pm standard deviation and were analyzed by Student's t test or ANOVA followed by the Tukey's multiple comparison; the significance level for all analyses was 5%.

Table 2-3 Primer sequences for RT-PCR experiments in HNSCC system

Genes	Sequences
Bcl-x	Bcl-xF: 5'- GAG GCA GGC GAC GAG TTT GAA -3'
	Bcl-xR: 5'- TGG GAG TTG AGA GTG GAT GGT -3'
Mcl-1	Mcl-1F: 5'- ATC TCT CGG TAC CTT CGG GAG C -3'
	Mcl-1R: 5'- CCT GAT GCC ACC TTC TAG GTC C -3'
	Mcl-2F: 5'- ATG TTT GGC CTC AAA AGA AAC GCG -3'
	Mcl-2R: 5'- GGC TAT CTT ATT AGA TAT GCC AA-3'
HPV16 E6	Forward: 5'- ATG CAC CAA AAG AGA ACT GC -3'
	Reverse: 5'- TTA CAG CTG GGT TTC TCT AC -3'
HPV16 E7	Forward: 5'- GTA ACC TTT TGT TGC AAG TGT GAC T -3'
	Reverse: 5'- TTA TGG TTT CTG AGA ACA GAT GG -3'
β -actin	Forward: 5'- GCA CCA CAC CTT CTA CAT GAG C -3'
	Reverse: 5'- TAG CAC AGC CTG GAT AGC AAC G -3'

2.4 MEAYAMYCIN B IN OTHER IN VITRO CELL MODELS

2.4.1 Cisplatin-resistant ovarian cancer cells

cis-diamminedichloroplatinum (II) (cisplatin) is an effective drug in the treatment of a variety of human tumors, including ovarian carcinoma. Unfortunately, a development of resistance is a major obstacle to the success of platinum-based chemotherapy, with fewer than 25% of the women diagnosed with advanced ovarian cancer showing progression-free survival after 4 years.²¹⁸ The cellular mechanisms of cisplatin-resistance are multifactorial, hence a longstanding challenge to circumvent in anticancer therapy.²¹⁹

The remarkable potency of the combination of meayamycin B and Bcl-x/bcl-2 inhibitor has been verified in NSCLC and HNSCC *in vitro* models. However, it is unclear whether it can overcome acquired drug resistance, such as the notorious cisplatin-resistance in ovarian cancer. To answer this question, we planned to determine whether meayamycin B (Figure 2-9), as single agent or in combination with ABT-737 (Figure 2-9), could enhance the efficacy of cisplatin, or overcome acquired cisplatin-resistance, in ovarian cancer models.

Cisplatin-resistant human ovarian carcinoma 2008C cell line was generated by repeated selection of the cisplatin-sensitive ovarian cancer cells 2008 with 1 μ M cisplatin.²²⁰ The resulted cells, named 2008C, exhibited 2.7-fold higher resistance to cisplatin compared with the parent cell line 2008. As shown in Figure 2-32A, single-agent cisplatin exhibited GI₅₀ values at 1.0 μ M and 3.1 μ M in 2008 and 2008C, respectively, consistent with literature.²²⁰ Single-agent meayamycin B caused ~50% inhibition of cell growth in 2008, but was inactive in 2008C. When combined simultaneously, meayamycin B and cisplatin did not affect each other in either cell

lines. These data demonstrated that cisplatin-resistant ovarian cancer cells are likely also resistant to meayamycin B and SF3b inhibition might not overcome cisplatin resistance.

Subsequently, we examined the interaction of meayamycin B and ABT-737 in these ovarian cancer cell lines. Concerning the multifactorial resistance mechanism and the specific activation of apoptosis pathway by the combination, we envisioned that 2008C cells would be less sensitive than 2008.²¹⁹ Indeed, 2008C was invariably more resistant to all treatments than 2008. Nonetheless, the combination could cause 100% cell death in 2008 and 2008C with GI₅₀ values at 0.077 μ M and 0.94 μ M, respectively (Figure 2-32B). Therefore, meayamycin B and ABT-737 combination could overcome cisplatin resistance, with minor compromise in the efficacy.

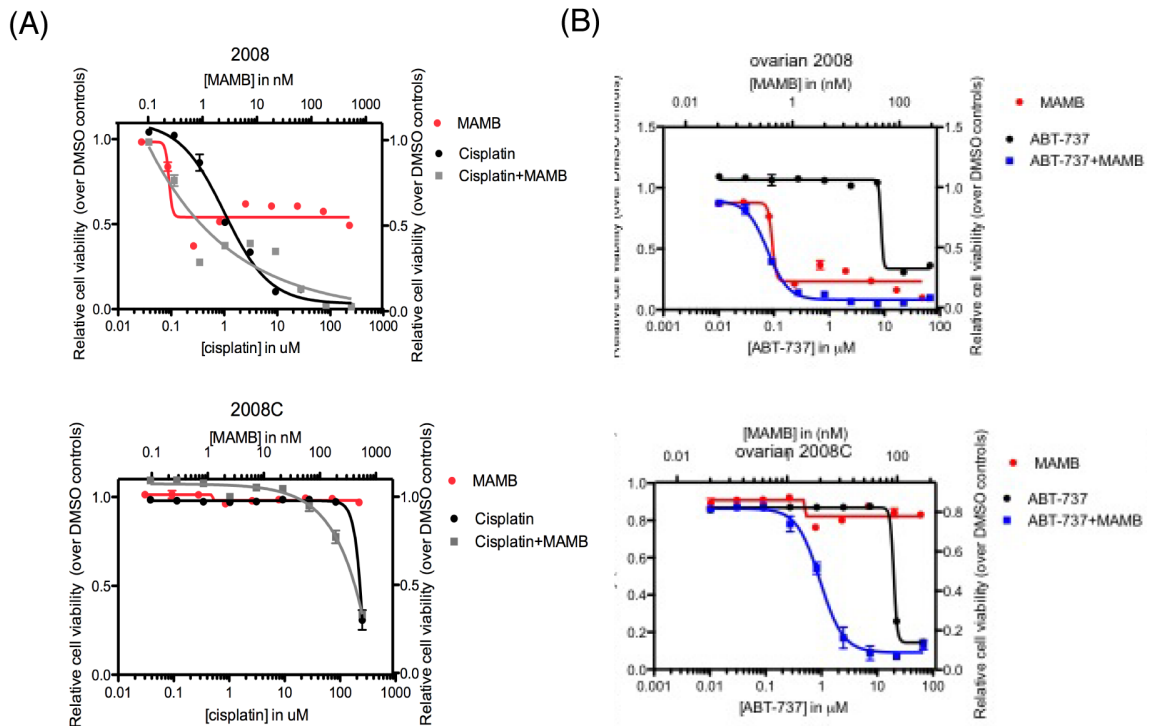


Figure 2-32 Meayamycin B and ABT-737 combination overcomes cisplatin resistance

2.4.2 Cervical cancer model cell lines

Besides in a subgroup of HNSCC, HPV DNA is detected in over 90% of cervical cancer world wide, ~60% and ~15% of which are HPV16 and HPV18, respectively.²²¹ In addition to this common molecular feature, cervical cancer and HNSCC share the risk factors that are common for sexually transmitted diseases.²²² Hence, it would be interesting to examine the efficacy of meayamycin B, as single agent or in combination with ABT-737, in cervical tumor cell lines.

To this end, we chose Caski and Siha, which have ~600 and 1–2 copies of genomically integrated HPV16 DNA, respectively.²²³ Figure 2-33A shows the caspase 3/7 activity in each cell line exposed to each single agent (10 nM meayamycin B or 5 μ M ABT-737) or the combination, for 9 h or 24 h. Within 9 h, the combination significantly induced the activity of caspase 3/7, while single agents led to negligible to minor increase. Of note, by 24 h, the cells were almost completely eliminated in the combination-treated samples. The GI₅₀ values for 72-h MTS assays indicated single agents or the combination was 2-fold more active in Caski than in Siha (Figure 2-33B). Although Caski harbors notably more copies of HPV16 than Siha, it is unknown how many of these copies are transcriptionally competent. Such differential responses to meayamycin B were also observed in HPV16 positive and HPV16 negative HNSCC cell lines. The functions of high-risk HPV oncogenic genes, especially those from HPV16, have been better understood in cervical cancer. Screening and characterizing more cervical cancer cell lines might provide us insights into the molecular mechanism underlying this differential meayamycin B-sensitivity.

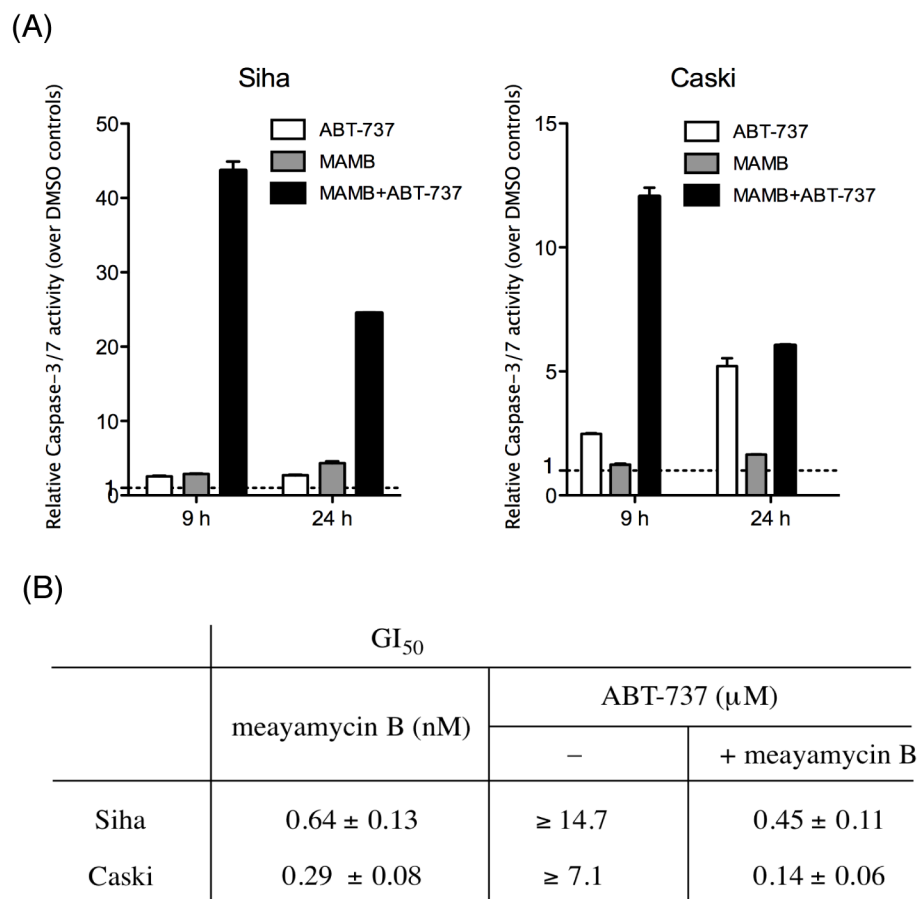


Figure 2-33 Antiproliferative and caspase 3/7 assays in cervical cancer cells

2.4.3 Experimental

Cell lines. Cisplatin sensitive 2008 and resistant 2008C cells are gifts from Dr. Van Houton (University of Pittsburgh Cancer Institute). Siha and Caski (gifts from Dr. Robert Ferris) were maintained in Dulbecco's Modified Eagle's Medium (Gibco, NY). Cells were maintained at 37 °C in air containing 5% CO₂.

Caspase 3/7 activity assays. The cells, seeded at 1.0×10^4 per well in triplicate in white solid-bottom 96-well plates, were treated with 3 nM meayamycin B and 5 μM ABT-737 (alone or in combination) or an equal volume of DMSO as a negative control for 9 h and 24 h. Then,

caspase 3/7 activity was monitored using Caspase-Glo® 3/7 reagent (Promega, WI) with a Modulus II Microplate Reader (Promega, WI) following the manufacturers' protocols. The caspase 3/7 activity was expressed as the mean luminescence signal from the compound-treated wells divided by that from vehicle-treated wells.

Cell proliferation assay. Cell proliferation was evaluated using the MTS dye reduction assay with PMS as the electron acceptor assay performed in triplicate. To this end, cells were seeded in 96-well plates at 6×10^3 cells per well and incubated for 24 h at 37 °C. Cells were then exposed to various concentrations (serial three-fold dilutions) of the meayamycin B and ABT-737 or cisplatin, as single agents or in 1:500 constant ratio, for 72 h at 37 °C. An MTS solution (20 µL of MTS: PMS at 20:1) was added, and cells were incubated for 2 h at 37 °C before the absorption signals were measured at 490 and 650 nm. Growth inhibition was calculated as defined by the National Cancer Institute [$GI_{50} = 100 \times (T - T_0) / (C - T_0)$; T_0 = cell density at time zero; T = cell density of the test well after period of exposure to test compound; C = cell density of the vehicle treated].

Statistics. Data analysis and graph plotting were carried out using a GraphPad Prism 5.0c for Mac (GraphPad Software). All of the data were presented as mean \pm standard deviation and were analyzed by Student's t test or ANOVA followed by the Tukey's multiple comparison; the significance level for all analyses was 5%.

3.0 ACTIVATION OF SV40 PROMOTER AND INHIBITION OF LUCIFERASE BY TMC-205 AND ANALOGS

This section is in part taken from the manuscript “Gao, Y., Osman, S., and Koide, K. Total synthesis and biological studies of TMC-205 and analogs as anticancer agents and activators of SV40 promoter”, submitted to *ACS Med. Chem. Lett.*

3.1 RESEARCH PLAN

TMC-205, an indole derivative isolated from an unidentified fungal strain TC 1630. The natural product was cytotoxic against various human cancer cell lines with GI₅₀ values in the range of 52–203 μM.²²⁴ TMC-205 showed light- and air- sensitivity, preventing thorough exploitation of its potential as cancer therapeutics. Being isolated as a transcription activator, TMC-205 activated the expression of Simian virus 40 (SV40) promoter via an unknown mechanism. Other natural products discovered by this route include azelaic bishydroxamic acid,²²⁵ trichostatin A,²²⁶ FR901228,²²⁷ herboxidiene^{87, 121} and FR901464.⁸²⁻⁸⁴ Mechanistic studies using these small molecules demonstrated that inhibitions of histone deacetylases and spliceosome are viable cancer therapeutic approaches.^{100, 228-232}

To fully exploit the potential of TMC-205 as an antiproliferative agent against cancer, herein we performed the synthesis of TMC-205 and its light- and air-stable analogs, which were subsequently applied in biological activity evaluations. Two activities examined include SV40 promoter-activation and direct luciferase binding.²³³⁻²³⁶

TMC-205 experiences photosensitized singlet oxygen-mediated degradation. Its trifluoro-substituted stable analogue maintains the activity to inhibit cell growth and activate SV40 promoter-driven luciferase expression, and also inhibit firefly luciferase. These data prime for further development of these novel anticancer agents with multifactorial mode of action.

3.2 RESULTS AND DISCUSSION

This project was completed in collaboration with Dr. Sami Osman, who accomplished the synthesis of TMC-205 and its analogs. The anti-proliferative activities of these compounds were obtained in HCT-116 cell line (Table 3-1). He also discovered that TMC-205 selectively reacts with singlet oxygen, which affords its sensitivity to air and light under laboratory ambient conditions.

The biological studies presented herein were mainly carried out using TMC-205 and its stable analogs including **12** and **14** that are 2–8 fold more potent than TMC-205 against HCT-116 (Table 3-1).

Table 3-1 Antiproliferative activity of TMC-205 and its analogs against HCT-116

Analog	R ¹	R ²	R ³	GI ₅₀ (μM)
1	CO ₂ H	H		68 ± 3
10	H	H		147 ± 10
11	CH ₂ OH	H		79 ± 15
12	C(O)CF ₃	H		39 ± 12
13	C(O)CF ₃	H		14 ± 4
14	C(O)CF ₃	H		8 ± 6
15	C(O)CF ₃	H		>500
16	CO ₂ H	H		>500
17	C(O)CF ₃	CH ₃		>500

3.2.1 Viral promoter activation

Previously, TMC-205 was found to activate a luciferase gene driven by an SV40 promoter in an SV40 enhancer-dependent manner using the pGL3-control® (Promega).²²⁴ The activation of the luciferase gene driven by the SV40 promoter without the SV40 enhancer (pGL3-promoter®, Promega) was negligible in the presence of TMC-205 (Figure 3-1).

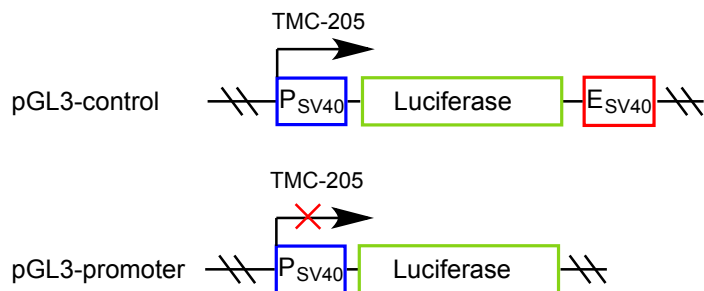


Figure 3-1 SV40 enhancer-dependent activation of SV40 promoter

With 24-h exposure, TMC-205 and **12** activated SV40 promoter in the presence of enhancer in HeLa cells stably transfected with pGL3-control (Figure 3-2A and B). Interestingly, in our hands, pGL3-promoter could be activated by TMC-205 as well (Figure 3-2C, transient transfection) – meaning the gene activation was independent of SV40 enhancer.

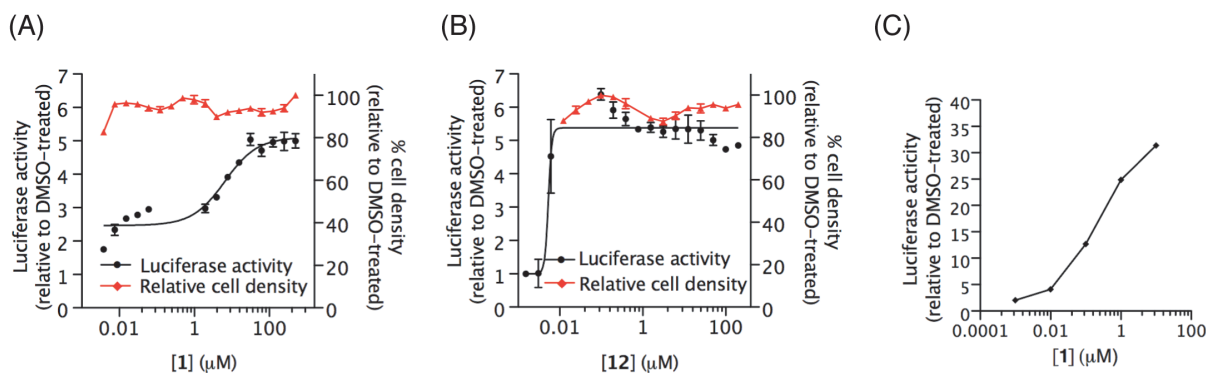


Figure 3-2 TMC-205 activates SV40 promoter independent of enhancer

Analogs **12** and **14** also activated the expression of SV40:*luciferase* without inhibiting cell growth (Figure 3-3A and B). It is noteworthy that within the 24-h time frame before cell growth can be influenced, analogue **12** activated gene transcription in a nanomolar range (Figure 3-2B); such a property is critical for gain-of-function techniques used in live cell models.

Previously, it was discovered that singlet oxygen reacts with TMC-205. Therefore, resveratrol was also examined for SV40 promoter activation because of its selective reactivity to singlet oxygen. Interestingly, resveratrol also activated SV40 promoter in pGL3-promoter in a dose-dependent manner (Figure 3-3C).

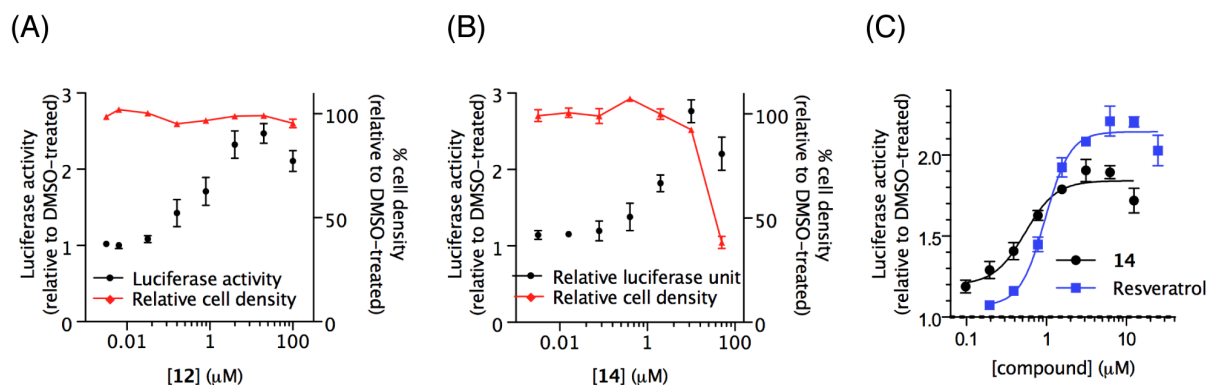


Figure 3-3 Compounds 12, 14 and resveratrol activate SV40 promoter

3.2.2 Luciferase inhibition

Firefly luciferase is the reporter enzyme in the vectors used both in the original isolation study and our current SAR studies for TMC-205 and its analogs. Recently, it was discovered that luciferase catalyzed luminescence-emission is prone to perturbation by certain heterocyclic small molecules either through luciferase binding or compound-specific luminescence absorbance or scattering.²³³⁻²³⁴ In the case of direct binding, these small molecules inhibit luciferase, competitively or non-competitively with D-luciferin and/or ATP. Concerns arise when the tested compounds that are active against luciferase might also be active against a target of interest. For example, high throughput screenings for enzymes, such as kinases that are also ATP-dependent, would inevitably be susceptible to luciferase inhibitory activity of the hits.²³⁷⁻²³⁸ For the current

study, direct attenuation of luminescence was not a concern for two reasons: first, as shown in Figure 3-4, analogue **12** absorbs UV light with a peak at 290 nm, with no absorption in the range of visible light (400–700 nm); second, compound-containing cell medium was thoroughly removed for the luciferase reporter assay.

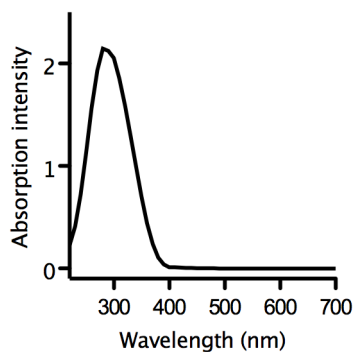


Figure 3-4 Absorption spectra of compound **12**

We decided to examine the interaction between recombinant luciferase and analogue **12**. Resveratrol was applied in parallel as a positive control since it was confirmed to be a non-competitive luciferase inhibitor.²³⁹ Substrate competition assays were carried out by varying concentrations of ATP or D-luciferin to acquire the dose-response curves of luciferase inhibition by **12** and resveratrol. If a test compound antagonizes either of the native ligands, increasing the concentration of this ligand would abolish the inhibition caused by the test compound. As shown in Figure 3-5, varying ATP concentration did not significantly change the IC_{50} values of **12** or resveratrol, which implies that **12** or resveratrol does not antagonize ATP.²⁴⁰ D-luciferin, on the other hand, perturbed the inhibitory capability of **12** in a dose-dependent manner, indicating that **12** might share the same binding pocket with D-luciferin.

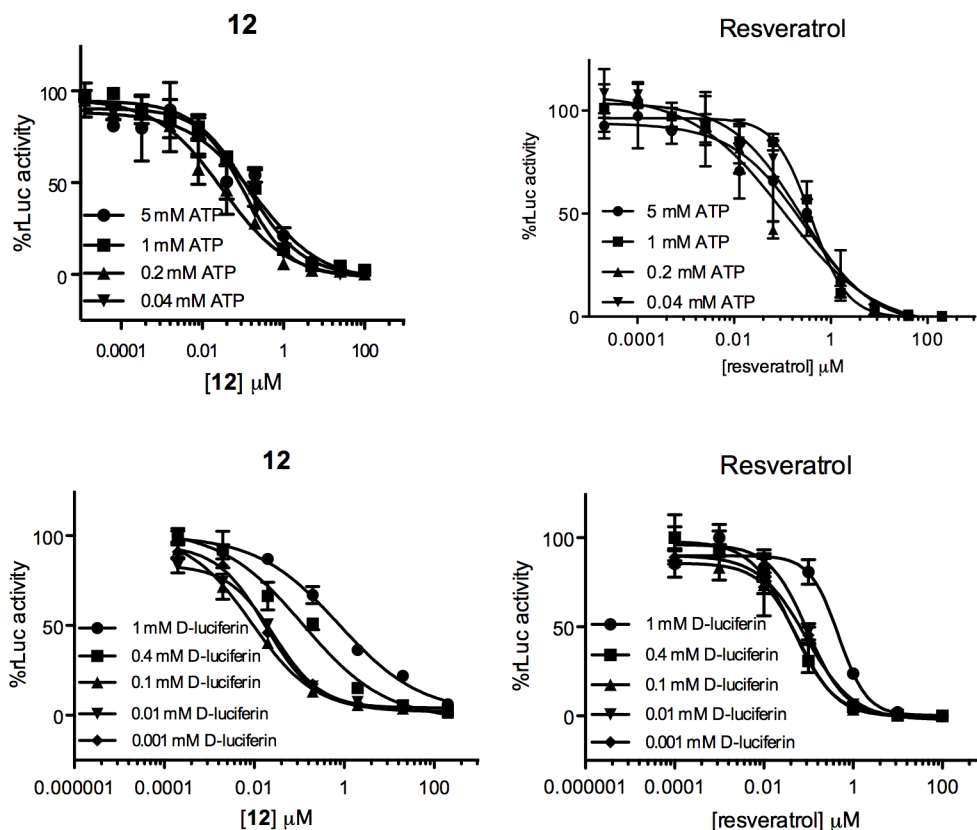


Figure 3-5 Compound **12** and resveratrol non-competitively inhibit luciferase

Based on these data, we speculated that the strong luciferase inhibition would result in an underestimate of expression activation of luciferase by **12**. We set out to examine the expression of luciferase at the mRNA level. To this end, the total RNA extracted from **12**-, resveratrol-, meayamycin-, and DMSO-treated HeLa cells expressing pGL3-promoter was analyzed by RT-PCR for luciferase level (Figure 3-6). Meayamycin was included as a positive control for SV40 promoter activation. In a dose-dependent manner, **12**, resveratrol (RSV), and meayamycin (MAM) exhibited moderate activation of the SV40 promoter. This data demonstrated that **12** and resveratrol share the common activities of luciferase inhibition and SV40 promoter activation, while meayamycin only activates SV40 promoter.

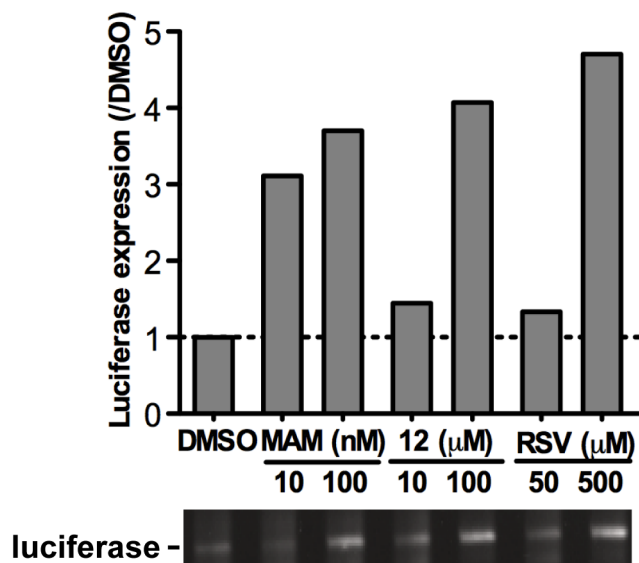


Figure 3-6 Activation of Luciferase expression at the mRNA level

3.3 CONCLUSION

In conclusion, TMC-205 and its stable analogs **12** and **14** activated SV40 promoter in an enhancer-independent manner. Through biochemical assays and RT-PCR, we proved that **12** also exhibited nanomolar binding-affinity for firefly luciferase.

3.4 EXPERIMENTAL

Cells, reagents and plasmids. HeLa cells are gifts from Professors Andreas Vogt and Billy Day (University of Pittsburgh), respectively. HeLa cells were maintained at 37 °C in an atmosphere containing 5% carbon dioxide in Corning cell culture dishes (150 mm) in RPMI cell culture medium containing 10% fetal bovine serum, 1% L-glutamine, and 1% penicillin-streptomycin

solution (Invitrogen). pGL3-control and pGL3-promoter vectors were purchased from Promega (cat# E1741, E1761). GenCarrier-1 was purchased Epoch Biolabs. All synthetic compounds were dissolved in DMSO as stock solutions and stored at -20 °C. For the experiments, aliquots were thawed at room temperature in a dark environment, and diluted solutions were prepared in cell culture medium containing 1% DMSO prior to addition to the cell culture media.

Luciferase reporter assay with TMC-205 and its analogs. All compounds were diluted to 10 mM stock solutions and stored at -20 °C. Diluted solutions in DMSO were prepared immediately before use and administered directly into cell cultures. The final DMSO concentration was 0.5% (v/v), which was demonstrated to be nontoxic for cells. For transfection, HeLa cells were seeded in 35-mm tissue culture dishes in RPMI medium and allowed to reach 70% confluency upon transfection.

For transient transfection, cells were transfected with a pGL3-control or a pGL3-promoter vector and GenCarrier-1 in serum-free medium containing vector and GenCarrier-1 (1 µg and 2 µL per dish). After 48 h of transfection, cells were trypsinized and seeded at a density of approximately 15,000 cells per well in a 96-well plate in RPMI medium (200 µL), and allowed to attach overnight. The cells were then treated with synthetic TMC-205 at the indicated concentrations for 24 h. The cell culture medium was then removed, and cells were rinsed once with phosphate-buffered saline (PBS) before 1 × cell lysis buffer (20 µL) was added to each well. After homogenization for 10 min at room temperature, cell lysates were subjected to luciferase assay reagent (100 µL; Promega) and luminescence was measured immediately on a Spectromax M5 plate reader (Molecular Devices) or Modulus II Microplate Multimode Reader (Turner BioSystems). With the M5 plate reader, white 96-well plates with clear bottom were used. With the Modulus II, white solid-bottomed 96-well plates were used.

For stable transfection, HeLa cells were transfected with a 9:1 w/w pGL3-control or pGL3-promoter and pREP4. Stable transfectants selection, in a medium containing 250 µg/mL of hygromycin B, started 48 h post transfection in the same dish where transfection took place. After 2 weeks of continuous selection, hygromycin B-resistant cells formed colonies, each of which consisted of hundreds of cells. These single cell colonies were amplified and maintained for five passages and assayed for luciferase expression and response to the activation of the SV40 promoter. Thereafter, luciferase-expressing colonies that most strongly responded to the promoter activation were reserved and maintained for another 15 generations prior to being used. Approximately 10,000 cells were seeded in each well of a 96-well plate in an RPMI medium (200 µL) and were allowed to attach overnight. The cells were treated with the compounds at the indicated concentrations for 24 h before luciferase assay analysis was undertaken as mentioned above.

Firefly luciferase inhibition assay. To determine whether ketone **12** competes with ATP or D-luciferin (i.e. competitively inhibits luciferase by direct binding), dose-dependence studies for ketone **12** were carried out with varying concentrations of ATP or D-luciferin for recombinant firefly luciferase (Promega) activity assays. Each assay reaction was performed in white solid-bottom 96 well plates. To each well, the following reagents were added sequentially: ketone **12** or resveratrol (2 µL of stock solution at appropriate concentration), 181 µL luciferase assay buffer (pH 7.5 Tris acetate 50 mM, MgSO₄ 10 mM, pH 8.0 EDTA 2 mM, sodium pyrophosphate 1 µM, DTT 5 mM, and ATP at various concentrations, see below) and recombinant luciferase (1 µL at 1 mg/mL). Then the mixture was incubated at room temperature for 5 min before 16 µL D-luciferin (at appropriate concentration dissolved in MiliQ H₂O) was added. To study the competition between ATP and ketone **12**, the final concentration of D-

luciferin was controlled at 0.4 mM, and various amounts of ATP (0.04–5 mM) were included in the assay buffer. To study the competition between D-luciferin and ketone **12**, ATP was controlled at 1 mM and various amounts of D-luciferin (0.001–1 mM) were added to the assay. For each study, resveratrol (10 mM in DMSO) or ketone **12** (20 mM in DMSO) were diluted in DMSO and directly added to the reaction mixtures. Each treatment was performed in duplicate.

BIBLIOGRAPHY

1. Moore, M. J.; Proudfoot, N. J., Pre-mRNA processing reaches back to transcription and ahead to translation. *Cell* **2009**, *136* (4), 688–700.
2. Wahl, M. C.; Will, C. L.; Luhrmann, R., The spliceosome: design principles of a dynamic RNP machine. *Cell* **2009**, *136* (4), 701–718.
3. Cech, T. R., Self-splicing of group-I introns. *Annu. Rev. Biochem.* **1990**, *59*, 543–568.
4. Will, C. L.; Luhrmann, R., Spliceosome structure and function. *Cold Spring Harb. Perspect. Biol.* **2011**, *3* (7), a003707.
5. Burge, C. B.; Tuschl, T.; Sharp, P. A., The RNA World. **1999**, 525–560.
6. Mount, S. M., A catalog of splice junction sequences. *Nucleic Acids Res.* **1982**, *10* (2), 459–472.
7. Mount, S. M.; Pettersson, I.; Hinterberger, M.; Karmas, A.; Steitz, J. A., The U1 small nuclear RNA-protein complex selectively binds a 5' splice site in vitro. *Cell* **1983**, *33* (2), 509–518.
8. Zamore, P. D.; Green, M. R., Identification, purification, and biochemical characterization of U2 small nuclear ribonucleoprotein auxiliary factor. *Proc. Natl. Acad. Sci. U S A* **1989**, *86* (23), 9243–9247.
9. Berglund, J. A.; Chua, K.; Abovich, N.; Reed, R.; Rosbash, M., The splicing factor BBP interacts specifically with the pre-mRNA branchpoint sequence UACUAAC. *Cell* **1997**, *89* (5), 781–787.
10. Pikielny, C. W.; Rymond, B. C.; Rosbash, M., Electrophoresis of ribonucleoproteins reveals an ordered assembly pathway of yeast splicing complexes. *Nature* **1986**, *324* (6095), 341–345.
11. Konarska, M. M.; Sharp, P. A., Interactions between small nuclear ribonucleoprotein-particles in formation of spliceosomes. *Cell* **1987**, *49* (6), 763–774.
12. Rutz, B.; Seraphin, B., Transient interaction of BBP/ScSF1 and Mud2 with the splicing machinery affects the kinetics of spliceosome assembly. *Rna* **1999**, *5* (6), 819–831.
13. Staley, J. P.; Guthrie, C., Mechanical devices of the spliceosome: Motors, clocks, springs, and things. *Cell* **1998**, *92* (3), 315–326.
14. Kiss, T., Biogenesis of small nuclear RNPs. *J Cell Sci* **2004**, *117* (25), 5949-+.
15. Nilsen, T. W.; Graveley, B. R., Expansion of the eukaryotic proteome by alternative splicing. *Nature* **2010**, *463* (7280), 457–463.
16. Meyer, I. M.; Durbin, R., Gene structure conservation aids similarity based gene prediction. *Nucleic Acids Res.* **2004**, *32* (2), 776–783.
17. Wang, E. T.; Sandberg, R.; Luo, S. J.; Khrebtkova, I.; Zhang, L.; Mayr, C.; Kingsmore, S. F.; Schroth, G. P.; Burge, C. B., Alternative isoform regulation in human tissue transcriptomes. *Nature* **2008**, *456* (7221), 470–476.

18. Kalsotra, A.; Cooper, T. A., Functional consequences of developmentally regulated alternative splicing. *Nat. Rev. Genet.* **2011**, *12* (10), 715–729.
19. Singh, R. K.; Cooper, T. A., Pre-mRNA splicing in disease and therapeutics. *Trends Mol. Med.* **2012**, *18* (8), 472–482.
20. David, C. J.; Manley, J. L., Alternative pre-mRNA splicing regulation in cancer: pathways and programs unhinged. *Gene Dev* **2010**, *24* (21), 2343–2364.
21. Kaida, D.; Schneider-Poetsch, T.; Yoshida, M., Splicing in oncogenesis and tumor suppression. *Cancer Sci.* **2012**, *103* (9), 1611–1616.
22. Black, D. L., Mechanisms of alternative pre-messenger RNA splicing. *Annu. Rev. Biochem.* **2003**, *72*, 291–336.
23. Barash, Y.; Calarco, J. A.; Gao, W. J.; Pan, Q.; Wang, X. C.; Shai, O.; Blencowe, B. J.; Frey, B. J., Deciphering the splicing code. *Nature* **2010**, *465* (7294), 53–59.
24. Lander, E. S.; Consortium, I. H. G. S.; Linton, L. M.; Birren, B.; Nusbaum, C.; Zody, M. C.; Baldwin, J.; Devon, K.; Dewar, K.; Doyle, M.; FitzHugh, W.; Funke, R.; Gage, D.; Harris, K.; Heaford, A.; Howland, J.; Kann, L.; Lehoczky, J.; LeVine, R.; McEwan, P.; McKernan, K.; Meldrim, J.; Mesirov, J. P.; Miranda, C.; Morris, W.; Naylor, J.; Raymond, C.; Rosetti, M.; Santos, R.; Sheridan, A.; Sougnez, C.; Stange-Thomann, N.; Stojanovic, N.; Subramanian, A.; Wyman, D.; Rogers, J.; Sulston, J.; Ainscough, R.; Beck, S.; Bentley, D.; Burton, J.; Clee, C.; Carter, N.; Coulson, A.; Deadman, R.; Deloukas, P.; Dunham, A.; Dunham, I.; Durbin, R.; French, L.; Grafham, D.; Gregory, S.; Hubbard, T.; Humphray, S.; Hunt, A.; Jones, M.; Lloyd, C.; McMurray, A.; Matthews, L.; Mercer, S.; Milne, S.; Mullikin, J. C.; Mungall, A.; Plumb, R.; Ross, M.; Shownkeen, R.; Sims, S.; Waterston, R. H.; Wilson, R. K.; Hillier, L. W.; McPherson, J. D.; Marra, M. A.; Mardis, E. R.; Fulton, L. A.; Chinwalla, A. T.; Pepin, K. H.; Gish, W. R.; Chissole, S. L.; Wendl, M. C.; Delehaunty, K. D.; Miner, T. L.; Delehaunty, A.; Kramer, J. B.; Cook, L. L.; Fulton, R. S.; Johnson, D. L.; Minx, P. J.; Clifton, S. W.; Hawkins, T.; Branscomb, E.; Predki, P.; Richardson, P.; Wenning, S.; Slezak, T.; Doggett, N.; Cheng, J. F.; Olsen, A.; Lucas, S.; Elkin, C.; Uberbacher, E.; Frazier, M.; Gibbs, R. A.; Muzny, D. M.; Scherer, S. E.; Bouck, J. B.; Sodergren, E. J.; Worley, K. C.; Rives, C. M.; Gorrell, J. H.; Metzker, M. L.; Naylor, S. L.; Kucherlapati, R. S.; Nelson, D. L.; Weinstock, G. M.; Sakaki, Y.; Fujiyama, A.; Hattori, M.; Yada, T.; Toyoda, A.; Itoh, T.; Kawagoe, C.; Watanabe, H.; Totoki, Y.; Taylor, T.; Weissenbach, J.; Heilig, R.; Saurin, W.; Artiguenave, F.; Brottier, P.; Bruls, T.; Pelletier, E.; Robert, C.; Wincker, P.; Rosenthal, A.; Platzer, M.; Nyakatura, G.; Taudien, S.; Rump, A.; Yang, H. M.; Yu, J.; Wang, J.; Huang, G. Y.; Gu, J.; Hood, L.; Rowen, L.; Madan, A.; Qin, S. Z.; Davis, R. W.; Federspiel, N. A.; Abola, A. P.; Proctor, M. J.; Myers, R. M.; Schmutz, J.; Dickson, M.; Grimwood, J.; Cox, D. R.; Olson, M. V.; Kaul, R.; Raymond, C.; Shimizu, N.; Kawasaki, K.; Minoshima, S.; Evans, G. A.; Athanasiou, M.; Schultz, R.; Roe, B. A.; Chen, F.; Pan, H. Q.; Ramser, J.; Lehrach, H.; Reinhardt, R.; McCombie, W. R.; de la Bastide, M.; Dedhia, N.; Blocker, H.; Hornischer, K.; Nordtsiek, G.; Agarwala, R.; Aravind, L.; Bailey, J. A.; Bateman, A.; Batzoglou, S.; Birney, E.; Bork, P.; Brown, D. G.; Burge, C. B.; Cerutti, L.; Chen, H. C.; Church, D.; Clamp, M.; Copley, R. R.; Doerks, T.; Eddy, S. R.; Eichler, E. E.; Furey, T. S.; Galagan, J.; Gilbert, J. G. R.; Harmon, C.; Hayashizaki, Y.; Haussler, D.; Hermjakob, H.; Hokamp, K.; Jang, W. H.; Johnson, L. S.; Jones, T. A.; Kasif, S.; Kasprzyk, A.; Kennedy, S.; Kent, W. J.; Kitts, P.; Koonin, E. V.; Korf, I.; Kulp, D.; Lancet, D.; Lowe, T. M.; McLysaght, A.; Mikkelsen, T.; Moran, J. V.; Mulder, N.; Pollara, V. J.; Ponting, C. P.; Schuler, G.; Schultz, J. R.; Slater, G.; Smit, A. F. A.; Stupka, E.; Szustakowki, J.; Thierry-Mieg, D.; Thierry-Mieg, J.; Wagner, L.; Wallis, J.; Wheeler, R.; Williams, A.; Wolf, Y. I.; Wolfe, K. H.; Yang, S. P.; Yeh,

- R. F.; Collins, F.; Guyer, M. S.; Peterson, J.; Felsenfeld, A.; Wetterstrand, K. A.; Patrinos, A.; Morgan, M. J.; Conso, I. H. G. S., Initial sequencing and analysis of the human genome. *Nature* **2001**, *409* (6822), 860–921.
25. Berget, S. M., Exon recognition in vertebrate splicing. *J. Biol. Chem.* **1995**, *270* (6), 2411–2414.
26. Reed, R., Initial splice-site recognition and pairing during pre-mRNA splicing. *Curr. Opin. Genetics Dev.* **1996**, *6* (2), 215–220.
27. Cartegni, L.; Chew, S. L.; Krainer, A. R., Listening to silence and understanding nonsense: Exonic mutations that affect splicing. *Nat. Rev. Genet.* **2002**, *3* (4), 285–298.
28. Graveley, B. R., Sorting out the complexity of SR protein functions. *Rna* **2000**, *6* (9), 1197–1211.
29. Blencowe, B. J., Exonic splicing enhancers: mechanism of action, diversity and role in human genetic diseases. *Trends Biochem. Sci.* **2000**, *25* (3), 106–110.
30. Birney, E.; Kumar, S.; Krainer, A. R., Analysis of the RNA-recognition motif and RS and RGG domains: conservation in metazoan pre-mRNA splicing factors. *Nucleic Acids Res.* **1993**, *21* (25), 5803–5816.
31. Staknis, D.; Reed, R., SR proteins promote the first specific recognition of pre-mRNA and are present together with the U1 small nuclear ribonucleoprotein particle in a general splicing enhancer complex. *Mol. Cell Biol.* **1994**, *14* (11), 7670–7682.
32. Weighardt, F.; Biamonti, G.; Riva, S., Nucleo-cytoplasmic distribution of human hnRNP proteins: a search for the targeting domains in hnRNP A1. *J. Cell Sci.* **1995**, *108* (Pt 2), 545–555.
33. Krecic, A. M.; Swanson, M. S., hnRNP complexes: composition, structure, and function. *Curr. Opin. Cell Biol.* **1999**, *11* (3), 363–371.
34. Kashima, T.; Rao, N.; Manley, J. L., An intronic element contributes to splicing repression in spinal muscular atrophy. *Proc. Natl. Acad. Sci. USA* **2007**, *104* (9), 3426–3431.
35. Del Gatto-Konczak, F.; Olive, M.; Gesnel, M. C.; Breathnach, R., hnRNP A1 recruited to an exon in vivo can function as an exon splicing silencer. *Mol. Cell Biol.* **1999**, *19* (1), 251–260.
36. Piekielko-Witkowska, A.; Wiszomirska, H.; Wojcicka, A.; Poplawski, P.; Boguslawska, J.; Tanski, Z.; Nauman, A., Disturbed expression of splicing factors in renal cancer affects alternative splicing of apoptosis regulators, oncogenes, and tumor suppressors. *PLoS One* **2010**, *5* (10), e13690.
37. Karni, R.; de Stanchina, E.; Lowe, S. W.; Sinha, R.; Mu, D.; Krainer, A. R., The gene encoding the splicing factor SF2/ASF is a proto-oncogene. *Nat. Struct. Mol. Biol.* **2007**, *14* (3), 185–193.
38. Anczukow, O.; Rosenberg, A. Z.; Akerman, M.; Das, S.; Zhan, L. X.; Karni, R.; Muthuswamy, S. K.; Krainer, A. R., The splicing factor SRSF1 regulates apoptosis and proliferation to promote mammary epithelial cell transformation. *Nat. Struct. Mol. Biol.* **2012**, *19* (2), 220–228.
39. Jensen, M. A.; Wilkinson, J. E.; Krainer, A. R., Splicing factor SRSF6 promotes hyperplasia of sensitized skin. *Nat. Struct. Mol. Biol.* **2014**, doi: 10.1038/nsmb.2756. Epub ahead of print.
40. Jia, R.; Li, C. L.; McCoy, J. P.; Deng, C. X.; Zheng, Z. M., SRp20 is a proto-oncogene critical for cell proliferation and tumor induction and maintenance. *Int. J. Biol. Sci.* **2010**, *6* (7), 806–826.

41. Quidville, V.; Alsafadi, S.; Goubar, A.; Commo, F.; Scott, V.; Pioche-Durieu, C.; Girault, I.; Bacconnais, S.; Le Cam, E.; Lazar, V.; Delaloue, S.; Saghatchian, M.; Pautier, P.; Morice, P.; Dessen, P.; Vagner, S.; Andre, F., Targeting the deregulated spliceosome core machinery in cancer cells triggers mTOR blockade and autophagy. *Cancer Res.* **2013**, *73* (7), 2247–2258.
42. Will, C. L.; Luhrmann, R., Spliceosomal UsnRNP biogenesis, structure and function. *Curr. Opin. Cell Biol.* **2001**, *13* (3), 290–301.
43. Brosi, R.; Hauri, H. P.; Kramer, A., Separation of splicing factor SF3 into two components and purification of SF3a activity. *J. Biol. Chem.* **1993**, *268* (23), 17640–17646.
44. Das, B. K.; Xia, L.; Palandjian, L.; Gozani, O.; Chyung, Y.; Reed, R., Characterization of a protein complex containing spliceosomal proteins SAPs 49, 130, 145, and 155. *Mol. Cell. Biol.* **1999**, *19* (10), 6796–6802.
45. Kramer, A.; Gruter, P.; Groning, K.; Kastner, B., Combined biochemical and electron microscopic analyses reveal the architecture of the mammalian U2 snRNP. *J. Cell Biol.* **1999**, *145* (7), 1355–1368.
46. Will, C. L.; Schneider, C.; MacMillan, A. M.; Katopodis, N. F.; Neubauer, G.; Wilm, M.; Luhrmann, R.; Query, C. C., A novel U2 and U11/U12 snRNP protein that associates with the pre-mRNA branch site. *EMBO J.* **2001**, *20* (16), 4536–4546.
47. Will, C. L.; Urlaub, H.; Achsel, T.; Gentzel, M.; Wilm, M.; Luhrmann, R., Characterization of novel SF3b and 17S U2 snRNP proteins, including a human Prp5p homologue and an SF3b DEAD-box protein. *EMBO J.* **2002**, *21* (18), 4978–4988.
48. Golas, M. M.; Sander, B.; Will, C. L.; Luhrmann, R.; Stark, H., Molecular architecture of the multiprotein splicing factor SF3b. *Science* **2003**, *300* (5621), 980–984.
49. Gozani, O.; Potashkin, J.; Reed, R., A potential role for U2AF-SAP 155 interactions in recruiting U2 snRNP to the branch site. *Mol. Cell. Biol.* **1998**, *18* (8), 4752–4760.
50. Seghezzi, W.; Chua, K.; Shanahan, F.; Gozani, O.; Reed, R.; Lees, E., Cyclin E associates with components of the pre-mRNA splicing machinery in mammalian cells. *Mol. Cellular Biol.* **1998**, *18* (8), 4526–4536.
51. Boudrez, A.; Beullens, M.; Waelkens, E.; Stalmans, W.; Bollen, M., Phosphorylation-dependent interaction between the splicing factors SAP155 and NIPP1. *J. Biol. Chem.* **2002**, *277* (35), 31834–31841.
52. Schellenberg, M. J.; Dul, E. L.; MacMillan, A. M., Structural model of the p14/SF3b155 branch duplex complex. *Rna* **2011**, *17* (1), 155–165.
53. Kuwasako, K.; Dohmae, N.; Inoue, M.; Shirouzu, M.; Taguchi, S.; Guntert, P.; Seraphin, B.; Muto, Y.; Yokoyama, S., Complex assembly mechanism and an RNA-binding mode of the human p14-SF3b155 spliceosomal protein complex identified by NMR solution structure and functional analyses. *Proteins* **2008**, *71* (4), 1617–1636.
54. Thickman, K. R.; Swenson, M. C.; Kabogo, J. M.; Gryczynski, Z.; Kielkopf, C. L., Multiple U2AF65 binding sites within SF3b155: thermodynamic and spectroscopic characterization of protein-protein interactions among pre-mRNA splicing factors. *J. Mol. Biol.* **2006**, *356* (3), 664–683.
55. Cass, D. M.; Berglund, J. A., The SF3b155 N-terminal domain is a scaffold important for splicing. *Biochemistry-Us* **2006**, *45* (33), 10092–10101.
56. Kielkopf, C. L.; Lucke, S.; Green, A. R., U2AF homology motifs: protein recognition in the RRM world. *Gene Dev* **2004**, *18* (13), 1513–1526.
57. Spadaccini, R.; Reidt, U.; Dybkov, O.; Will, C.; Frank, R.; Stier, G.; Corsini, L.; Wahl, M. C.; Luhrmann, R.; Sattler, M., Biochemical and NMR analyses of an SF3b155-p14-U2AF-

RNA interaction network involved in branch point definition during pre-mRNA splicing. *Rna* **2006**, *12* (3), 410–425.

58. Selenko, P.; Gregorovic, G.; Sprangers, R.; Stier, G.; Rhani, Z.; Kramer, A.; Sattler, M., Structural basis for the molecular recognition between human splicing factors U2AF65 and SF1/mBBP. *Mol. Cell* **2003**, *11* (4), 965–976.

59. Warkocki, Z.; Odenwalder, P.; Schmitzova, J.; Platzmann, F.; Stark, H.; Urlaub, H.; Ficner, R.; Fabrizio, P.; Luhrmann, R., Reconstitution of both steps of *Saccharomyces cerevisiae* splicing with purified spliceosomal components. *Nat. Struct. Mol. Biol.* **2009**, *16* (12), 1237–1250.

60. Lardelli, R. M.; Thompson, J. X.; Yates, J. R., 3rd; Stevens, S. W., Release of SF3 from the intron branchpoint activates the first step of pre-mRNA splicing. *Rna* **2010**, *16* (3), 516–528.

61. Wang, C. Y.; Chua, K.; Seghezzi, W.; Lees, E.; Gozani, O.; Reed, R., Phosphorylation of spliceosomal protein SAP 155 coupled with splicing catalysis. *Gene Dev* **1998**, *12* (10), 1409–1414.

62. Tanuma, N.; Kim, S. E.; Beullens, M.; Tsubaki, Y.; Mitsuhashi, S.; Nomura, M.; Kawamura, T.; Isono, K.; Koseki, H.; Sato, M.; Bollen, M.; Kikuchi, K.; Shima, H., Nuclear inhibitor of protein phosphatase-1 (NIPPI) directs protein phosphatase-1 (PP1) to dephosphorylate the U2 small nuclear ribonucleoprotein particle (snRNP) component, spliceosome-associated protein 155 (Sap155). *J. Biol. Chem.* **2008**, *283* (51), 35805–35814.

63. de Graaf, K.; Czajkowska, H.; Rottmann, S.; Packman, L. C.; Lilischkis, R.; Luscher, B.; Becker, W., The protein kinase DYRK1A phosphorylates the splicing factor SF3b1/SAP155 at Thr434, a novel in vivo phosphorylation site. *BMC biochem.* **2006**, *7*, 7.

64. Massiello, A.; Roesser, J. R.; Chalfant, C. E., SAP155 Binds to ceramide-responsive RNA cis-element 1 and regulates the alternative 5' splice site selection of Bcl-x pre-mRNA. *FASEB J.* **2006**, *20* (10), 1680–1682.

65. Corsini, L.; Bonnal, S.; Basquin, J.; Hothorn, M.; Scheffzek, K.; Valcarcel, J.; Sattler, M., U2AF-homology motif interactions are required for alternative splicing regulation by SPF45. *Nat. Struct. Mol. Biol.* **2007**, *14* (7), 620–629.

66. Corsini, L.; Hothorn, M.; Stier, G.; Rybin, V.; Scheffzek, K.; Gibson, T. J.; Sattler, M., Dimerization and protein binding specificity of the U2AF homology motif of the splicing factor Puf60. *J. Biol. Chem.* **2009**, *284* (1), 630–639.

67. Hastings, M. L.; Allemand, E.; Duelli, D. M.; Myers, M. P.; Krainer, A. R., Control of pre-mRNA splicing by the general splicing factors PUF60 and U2AF(65). *PLoS One* **2007**, *2* (6), e538.

68. Matsushita, K.; Kajiwara, T.; Tamura, M.; Satoh, M.; Tanaka, N.; Tomonaga, T.; Matsubara, H.; Shimada, H.; Yoshimoto, R.; Ito, A.; Kubo, S.; Natsume, T.; Levens, D.; Yoshida, M.; Nomura, F., SAP155-mediated splicing of FUSE-binding protein-interacting repressor serves as a molecular switch for c-myc gene expression. *Mol. Cancer Res.* **2012**, *10* (6), 787–799.

69. Matsushita, K.; Tamura, M.; Tanaka, N.; Tomonaga, T.; Matsubara, H.; Shimada, H.; Levens, D.; He, L. S.; Liu, J. H.; Yoshida, M.; Nomura, F., Interactions between SAP155 and FUSE-binding protein-interacting repressor bridges c-Myc and p27Kip1 expression. *Mol. Cancer Res.* **2013**, *11* (7), 689–698.

70. Kajiwara, T.; Matsushita, K.; Itoga, S.; Tamura, M.; Tanaka, N.; Tomonaga, T.; Matsubara, H.; Shimada, H.; Habara, Y.; Matsuo, M.; Nomura, F., SAP155-mediated c-myc

suppressor far-upstream element-binding protein-interacting repressor splicing variants are activated in colon cancer tissues. *Cancer Sci.* **2013**, *104* (2), 149–156.

71. Haferlach, T.; Nagata, Y.; Grossmann, V.; Okuno, Y.; Bacher, U.; Nagae, G.; Schnittger, S.; Sanada, M.; Kon, A.; Alpermann, T.; Yoshida, K.; Roller, A.; Nadarajah, N.; Shiraishi, Y.; Shiozawa, Y.; Chiba, K.; Tanaka, H.; Koeffler, H. P.; Klein, H. U.; Dugas, M.; Aburatani, H.; Kohlmann, A.; Miyano, S.; Haferlach, C.; Kern, W.; Ogawa, S., Landscape of genetic lesions in 944 patients with myelodysplastic syndromes. *Leukemia* **2014**, *28* (2), 241–247.

72. On the way towards a “CLL prognostic index”: focus on TP53, BIRC3, SF3B1, NOTCH1 and MYD88 in a population-based cohort. *Leukemia* **2013**, doi: 10.1038/leu.2013.333. *Epub ahead of print.*

73. Papaemmanuil, E.; Cazzola, M.; Boulton, J.; Malcovati, L.; Vyas, P.; Bowen, D.; Pellagatti, A.; Wainscoat, J. S.; Hellstrom-Lindberg, E.; Gambacorti-Passerini, C.; Godfrey, A. L.; Rapado, I.; Cvejic, A.; Rance, R.; McGee, C.; Ellis, P.; Mudie, L. J.; Stephens, P. J.; McLaren, S.; Massie, C. E.; Tarpey, P. S.; Varela, I.; Nik-Zainal, S.; Davies, H. R.; Shlien, A.; Jones, D.; Raine, K.; Hinton, J.; Butler, A. P.; Teague, J. W.; Baxter, E. J.; Score, J.; Galli, A.; Della Porta, M. G.; Travaglino, E.; Groves, M.; Tauro, S.; Munshi, N. C.; Anderson, K. C.; El-Naggar, A.; Fischer, A.; Mustonen, V.; Warren, A. J.; Cross, N. C.; Green, A. R.; Futreal, P. A.; Stratton, M. R.; Campbell, P. J., Somatic SF3B1 mutation in myelodysplasia with ring sideroblasts. *New Engl. J. Med.* **2011**, *365* (15), 1384–1395.

74. Wan, Y.; Wu, C. J., SF3B1 mutations in chronic lymphocytic leukemia. *Blood* **2013**, *121* (23), 4627–4234.

75. Quesada, V.; Conde, L.; Villamor, N.; Ordonez, G. R.; Jares, P.; Bassaganyas, L.; Ramsay, A. J.; Bea, S.; Pinyol, M.; Martinez-Trillos, A.; Lopez-Guerra, M.; Colomer, D.; Navarro, A.; Baumann, T.; Aymerich, M.; Rozman, M.; Delgado, J.; Gine, E.; Hernandez, J. M.; Gonzalez-Diaz, M.; Puente, D. A.; Velasco, G.; Freije, J. M.; Tubio, J. M.; Royo, R.; Gelpi, J. L.; Orozco, M.; Pisano, D. G.; Zamora, J.; Vazquez, M.; Valencia, A.; Himmelbauer, H.; Bayes, M.; Heath, S.; Gut, M.; Gut, I.; Estivill, X.; Lopez-Guillermo, A.; Puente, X. S.; Campo, E.; Lopez-Otin, C., Exome sequencing identifies recurrent mutations of the splicing factor SF3B1 gene in chronic lymphocytic leukemia. *Nat. Genet.* **2012**, *44* (1), 47–52.

76. Wu, X.; Tschumper, R. C.; Jelinek, D. F., Genetic characterization of SF3B1 mutations in single chronic lymphocytic leukemia cells. *Leukemia* **2013**, *27* (11), 2264–2267.

77. Isono, K.; Mizutani-Koseki, Y.; Komori, T.; Schmidt-Zachmann, M. S.; Koseki, H., Mammalian polycomb-mediated repression of Hox genes requires the essential spliceosomal protein Sf3b1. *Gene Dev* **2005**, *19* (5), 536–541.

78. Koboldt, D. C.; Fulton, R. S.; McLellan, M. D.; Schmidt, H.; Kalicki-Veizer, J.; McMichael, J. F.; Fulton, L. L.; Dooling, D. J.; Ding, L.; Mardis, E. R.; Wilson, R. K.; Ally, A.; Balasundaram, M.; Butterfield, Y. S. N.; Carlsen, R.; Carter, C.; Chu, A.; Chuah, E.; Chun, H. J. E.; Coope, R. J. N.; Dhalla, N.; Guin, R.; Hirst, C.; Hirst, M.; Holt, R. A.; Lee, D.; Li, H. Y. I.; Mayo, M.; Moore, R. A.; Mungall, A. J.; Pleasance, E.; Robertson, A. G.; Schein, J. E.; Shafiei, A.; Sipahimalani, P.; Slobodan, J. R.; Stoll, D.; Tam, A.; Thiessen, N.; Varhol, R. J.; Wye, N.; Zeng, T.; Zhao, Y. J.; Birol, I.; Jones, S. J. M.; Marra, M. A.; Cherniack, A. D.; Saksena, G.; Onofrio, R. C.; Pho, N. H.; Carter, S. L.; Schumacher, S. E.; Tabak, B.; Hernandez, B.; Gentry, J.; Nguyen, H.; Crenshaw, A.; Ardlie, K.; Beroukhi, R.; Winckler, W.; Getz, G.; Gabriel, S. B.; Meyerson, M.; Chin, L.; Park, P. J.; Kucherlapati, R.; Hoadley, K. A.; Auman, J. T.; Fan, C.; Turman, Y. J.; Shi, Y.; Li, L.; Topal, M. D.; He, X. P.; Chao, H. H.; Prat, A.; Silva, G. O.; Iglesia, M. D.; Zhao, W.; Usary, J.; Berg, J. S.; Adams, M.; Booker, J.; Wu, J. Y.; Gulabani, A.;

Bodenheimer, T.; Hoyle, A. P.; Simons, J. V.; Soloway, M. G.; Mose, L. E.; Jefferys, S. R.; Balu, S.; Parker, J. S.; Hayes, D. N.; Perou, C. M.; Malik, S.; Mahurkar, S.; Shen, H.; Weisenberger, D. J.; Triche, T.; Lai, P. H.; Bootwalla, M. S.; Maglinte, D. T.; Berman, B. P.; Van den Berg, D. J.; Baylin, S. B.; Laird, P. W.; Creighton, C. J.; Donehower, L. A.; Getz, G.; Noble, M.; Voet, D.; Saksena, G.; Gehlenborg, N.; DiCara, D.; Zhang, J. H.; Zhang, H. L.; Wu, C. J.; Liu, S. Y.; Lawrence, M. S.; Zou, L. H.; Sivachenko, A.; Lin, P.; Stojanov, P.; Jing, R.; Cho, J.; Sinha, R.; Park, R. W.; Nazaire, M. D.; Robinson, J.; Thorvaldsdottir, H.; Mesirov, J.; Park, P. J.; Chin, L.; Reynolds, S.; Kreisberg, R. B.; Bernard, B.; Bressler, R.; Erkkila, T.; Lin, J.; Thorsson, V.; Zhang, W.; Shmulevich, I.; Ciriello, G.; Weinhold, N.; Schultz, N.; Gao, J. J.; Cerami, E.; Gross, B.; Jacobsen, A.; Sinha, R.; Aksoy, B. A.; Antipin, Y.; Reva, B.; Shen, R. L.; Taylor, B. S.; Ladanyi, M.; Sander, C.; Anur, P.; Spellman, P. T.; Lu, Y. L.; Liu, W. B.; Verhaak, R. R. G.; Mills, G. B.; Akbani, R.; Zhang, N. X.; Broom, B. M.; Casavant, T. D.; Wakefield, C.; Unruh, A. K.; Baggerly, K.; Coombes, K.; Weinstein, J. N.; Haussler, D.; Benz, C. C.; Stuart, J. M.; Benz, S. C.; Zhu, J. C.; Szeto, C. C.; Scott, G. K.; Yau, C.; Paul, E. O.; Carlin, D.; Wong, C.; Sokolov, A.; Thusberg, J.; Mooney, S.; Ng, S.; Goldstein, T. C.; Ellrott, K.; Grifford, M.; Wilks, C.; Ma, S.; Craft, B.; Yan, C. H.; Hu, Y.; Meerzaman, D.; Gastier-Foster, J. M.; Bowen, J.; Ramirez, N. C.; Black, A. D.; Pyatt, R. E.; White, P.; Zmuda, E. J.; Frick, J.; Lichtenberg, T.; Broekmans, R.; George, M. M.; Gerken, M. A.; Harper, H. A.; Leraas, K. M.; Wise, L. J.; Tabler, T. R.; McAllister, C.; Barr, T.; Hart-Kothari, M.; Tarvin, K.; Saller, C.; Sandusky, G.; Mitchell, C.; Iacocca, M. V.; Brown, J.; Rabeno, B.; Czerwinski, C.; Petrelli, N.; Dolzhansky, O.; Abramov, M.; Voronina, O.; Potapova, O.; Marks, J. R.; Suchorska, W. M.; Murawa, D.; Kycler, W.; Ibbs, M.; Korski, K.; Szychala, A.; Murawa, P.; Brzezinski, J. J.; Perz, H.; Lazniak, R.; Teresiak, M.; Tatka, H.; Leporowska, E.; Bogusz-Czerniewicz, M.; Malicki, J.; Mackiewicz, A.; Wiznerowicz, M.; Le, X. V.; Kohl, B.; Tien, N. V.; Thorp, R.; Bang, N. V.; Sussman, H.; Phu, B. D.; Hajek, R.; Hung, N. P.; Tran, V. T. P.; Thang, H. Q.; Khan, K. Z.; Penny, R.; Mallery, D.; Curley, E.; Shelton, C.; Yena, P.; Ingle, J. N.; Couch, F. J.; Lingle, W. L.; King, T. A.; Gonzalez-Angulo, A. M.; Mills, G. B.; Dyer, M. D.; Liu, S. Y.; Meng, X. L.; Patangan, M.; Waldman, F.; Stoppler, H.; Rathmell, W. K.; Thorne, L.; Huang, M.; Boice, L.; Hill, A.; Morrison, C.; Gaudioso, C.; Bshara, W.; Daily, K.; Egea, S. C.; Pegram, M. D.; Gomez-Fernandez, C.; Dhir, R.; Bhargava, R.; Brufsky, A.; Shriver, C. D.; Hooke, J. A.; Campbell, J. L.; Mural, R. J.; Hu, H.; Somiari, S.; Larson, C.; Deyarmin, B.; Kvecher, L.; Kovatich, A. J.; Ellis, M. J.; King, T. A.; Hu, H.; Couch, F. J.; Mural, R. J.; Stricker, T.; White, K.; Olopade, O.; Ingle, J. N.; Luo, C. Q.; Chen, Y. Q.; Marks, J. R.; Waldman, F.; Wiznerowicz, M.; Bose, R.; Chang, L. W.; Beck, A. H.; Gonzalez-Angulo, A. M.; Pihl, T.; Jensen, M.; Sfeir, R.; Kahn, A.; Chu, A.; Kothiyal, P.; Wang, Z. N.; Snyder, E.; Pontius, J.; Ayala, B.; Backus, M.; Walton, J.; Baboud, J.; Berton, D.; Nicholls, M.; Srinivasan, D.; Raman, R.; Girshik, S.; Kigonya, P.; Alonso, S.; Sanbhadti, R.; Barletta, S.; Pot, D.; Sheth, M.; Demchok, J. A.; Shaw, K. R. M.; Yang, L. M.; Eley, G.; Ferguson, M. L.; Tarnuzzer, R. W.; Zhang, J. S.; Dillon, L. A. L.; Buetow, K.; Fielding, P.; Ozenberger, B. A.; Guyer, M. S.; Sofia, H. J.; Palchik, J. D.; Network, C. G. A., Comprehensive molecular portraits of human breast tumours. *Nature* **2012**, *490* (7418), 61–70.

79. Biankin, A. V.; Waddell, N.; Kassahn, K. S.; Gingras, M. C.; Muthuswamy, L. B.; Johns, A. L.; Miller, D. K.; Wilson, P. J.; Patch, A. M.; Wu, J. M.; Chang, D. K.; Cowley, M. J.; Gardiner, B. B.; Song, S.; Harliwong, I.; Idrisoglu, S.; Nourse, C.; Nourbakhsh, E.; Manning, S.; Wani, S.; Gongora, M.; Pajic, M.; Scarlett, C. J.; Gill, A. J.; Pinho, A. V.; Rooman, I.; Anderson, M.; Holmes, O.; Leonard, C.; Taylor, D.; Wood, S.; Xu, Q. Y.; Nones, K.; Fink, J. L.; Christ, A.; Bruxner, T.; Cloonan, N.; Kolle, G.; Newell, F.; Pinese, M.; Mead, R. S.; Humphris, J. L.;

- Kaplan, W.; Jones, M. D.; Colvin, E. K.; Nagrial, A. M.; Humphrey, E. S.; Chou, A.; Chin, V. T.; Chantrill, L. A.; Mawson, A.; Samra, J. S.; Kench, J. G.; Lovell, J. A.; Daly, R. J.; Merrett, N. D.; Toon, C.; Epari, K.; Nguyen, N. Q.; Barbour, A.; Zeps, N.; Kakkar, N.; Zhao, F. M.; Wu, Y. Q.; Wang, M.; Muzny, D. M.; Fisher, W. E.; Brunicardi, F. C.; Hodges, S. E.; Reid, J. G.; Drummond, J.; Chang, K.; Han, Y.; Lewis, L. R.; Dinh, H.; Buhay, C. J.; Beck, T.; Timms, L.; Sam, M.; Begley, K.; Brown, A.; Pai, D.; Panchal, A.; Buchner, N.; De Borja, R.; Denroche, R. E.; Yung, C. K.; Serra, S.; Onetto, N.; Mukhopadhyay, D.; Tsao, M. S.; Shaw, P. A.; Petersen, G. M.; Gallinger, S.; Hruban, R. H.; Maitra, A.; Iacobuzio-Donahue, C. A.; Schulick, R. D.; Wolfgang, C. L.; Morgan, R. A.; Lawlor, R. T.; Capelli, P.; Corbo, V.; Scardoni, M.; Tortora, G.; Tempero, M. A.; Mann, K. M.; Jenkins, N. A.; Perez-Mancera, P. A.; Adams, D. J.; Largaespada, D. A.; Wessels, L. F. A.; Rust, A. G.; Stein, L. D.; Tuveson, D. A.; Copeland, N. G.; Musgrove, E. A.; Scarpa, A.; Eshleman, J. R.; Hudson, T. J.; Sutherland, R. L.; Wheeler, D. A.; Pearson, J. V.; McPherson, J. D.; Gibbs, R. A.; Grimmond, S. M.; Genome, A. P. C., Pancreatic cancer genomes reveal aberrations in axon guidance pathway genes. *Nature* **2012**, *491* (7424), 399–405.
80. Harbour, J. W.; Roberson, E. D. O.; Anbunathan, H.; Onken, M. D.; Worley, L. A.; Bowcock, A. M., Recurrent mutations at codon 625 of the splicing factor SF3B1 in uveal melanoma. *Nat. Genet.* **2013**, *45* (2), 133–135.
81. Fan, L. Y.; Lagisetti, C.; Edwards, C. C.; Webb, T. R.; Potter, P. M., Sudemycins, novel small molecule analogues of FR901464, induce alternative gene splicing. *ACS Chem. Biol.* **2011**, *6* (6), 582–589.
82. Nakajima, H.; Takase, S.; Terano, H.; Tanaka, H., New antitumor substances, FR901463, FR901464 and FR901465. III. Structures of FR901463, FR901464 and FR901465. *J. Antibiot.* **1997**, *50* (1), 96–99.
83. Nakajima, H.; Sato, B.; Fujita, T.; Takase, S.; Terano, H.; Okuhara, M., New antitumor substances, FR901463, FR901464 and FR901465. I. Taxonomy, fermentation, isolation, physico-chemical properties and biological activities. *J. Antibiot.* **1996**, *49* (12), 1196–1203.
84. Nakajima, H.; Hori, Y.; Terano, H.; Okuhara, M.; Manda, T.; Matsumoto, S.; Shimomura, K., New antitumor substances, FR901463, FR901464 and FR901465. II. Activities against experimental tumors in mice and mechanism of action. *J. Antibiot.* **1996**, *49* (12), 1204–1211.
85. Sakai, T.; Sameshima, T.; Matsufuji, M.; Kawamura, N.; Dobashi, K.; Mizui, Y., Pladienolides, new substances from culture of *Streptomyces platensis* Mer-11107. I. Taxonomy, fermentation, isolation and screening. *J. Antibiot.* **2004**, *57* (3), 173–179.
86. Mizui, Y.; Sakai, T.; Iwata, M.; Uenaka, T.; Okamoto, K.; Shimizu, H.; Yamori, T.; Yoshimatsu, K.; Asada, M., Pladienolides, new substances from culture of *Streptomyces platensis* Mer-11107. III. In vitro and in vivo antitumor activities. *J. Antibiot.* **2004**, *57* (3), 188–196.
87. Sakai, Y. T., T.; Akiyama, T.; Yoshida, T.; Mizukami, T.; Akinaga, S.; Horinouchi, S.; Yoshida, M.; Yoshida, T., GEX1 compounds, novel antitumor antibiotics related to herboxidiene, produced by *streptomyces* sp. II The effects on cell cycle progression and gene expression. *J. Antibiot.* **2002**, *55* (10), 863–872.
88. Taunton, J.; Hassig, C. A.; Schreiber, S. L., A mammalian histone deacetylase related to the yeast transcriptional regulator Rpd3p. *Science* **1996**, *272* (5260), 408–411.

89. Nakajima, H.; Kim, Y. B.; Terano, H.; Yoshida, M.; Horinouchi, S., FR901228, a potent antitumor antibiotic, is a novel histone deacetylase inhibitor. *Exp. Cell Res.* **1998**, *241* (1), 126–133.
90. Thompson, C. F.; Jamison, T. F.; Jacobsen, E. N., FR901464: total synthesis, proof of structure, and evaluation of synthetic analogues. *J. Am. Chem. Soc.* **2001**, *123* (41), 9974–9983.
91. Motoyoshi, H.; Horigome, M.; Ishigami, K.; Yoshida, T.; Horinouchi, S.; Yoshida, M.; Watanabe, H.; Kitahara, T., Structure-activity relationship for FR901464: a versatile method for the conversion and preparation of biologically active biotinylated probes. *Biosci. Biotechnol. Biochem.* **2004**, *68* (10), 2178–2182.
92. Motoyoshi, H.; Horigome, M.; Watanabe, H.; Kitahara, T., Total synthesis of FR901464: second generation. *Tetrahedron* **2006**, *62* (7), 1378–1389.
93. Horigome, M., Motoyoshi, H., Watanabe, H., and Kitahara, T., A synthesis of FR901464. *Tetrahedron Lett.* **2001**, *42*, 8207–8210.
94. Osman, S.; Albert, B. J.; Wang, Y.; Li, M.; Czaicki, N. L.; Koide, K., Structural requirements for the antiproliferative activity of pre-mRNA splicing inhibitor FR901464. *Chemistry* **2011**, *17* (3), 895–904.
95. Albert, B. J.; Sivaramakrishnan, A.; Naka, T.; Koide, K., Total synthesis of FR901464, an antitumor agent that regulates the transcription of oncogenes and tumor suppressor genes. *J. Am. Chem. Soc.* **2006**, *128* (9), 2792–2793.
96. Ghosh, A. K.; Chen, Z. H., Enantioselective syntheses of FR901464 and spliceostatin A: potent inhibitors of spliceosome. *Org. Lett.* **2013**, *15* (19), 5088–5091.
97. Liu, X. Y.; Biswas, S.; Berg, M. G.; Antapli, C. M.; Xie, F.; Wang, Q.; Tang, M. C.; Tang, G. L.; Zhang, L. X.; Dreyfuss, G.; Cheng, Y. Q., Genomics-guided discovery of thailanstatins A, B, and C as pre-mRNA splicing inhibitors and antiproliferative agents from *Burkholderia thailandensis* MSMB43. *J. Nat. Prod.* **2013**, *76* (4), 685–693.
98. Liu, X.; Biswas, S.; Tang, G. L.; Cheng, Y. Q., Isolation and characterization of spliceostatin B, a new analogue of FR901464, from *Pseudomonas* sp. No. 2663. *J. Antibiot.* **2013**, *66* (9), 555–558.
99. Tashiro, E.; Imoto, M.; Yoshida, M.; Kitahara, T.; Watanabe, H.; Nakajima, H., Method for screening antitumor agent. *Japan Kokai Tokkyo Koho* **2005**, *JP 2005323514*.
100. Kaida, D.; Motoyoshi, H.; Tashiro, E.; Nojima, T.; Hagiwara, M.; Ishigami, K.; Watanabe, H.; Kitahara, T.; Yoshida, T.; Nakajima, H.; Tani, T.; Horinouchi, S.; Yoshida, M., Spliceostatin A targets SF3b and inhibits both splicing and nuclear retention of pre-mRNA. *Nat. Chem. Biol.* **2007**, *3* (9), 576–583.
101. Roybal, G. A.; Jurica, M. S., Spliceostatin A inhibits spliceosome assembly subsequent to prespliceosome formation. *Nucleic Acids Res.* **2010**, *38* (19), 6664–6672.
102. Konarska, M. M.; Sharp, P. A., Electrophoretic Separation of Complexes Involved in the Splicing of Precursors to Messenger-Rnas. *Cell* **1986**, *46* (6), 845–855.
103. Weng, M. T.; Lee, J. H.; Wei, S. C.; Li, Q. N.; Shahamatdar, S.; Hsu, D.; Schetter, A. J.; Swatkoski, S.; Mannan, P.; Garfield, S.; Gucek, M.; Kim, M. K. H.; Annunziata, C. M.; Creighton, C. J.; Emanuele, M. J.; Harris, C. C.; Sheu, J. C.; Giaccone, G.; Luo, J., Evolutionarily conserved protein ERH controls CENP-E mRNA splicing and is required for the survival of KRAS mutant cancer cells. *Proc. Natl. Acad. Sci. USA* **2012**, *109* (52), E3659–E3667.
104. McGlincy, N. J.; Smith, C. W., Alternative splicing resulting in nonsense-mediated mRNA decay: what is the meaning of nonsense? *Trends Biochem. Sci.* **2008**, *33* (8), 385–393.

105. Corrionero, A.; Minana, B.; Valcarcel, J., Reduced fidelity of branch point recognition and alternative splicing induced by the anti-tumor drug spliceostatin A. *Gene Dev* **2011**, *25* (5), 445–459.
106. Shiimori, M.; Inoue, K.; Sakamoto, H., A specific set of exon junction complex subunits is required for the nuclear retention of unspliced RNAs in *Caenorhabditis elegans*. *Mol. Cell. Biol.* **2013**, *33* (2), 444–456.
107. Michelle, L.; Cloutier, A.; Toutant, J.; Shkreta, L.; Thibault, P.; Durand, M.; Garneau, D.; Gendron, D.; Lapointe, E.; Couture, S.; Le Hir, H.; Klinck, R.; Abou Elela, S.; Prinos, P.; Chabot, B., Proteins associated with the exon junction complex also control the alternative splicing of apoptotic regulators. *Mol. Cell. Biol.* **2012**, *32* (5), 954–967.
108. Furumai, R.; Uchida, K.; Komi, Y.; Yoneyama, M.; Ishigami, K.; Watanabe, H.; Kojima, S.; Yoshida, M., Spliceostatin A blocks angiogenesis by inhibiting global gene expression including VEGF. *Cancer Sci.* **2010**, *101* (11), 2483–3489.
109. Hong, D. S.; Kurzrock, R.; Naing, A.; Wheler, J. J.; Falchook, G. S.; Schiffman, J. S.; Faulkner, N.; Pilat, M. J.; O'Brien, J.; Lorusso, P., A phase I, open-label, single-arm, dose-escalation study of E7107, a precursor messenger ribonucleic acid (pre-mRNA) splicing inhibitor administered intravenously on days 1 and 8 every 21 days to patients with solid tumors. *Invest. New Drugs* **2013**, *Epub ahead of print*.
110. Eskens, F. A.; Ramos, F. J.; Burger, H.; O'Brien, J. P.; Piera, A.; de Jonge, M. J.; Mizui, Y.; Wiemer, E. A.; Carreras, M. J.; Baselga, J.; Tabernero, J., Phase I pharmacokinetic and pharmacodynamic study of the first-in-class spliceosome inhibitor E7107 in patients with advanced solid tumors. *Clin. Cancer Res.* **2013**, *19* (22), 6296–6304.
111. Kotake, Y.; Sagane, K.; Owa, T.; Mimori-Kiyosue, Y.; Shimizu, H.; Uesugi, M.; Ishihama, Y.; Iwata, M.; Mizui, Y., Splicing factor SF3b as a target of the antitumor natural product pladienolide. *Nat. Chem. Biol.* **2007**, *3* (9), 570–575.
112. Kanada, R. M.; Itoh, D.; Nagai, M.; Niiijima, J.; Asai, N.; Mizui, Y.; Abe, S.; Kotake, Y., Total synthesis of the potent antitumor macrolides pladienolide B and D. *Angew. Chem.* **2007**, *46* (23), 4350–4355.
113. Yokoi, A.; Kotake, Y.; Takahashi, K.; Kadowaki, T.; Matsumoto, Y.; Minoshima, Y.; Sugi, N. H.; Sagane, K.; Hamaguchi, M.; Iwata, M.; Mizui, Y., Biological validation that SF3b is a target of the antitumor macrolide pladienolide. *FEBS J.* **2011**, *278* (24), 4870–4880.
114. Groves, M. R.; Hanlon, N.; Turowski, P.; Hemmings, B. A.; Barford, D., The structure of the protein phosphatase 2A PR65/A subunit reveals the conformation of its 15 tandemly repeated HEAT motifs. *Cell* **1999**, *96* (1), 99–110.
115. Villa, R.; Kashyap, M. K.; Kumar, D.; Kipps, T. J.; Castro, J. E.; La Clair, J. J.; Burkart, M. D., Stabilized cyclopropane analogs of the splicing inhibitor FD-895. *J. Med. Chem.* **2013**, *56* (17), 6576–6582.
116. Lagisetti, C.; Pourpak, A.; Jiang, Q.; Cui, X.; Goronga, T.; Morris, S. W.; Webb, T. R., Antitumor compounds based on a natural product consensus pharmacophore. *J. Med. Chem.* **2008**, *51* (19), 6220–6224.
117. Lagisetti, C.; Pourpak, A.; Goronga, T.; Jiang, Q.; Cui, X.; Hyle, J.; Lahti, J. M.; Morris, S. W.; Webb, T. R., Synthetic mRNA splicing modulator compounds with in vivo antitumor activity. *J. Med. Chem.* **2009**, *52* (22), 6979–6990.
118. Lagisetti, C.; Palacios, G.; Goronga, T.; Freeman, B.; Caufield, W.; Webb, T. R., Optimization of antitumor modulators of pre-mRNA splicing. *J. Med. Chem.* **2013**, *56* (24), 10033–10044.

119. Miller-Wideman, M.; Makkar, N.; Tran, M.; Isaac, B.; Biest, N.; Stonard, R., Herboxidiene, a new herbicidal substance from *Streptomyces chromofuscus* A7847. Taxonomy, fermentation, isolation, physico-chemical and biological properties. *J. Antibiot.* **1992**, *45* (6), 914–921.
120. Koguchi, Y.; Nishio, M.; Kotera, J.; Omori, K.; Ohnuki, T.; Komatsubara, S., Trichostatin A and herboxidiene up-regulate the gene expression of low density lipoprotein receptor. *J. Antibiot.* **1997**, *50* (11), 970–971.
121. Sakai, Y. Y., T.; Ochiai, K.; Uosaki, Y.; Saitoh, Y.; Tanaka, F.; Akiyama, T.; Akinaga, S.; Mizukami, T., Gex1 Compounds, Novel antitumor antibiotics related to herboxidiene, produced by streptomyces, sp. I. Taxonomy, Production, Isolation, Physicochemical Properties and Biological Activities. *J. Antibiot.* **2002**, *55* (10), 855–862.
122. Hasegawa, M.; Miura, T.; Kuzuya, K.; Inoue, A.; Won Ki, S.; Horinouchi, S.; Yoshida, T.; Kunoh, T.; Koseki, K.; Mino, K.; Sasaki, R.; Yoshida, M.; Mizukami, T., Identification of SAP155 as the target of GEX1A (Herboxidiene), an antitumor natural product. *ACS Chem. Biol.* **2011**, *6* (3), 229–233.
123. Moore, M. J.; Wang, Q.; Kennedy, C. J.; Silver, P. A., An alternative splicing network links cell-cycle control to apoptosis. *Cell* **2010**, *142* (4), 625–636.
124. Albert, B. J.; Sivaramakrishnan, A.; Naka, T.; Czaicki, N. L.; Koide, K., Total syntheses, fragmentation studies, and antitumor/antiproliferative activities of FR901464 and its low picomolar analogue. *J. Am. Chem. Soc.* **2007**, *129* (9), 2648–2659.
125. Lo, C. W.; Kaida, D.; Nishimura, S.; Matsuyama, A.; Yashiroda, Y.; Taoka, H.; Ishigami, K.; Watanabe, H.; Nakajima, H.; Tani, T.; Horinouchi, S.; Yoshida, M., Inhibition of splicing and nuclear retention of pre-mRNA by spliceostatin A in fission yeast. *Biochem. Biophys. Res. Commun.* **2007**, *364* (3), 573–577.
126. Kaida, D.; Berg, M. G.; Younis, I.; Kasim, M.; Singh, L. N.; Wan, L.; Dreyfuss, G., U1 snRNP protects pre-mRNAs from premature cleavage and polyadenylation. *Nature* **2010**, *468* (7324), 664–668.
127. Schmidt, U.; Basyuk, E.; Robert, M. C.; Yoshida, M.; Villemin, J. P.; Auboeuf, D.; Aitken, S.; Bertrand, E., Real-time imaging of cotranscriptional splicing reveals a kinetic model that reduces noise: implications for alternative splicing regulation. *J. Cell Biol.* **2011**, *193* (5), 819–829.
128. Allende-Vega, N.; Dayal, S.; Agarwala, U.; Sparks, A.; Bourdon, J. C.; Saville, M. K., p53 is activated in response to disruption of the pre-mRNA splicing machinery. *Oncogene* **2012**, published online (DOI: 10.1038/onc.2012.38).
129. O'Brien, K.; Matlin, A. J.; Lowell, A. M.; Moore, M. J., The biflavonoid isoginkgetin is a general inhibitor of pre-mRNA splicing. *J. Biol. Chem.* **2008**, *283* (48), 33147–33154.
130. Brody, Y.; Neufeld, N.; Bieberstein, N.; Causse, S. Z.; Böhnlein, E.-M.; Neugebauer, K. M.; Darzacq, X.; Shav-Tal, Y., The in vivo kinetics of RNA polymerase II elongation during cotranscriptional splicing. *PLoS Biol.* **2011**, *9* (1), e1000573.
131. de Almeida, S. F.; Grosso, A. R.; Koch, F.; Fenouil, R.; Carvalho, S.; Andrade, J.; Levezinho, H.; Gut, M.; Eick, D.; Gut, I.; Andrau, J. C.; Ferrier, P.; Carmo-Fonseca, M., Splicing enhances recruitment of methyltransferase HYPB/Setd2 and methylation of histone H3 Lys36. *Nat. Struct. Mol. Biol.* **2011**, *18* (9), 977–983.
132. Visconte, V.; Rogers, H. J.; Singh, J.; Barnard, J.; Bupathi, M.; Traina, F.; McMahon, J.; Makishima, H.; Szpurka, H.; Jankowska, A.; Jerez, A.; Sekeres, M. A.; Sauntharajah, Y.; Advani, A. S.; Copelan, E.; Koseki, H.; Isono, K.; Padgett, R. A.; Osman, S.; Koide, K.

- O'Keefe, C.; Maciejewski, J. P.; Tiu, R. V., SF3B1 haploinsufficiency leads to formation of ring sideroblasts in myelodysplastic syndromes. *Blood* **2012**, 10.1182/blood-2012-05-430876.
133. Girard, C.; Will, C. L.; Peng, J.; Makarov, E. M.; Kastner, B.; Lemm, I.; Urlaub, H.; Hartmuth, K.; Lührmann, R., Post-transcriptional spliceosomes are retained in nuclear speckles until splicing completion. *Nat. Commun.* **2012**, 3, 994–1006.
134. Visconte, V.; Rogers, H. J.; Singh, J.; Barnard, J.; Bupathi, M.; Traina, F.; McMahan, J.; Makishima, H.; Szpurka, H.; Jankowska, A.; Jerez, A.; Sekeres, M. A.; Sauntharajah, Y.; Advani, A. S.; Copelan, E.; Koseki, H.; Isono, K.; Padgett, R. A.; Osman, S.; Koide, K.; O'Keefe, C.; Maciejewski, J. P.; Tiu, R. V., SF3B1 haploinsufficiency leads to formation of ring sideroblasts in myelodysplastic syndromes. *Blood* **2012**, 120 (16), 3173–3186.
135. Osman, S.; Waud, W. R.; Gorman, G. S.; Day, B. W.; Koide, K., Evaluation of FR901464 analogues in vitro and in vivo. *Medchemcomm* **2011**, 2 (1), 38–43.
136. Zaharieva, E.; Chipman, J. K.; Soller, M., Alternative splicing interference by xenobiotics. *Toxicology* **2012**, 296 (1-3), 1–12.
137. Rix, U.; Superti-Furga, G., Target profiling of small molecules by chemical proteomics. *Nat. Chem. Biol.* **2009**, 5 (9), 616–624.
138. Schneider-Poetsch, T.; Usui, T.; Kaida, D.; Yoshida, M., Garbled messages and corrupted translations. *Nat. Chem. Biol.* **2010**, 6 (3), 189–198.
139. Allende-Vega, N.; Dayal, S.; Agarwala, U.; Sparks, A.; Bourdon, J. C.; Saville, M. K., p53 is activated in response to disruption of the pre-mRNA splicing machinery. *Oncogene* **2013**, 32 (1), 1–14.
140. Zhang, J. H.; Chung, T. D. Y.; Oldenburg, K. R., A simple statistical parameter for use in evaluation and validation of high throughput screening assays. *J. Biomol. Screen.* **1999**, 4 (2), 67–73.
141. Ghosh, R. N.; Chen, Y. T.; DeBiasio, R.; DeBiasio, R. L.; Conway, B. R.; Minor, L. K.; Demarest, K. T., Cell-based, high-content screen for receptor internalization, recycling and intracellular trafficking. *Biotechniques* **2000**, 29 (1), 170–175.
142. Murray, T. J.; Forsyth, C. J., Total synthesis of GEX1A. *Org. Lett.* **2008**, 10 (16), 3429–3431.
143. Albert, B. J.; McPherson, P. A.; O'Brien, K.; Czaicki, N. L.; Destefino, V.; Osman, S.; Li, M.; Day, B. W.; Grabowski, P. J.; Moore, M. J.; Vogt, A.; Koide, K., Meayamycin inhibits pre-messenger RNA splicing and exhibits picomolar activity against multidrug-resistant cells. *Mol. Cancer Ther.* **2009**, 8 (8), 2308–2318.
144. Soper, H. E., Young, A. W., Cave, B. M., Lee, A., Pearson, K., On the distribution of the correlation coefficient in small samples. Appendix II to the papers of "Student" and R. A. Fisher. A co-operative study. *Biometrika* **1917**, 11, 328–413.
145. Boise, L. H.; González-García, M.; Postema, C. E.; Ding, L. Y.; Lindsten, T.; Turka, L. A.; Mao, X. H.; Nuñez, G.; Thompson, C. B., *bcl-x*, a *bcl-2*-related gene that functions as a dominant regulator of apoptotic cell death. *Cell* **1993**, 74 (4), 597–608.
146. Bae, J.; Leo, C. P.; Hsu, S. Y.; Hsueh, A. J. W., MCL-1S, a splicing variant of the antiapoptotic BCL-2 family member MCL-1, encodes a proapoptotic protein possessing only the BH3 domain. *J. Biol. Chem.* **2000**, 275 (33), 25255–25261.
147. Kim, J. H.; Sim, S. H.; Ha, H. J.; Ko, J. J.; Lee, K.; Bae, J., MCL-1ES, a novel variant of MCL-1, associates with MCL-1L and induces mitochondrial cell death. *FEBS Lett.* **2009**, 583 (17), 2758–2764.

148. Hanahan, D.; Weinberg, R. A., Hallmarks of Cancer: The Next Generation. *Cell* **2011**, *144* (5), 646-674.
149. Varin, E.; Denoyelle, C.; Brotin, E.; Meryet-Figuere, M.; Giffard, F.; Abeilard, E.; Goux, D.; Gauduchon, P.; Icard, P.; Poulain, L., Downregulation of Bcl-xL and Mcl-1 is sufficient to induce cell death in mesothelioma cells highly refractory to conventional chemotherapy. *Carcinogenesis* **2010**, *31* (6), 984–993.
150. Chen, L.; Willis, S. N.; Wei, A.; Smith, B. J.; Fletcher, J. I.; Hinds, M. G.; Colman, P. M.; Day, C. L.; Adams, J. M.; Huang, D. C. S., Differential targeting of prosurvival Bcl-2 proteins by their BH3-only ligands allows complementary apoptotic function. *Mol. Cell* **2005**, *17* (3), 393–403.
151. Oltersdorf, T.; Elmore, S. W.; Shoemaker, A. R.; Armstrong, R. C.; Augeri, D. J.; Belli, B. A.; Bruncko, M.; Deckwerth, T. L.; Dinges, J.; Hajduk, P. J.; Joseph, M. K.; Kitada, S.; Korsmeyer, S. J.; Kunzer, A. R.; Letai, A.; Li, C.; Mitten, M. J.; Nettlesheim, D. G.; Ng, S.; Nimmer, P. M.; O'Connor, J. M.; Oleksijew, A.; Petros, A. M.; Reed, J. C.; Shen, W.; Tahir, S. K.; Thompson, C. B.; Tomaselli, K. J.; Wang, B. L.; Wendt, M. D.; Zhang, H. C.; Fesik, S. W.; Rosenberg, S. H., An inhibitor of Bcl-2 family proteins induces regression of solid tumours. *Nature* **2005**, *435* (7042), 677–681.
152. Huang, S.; Sinicrope, F. A., BH3 mimetic ABT-737 potentiates TRAIL-mediated apoptotic signaling by unsequestering Bim and Bak in human pancreatic cancer cells. *Cancer Res.* **2008**, *68* (8), 2944–2951.
153. Wesarg, E.; Hoffarth, S.; Wiewrodt, R.; Kroll, M.; Biesterfeld, S.; Huber, C.; Schuler, M., Targeting BCL-2 family proteins to overcome drug resistance in non-small cell lung cancer. *Int. J. Cancer* **2007**, *121* (11), 2387–2394.
154. Lin, X.; Morgan-Lappe, S.; Huang, X.; Li, L.; Zakula, D. M.; Verneti, L. A.; Fesik, S. W.; Shen, Y., 'Seed' analysis of off-target siRNAs reveals an essential role of Mcl-1 in resistance to the small-molecule Bcl-2/Bcl-XL inhibitor ABT-737. *Oncogene* **2007**, *26* (27), 3972–3979.
155. Chen, S.; Dai, Y.; Harada, H.; Dent, P.; Grant, S., Mcl-1 down-regulation potentiates ABT-737 lethality by cooperatively inducing Bak activation and Bax translocation. *Cancer Res.* **2007**, *67* (2), 782–791.
156. Tahir, S. K.; Yang, X. F.; Anderson, M. G.; Morgan-Lappe, S. E.; Sarthy, A. V.; Chen, J.; Warner, R. B.; Ng, S. C.; Fesik, S. W.; Elmore, S. W.; Rosenberg, S. H.; Tse, C., Influence of Bcl-2 family members on the cellular response of small-cell lung cancer cell lines to ABT-737. *Cancer Res.* **2007**, *67* (3), 1176–1183.
157. van Delft, M. F.; Wei, A. H.; Mason, K. D.; Vandenberg, C. J.; Chen, L.; Czabotar, P. E.; Willis, S. N.; Scott, C. L.; Day, C. L.; Cory, S.; Adams, J. M.; Roberts, A. W.; Huang, D. C. S., The BH3 mimetic ABT-737 targets selective Bcl-2 proteins and efficiently induces apoptosis via Bak/Bax if Mcl-1 is neutralized. *Cancer Cell* **2006**, *10* (5), 389–399.
158. Kang, M. H.; Wan, Z.; Kang, Y. H.; Sposto, R.; Reynolds, C. P., Mechanism of synergy of N-(4-hydroxyphenyl)retinamide and ABT-737 in acute lymphoblastic leukemia cell lines: Mcl-1 inactivation. *J. Natl. Cancer Inst.* **2008**, *100* (8), 580–595.
159. Shieh, J. J.; Liu, K. T.; Huang, S. W.; Chen, Y. J.; Hsieh, T. Y., Modification of alternative splicing of Mcl-1 pre-mRNA using antisense morpholino oligonucleotides induces apoptosis in basal cell carcinoma cells. *J. Invest. Dermatol.* **2009**, *129* (10), 2497–4506.
160. Gao, Y.; Vogt, A.; Forsyth, C. J.; Koide, K., Comparison of splicing factor 3b inhibitors in human cells. *ChemBiochem* **2013**, *14* (1), 49–52.

161. Ikegaki, N.; Katsumata, M.; Minna, J.; Tsujimoto, Y., Expression of Bcl-2 in small-cell lung-carcinoma cells. *Cancer Res.* **1994**, *54* (1), 6–8.
162. Zhang, H.; Guttikonda, S.; Roberts, L.; Uziel, T.; Semizarov, D.; Elmore, S. W.; Levenson, J. D.; Lam, L. T., Mcl-1 is critical for survival in a subgroup of non-small-cell lung cancer cell lines. *Oncogene* **2011**, *30* (16), 1963–1968.
163. Song, L.; Coppola, D.; Livingston, S.; Cress, D.; Haura, E. B., Mcl-1 regulates survival and sensitivity to diverse apoptotic stimuli in human non-small cell lung cancer cells. *Cancer Biol. Ther.* **2005**, *4* (3), 267–276.
164. Yang, T.; Kozopas, K. M.; Craig, R. W., The intracellular distribution and pattern of expression of Mcl-1 overlap with, but are not identical to, those of Bcl-2. *J. Cell Biol.* **1995**, *128* (6), 1173–1184.
165. Kozopas, K. M.; Yang, T.; Buchan, H. L.; Zhou, P.; Craig, R. W., MCL1, a gene expressed in programmed myeloid cell differentiation, has sequence similarity to BCL2. *Proc. Natl. Acad. Sci. U S A* **1993**, *90* (8), 3516–3520.
166. Weiss, W. A.; Taylor, S. S.; Shokat, K. M., Recognizing and exploiting differences between RNAi and small-molecule inhibitors. *Nat. Chem. Biol.* **2007**, *3* (12), 739–744.
167. Yang, T. M.; Barbone, D.; Fennell, D. A.; Broaddus, V. C., Bcl-2 family proteins contribute to apoptotic resistance in lung cancer multicellular spheroids. *Am. J. Respir. Cell Mol. Biol.* **2009**, *41* (1), 14–23.
168. Chou, T. C.; Talalay, P., Generalized equations for the analysis of inhibitions of Michaelis-Menten and higher-order kinetic systems with two or more mutually exclusive and nonexclusive inhibitors. *Eur. J. Biochem.* **1981**, *115* (1), 207–216.
169. Yu, J.; Yue, W.; Wu, B.; Zhang, L., PUMA sensitizes lung cancer cells to chemotherapeutic agents and irradiation. *Clin. Cancer Res.* **2006**, *12* (9), 2928–2936.
170. Rho, J. K.; Choi, Y. J.; Ryoo, B. Y.; Na, H.; Yang, S. H.; Kim, C. H.; Lee, J. C., p53 enhances gefitinib-induced growth inhibition and apoptosis by regulation of Fas in non-small cell lung cancer. *Cancer Res.* **2007**, *67* (3), 1163–1169.
171. Vermes, I.; Haanen, C.; Steffens-Nakken, H.; Reutelingsperger, C., A novel assay for apoptosis. Flow cytometric detection of phosphatidylserine expression on early apoptotic cells using fluorescein labelled Annexin V. *J. Immunol. Methods* **1995**, *184* (1), 39–51.
172. Schmid, I.; Krall, W. J.; Uittenbogaart, C. H.; Braun, J.; Giorgi, J. V., Dead cell discrimination with 7-amino-actinomycin D in combination with dual color immunofluorescence in single laser flow cytometry. *Cytometry* **1992**, *13* (2), 204–208.
173. Jemal, A.; Siegel, R.; Xu, J.; Ward, E., Cancer statistics, 2010. *Cancer J. Clin.* **2010**, *60* (5), 277–300.
174. Kreimer, A. R.; Clifford, G. M.; Boyle, P.; Franceschi, S., Human papillomavirus types in head and neck squamous cell carcinomas worldwide: A systematic review. *Cancer Epidemiol. Biomarkers Prev.* **2005**, *14* (2), 467–475.
175. Koutsky, L. A.; Holmes, K. K.; Critchlow, C. W.; Stevens, C. E.; Paavonen, J.; Beckmann, A. M.; Derouen, T. A.; Galloway, D. A.; Vernon, D.; Kiviat, N. B., A Cohort Study of the Risk of Cervical Intraepithelial Neoplasia Grade-2 or Grade-3 in Relation to Papillomavirus Infection. *New Engl. J. Med.* **1992**, *327* (18), 1272–1278.
176. D'Souza, G.; Kreimer, A. R.; Viscidi, R.; Pawlita, M.; Fakhry, C.; Koch, W. M.; Westra, W. H.; Gillison, M. L., Case-control study of human papillomavirus and oropharyngeal cancer. *N. Engl. J. Med.* **2007**, *356* (19), 1944–1956.

177. Chaturvedi, A. K.; Engels, E. A.; Anderson, W. F.; Gillison, M. L., Incidence trends for human papillomavirus-related and -unrelated oral squamous cell carcinomas in the United States. *J. Clin. Oncol.* **2008**, *26* (4), 612–619.
178. Gillison, M. L.; Harris, J.; Westra, W.; Chung, C.; Jordan, R.; Rosenthal, D.; Nguyen-Tan, P.; Spanos, W. J.; Redmond, K. P.; Ang, K.; Grp, R. T. O., Survival outcomes by tumor human papillomavirus (HPV) status in stage III-IV oropharyngeal cancer (OPC) in RTOG 0129. *J. Clin. Oncol.* **2009**, *27* (15s), abstr 6003.
179. Spanos, W. C.; Nowicki, P.; Lee, D. W.; Hoover, A.; Hostager, B.; Gupta, A.; Anderson, M. E.; Lee, J. H., Immune response during therapy with cisplatin or radiation for human papillomavirus-related head and neck cancer. *Arch. Otolaryngol. Head Neck Surg.* **2009**, *135* (11), 1137–1146.
180. Nagel, R.; Martens-de Kemp, S. R.; Buijze, M.; Jacobs, G.; Braakhuis, B. J.; Brakenhoff, R. H., Treatment response of HPV-positive and HPV-negative head and neck squamous cell carcinoma cell lines. *Oral Oncol.* **2013**, *49* (6), 560–566.
181. Colevas, A. D., Chemotherapy options for patients with metastatic or recurrent squamous cell carcinoma of the head and neck. *J. Clin. Oncol.* **2006**, *24* (17), 2644–2652.
182. Walboomers, J. M. M.; Jacobs, M. V.; Manos, M. M.; Bosch, F. X.; Kummer, J. A.; Shah, K. V.; Snijders, P. J. F.; Peto, J.; Meijer, C. J. L. M.; Munoz, N., Human papillomavirus is a necessary cause of invasive cervical cancer worldwide. *J. Pathol.* **1999**, *189* (1), 12–19.
183. Danos, O.; Katinka, M.; Yaniv, M., Human Papillomavirus-1a Complete DNA-Sequence - a Novel Type of Genome Organization among Papovaviridae. *Embo J.* **1982**, *1* (2), 231–236.
184. Chow, L. T.; Broker, T. R.; Steinberg, B. M., The natural history of human papillomavirus infections of the mucosal epithelia. *Apmis* **2010**, *118* (6-7), 422–449.
185. Sedman, S. A.; Barbosa, M. S.; Vass, W. C.; Hubbert, N. L.; Haas, J. A.; Lowy, D. R.; Schiller, J. T., The Full-Length E6 Protein of Human Papillomavirus Type-16 Has Transforming and Trans-Activating Activities and Cooperates with E7 to immortalize Keratinocytes in Culture. *J. Virol.* **1991**, *65* (9), 4860–4866.
186. Smotkin, D.; Prokoph, H.; Wettstein, F. O., Oncogenic and nononcogenic human genital papillomaviruses generate the E7 mRNA by different mechanisms. *J. Virol.* **1989**, *63* (3), 1441–1447.
187. Rosenberger, S.; De-Castro Arce, J.; Langbein, L.; Steenbergen, R. D.; Rosl, F., Alternative splicing of human papillomavirus type-16 E6/E6* early mRNA is coupled to EGF signaling via Erk1/2 activation. *Proc. Natl. Acad. Sci. U S A* **2010**, *107* (15), 7006–7011.
188. Scheffner, M.; Werness, B. A.; Huibregtse, J. M.; Levine, A. J.; Howley, P. M., The E6 oncoprotein encoded by human papillomavirus types 16 and 18 promotes the degradation of p53. *Cell* **1990**, *63* (6), 1129–1136.
189. Munger, K.; Phelps, W. C.; Bubb, V.; Howley, P. M.; Schlegel, R., The E6 and E7 genes of the human papillomavirus type 16 together are necessary and sufficient for transformation of primary human keratinocytes. *J. Virol.* **1989**, *63* (10), 4417–4421.
190. Kosel, S.; Burggraf, S.; Engelhardt, W.; Olgemoller, B., Increased levels of HPV16 E6*I transcripts in high-grade cervical cytology and histology (CIN II+) detected by rapid real-time RT-PCR amplification. *Cytopathology* **2007**, *18* (5), 290–299.
191. Cricca, M.; Venturoli, S.; Leo, E.; Costa, S.; Musiani, M.; Zerbini, M., Molecular analysis of HPV 16 E6I/E6II spliced mRNAs and correlation with the viral physical state and the grade of the cervical lesion. *J. Med. Virol.* **2009**, *81* (7), 1276–1282.

192. Pim, D.; Massimi, P.; Banks, L., Alternatively spliced HPV-18 E6* protein inhibits E6 mediated degradation of p53 and suppresses transformed cell growth. *Oncogene* **1997**, *15* (3), 257–264.
193. Filippova, M.; Johnson, M. M.; Bautista, M.; Filippov, V.; Fodor, N.; Tungteakkhun, S. S.; Williams, K.; Duerksen-Hughes, P. J., The large and small isoforms of human papillomavirus type 16 E6 bind to and differentially affect procaspase 8 stability and activity. *J. Virol.* **2007**, *81* (8), 4116–4129.
194. Shirasawa, H.; Jin, M. H.; Shimizu, K.; Akutsu, N.; Shino, Y.; Simizu, B., Transcription-Modulatory Activity of Full-Length E6 and E6-Asterisk-I Proteins of Human Papillomavirus Type-16. *Virology* **1994**, *203* (1), 36–42.
195. Gao, Y.; Koide, K., Chemical perturbation of Mcl-1 pre-mRNA splicing to induce apoptosis in cancer cells. *ACS Chem. Biol.* **2013**, *8*, 895–900.
196. Laetsch, T. W.; Liu, X.; Vu, A.; Sliozberg, M.; Vido, M.; Elci, O. U.; Goldsmith, K. C.; Hogarty, M. D., Multiple components of the spliceosome regulate Mcl1 activity in neuroblastoma. *Cell Death Dis.* **2014**, *5*, e1072.
197. Ahrendt, S. A.; Chow, J. T.; Yang, S. C.; Wu, L.; Zhang, M. J.; Jen, J.; Sidransky, D., Alcohol consumption and cigarette smoking increase the frequency of p53 mutations in non-small cell lung cancer. *Cancer Res.* **2000**, *60* (12), 3155–3159.
198. Hashibe, M.; Brennan, P.; Benhamou, S.; Castellsague, X.; Chen, C.; Curado, M. P.; Dal Maso, L.; Daudt, A. W.; Fabianova, E.; Fernandez, L.; Wunsch-Filho, V.; Franceschi, S.; Hayes, R. B.; Herrero, R.; Koifman, S.; La Vecchia, C.; Lazarus, P.; Levi, F.; Mates, D.; Matos, E.; Menezes, A.; Muscat, J.; Eluf-Neto, J.; Olshan, A. F.; Rudnai, P.; Schwartz, S. M.; Smith, E.; Sturgis, E. M.; Szeszenia-Dabrowska, N.; Talamini, R.; Wei, Q.; Winn, D. M.; Zaridze, D.; Zatonski, W.; Zhang, Z. F.; Berthiller, J.; Boffetta, P., Alcohol drinking in never users of tobacco, cigarette smoking in never drinkers, and the risk of head and neck cancer: pooled analysis in the International Head and Neck Cancer Epidemiology Consortium. *J. Natl. Cancer Inst.* **2007**, *99* (10), 777–789.
199. Loewe, S., The problem of synergism and antagonism of combined drugs. *Arzneimittelforschung* **1953**, *3* (6), 285–290.
200. Greco, W. R.; Bravo, G.; Parsons, J. C., The search for synergy: a critical review from a response surface perspective. *Pharmacol. Rev.* **1995**, *47* (2), 331–385.
201. Silva, M. T., Secondary necrosis: the natural outcome of the complete apoptotic program. *FEBS Lett.* **2010**, *584* (22), 4491–4499.
202. Germain, M.; Nguyen, A. P.; Le Grand, J. N.; Arbour, N.; Vanderluit, J. L.; Park, D. S.; Opferman, J. T.; Slack, R. S., MCL-1 is a stress sensor that regulates autophagy in a developmentally regulated manner. *EMBO J.* **2011**, *30* (2), 395–407.
203. Shkreta, L.; Froehlich, U.; Paquet, E. R.; Toutant, J.; Elela, S. A.; Chabot, B., Anticancer drugs affect the alternative splicing of Bcl-x and other human apoptotic genes. *Mol. Cancer Ther.* **2008**, *7* (6), 1398–1409.
204. Smotkin, D.; Wettstein, F. O., Transcription of human papillomavirus type 16 early genes in a cervical cancer and a cancer-derived cell line and identification of the E7 protein. *Proc. Natl. Acad. Sci. USA* **1986**, *83* (13), 4680–4684.
205. Cumming, S. A.; McPhillips, M. G.; Veerapraditsin, T.; Milligan, S. G.; Graham, S. V., Activity of the human papillomavirus type 16 late negative regulatory element is partly due to four weak consensus 5' splice sites that bind a U1 snRNP-like complex. *J. Virol.* **2003**, *77* (9), 5167–5177.

206. Mole, S.; Milligan, S. G.; Graham, S. V., Human papillomavirus type 16 E2 protein transcriptionally activates the promoter of a key cellular splicing factor, SF2/ASF *J. Virol.* **2009**, *83* (7), 3418–3418.
207. Ramirez-Salazar, E.; Centeno, F.; Nieto, K.; Valencia-Hernandez, A.; Salcedo, M.; Garrido, E., HPV16 E2 could act as down-regulator in cellular genes implicated in apoptosis, proliferation and cell differentiation. *Virol. J.* **2011**, *8*, 247–256.
208. Lee, J. O.; Russo, A. A.; Pavletich, N. P., Structure of the retinoblastoma tumour-suppressor pocket domain bound to a peptide from HPV E7. *Nature* **1998**, *391* (6670), 859–865.
209. Quinn, B. A.; Dash, R.; Azab, B.; Sarkar, S.; Das, S. K.; Kumar, S.; Oyesanya, R. A.; Dasgupta, S.; Dent, P.; Grant, S.; Rahmani, M.; Curiel, D. T.; Dmitriev, I.; Hedvat, M.; Wei, J.; Wu, B. N.; Stebbins, J. L.; Reed, J. C.; Pellecchia, M.; Sarkar, D.; Fisher, P. B., Targeting Mcl-1 for the therapy of cancer. *Expert Opin. Investig. Drugs* **2011**, *20* (10), 1397–1411.
210. Gwodz, C.; Balz, V.; Scheckenbach, K.; Bier, H., p53, p63 and p73 expression in squamous cell carcinomas of the head and neck and their response to cisplatin exposure. *Adv. Otorhinolaryngol.* **2005**, *62*, 58–71.
211. Brenner, J. C.; Graham, M. P.; Kumar, B.; Saunders, L. M.; Kupfer, R.; Lyons, R. H.; Bradford, C. R.; Carey, T. E., Genotyping of 73 UM-SCC head and neck squamous cell carcinoma cell lines. *Head Neck* **2010**, *32* (4), 417–426.
212. Bradford, C. R.; Zhu, S.; Ogawa, H.; Ogawa, T.; Ubell, M.; Narayan, A.; Johnson, G.; Wolf, G. T.; Fisher, S. G.; Carey, T. E., P53 mutation correlates with cisplatin sensitivity in head and neck squamous cell carcinoma lines. *Head Neck* **2003**, *25* (8), 654–661.
213. Steenbergen, R. D.; Hermsen, M. A.; Walboomers, J. M.; Joenje, H.; Arwert, F.; Meijer, C. J.; Snijders, P. J., Integrated human papillomavirus type 16 and loss of heterozygosity at 11q22 and 18q21 in an oral carcinoma and its derivative cell line. *Cancer Res.* **1995**, *55* (22), 5465–5471.
214. Ferris, R. L.; Martinez, I.; Sirianni, N.; Wang, J.; Lopez-Albaitero, A.; Gollin, S. M.; Johnson, J. T.; Khan, S., Human papillomavirus-16 associated squamous cell carcinoma of the head and neck (SCCHN): a natural disease model provides insights into viral carcinogenesis. *Eur. J. Cancer* **2005**, *41* (5), 807–815.
215. Chikamatsu, K.; Nakano, K.; Storkus, W. J.; Appella, E.; Lotze, M. T.; Whiteside, T. L.; DeLeo, A. B., Generation of anti-p53 cytotoxic T lymphocytes from human peripheral blood using autologous dendritic cells. *Clin. Cancer Res.* **1999**, *5* (6), 1281–1288.
216. Krause, C. J.; Carey, T. E.; Ott, R. W.; Hurbis, C.; McClatchey, K. D.; Regezi, J. A., Human squamous cell carcinoma. Establishment and characterization of new permanent cell lines. *Arch. Otolaryngol.* **1981**, *107* (11), 703–710.
217. Wei, M. C.; Zong, W. X.; Cheng, E. H.; Lindsten, T.; Panoutsakopoulou, V.; Ross, A. J.; Roth, K. A.; MacGregor, G. R.; Thompson, C. B.; Korsmeyer, S. J., Proapoptotic BAX and BAK: a requisite gateway to mitochondrial dysfunction and death. *Science* **2001**, *292* (5517), 727–730.
218. McGuire, W. P.; Hoskins, W. J.; Brady, M. F.; Kucera, P. R.; Partridge, E. E.; Look, K. Y.; Clarke-Pearson, D. L.; Davidson, M., Cyclophosphamide and cisplatin compared with paclitaxel and cisplatin in patients with stage III and stage IV ovarian cancer. *New Engl. J. Med.* **1996**, *334* (1), 1–6.
219. Galluzzi, L.; Senovilla, L.; Vitale, I.; Michels, J.; Martins, I.; Kepp, O.; Castedo, M.; Kroemer, G., Molecular mechanisms of cisplatin resistance. *Oncogene* **2012**, *31* (15), 1869–1883.

220. Andrews, P. A.; Murphy, M. P.; Howell, S. B., Differential potentiation of alkylating and platinating agent cytotoxicity in human ovarian carcinoma cells by glutathione depletion. *Cancer Res.* **1985**, *45* (12 Pt 1), 6250–6253.
221. Munoz, N.; Bosch, F. X.; de Sanjose, S.; Herrero, R.; Castellsague, X.; Shah, K. V.; Snijders, P. J. F.; Meijer, C. J. L. M., Epidemiologic classification of human papillomavirus types associated with cervical cancer. *New Engl. J. Med.* **2003**, *348* (6), 518–527.
222. Heck, J. E.; Berthiller, J.; Vaccarella, S.; Winn, D. M.; Smith, E. M.; Shan'gina, O.; Schwartz, S. M.; Purdue, M. P.; Pilarska, A.; Eluf-Neto, J.; Menezes, A.; McClean, M. D.; Matos, E.; Koifman, S.; Kelsey, K. T.; Herrero, R.; Hayes, R. B.; Franceschi, S.; Wunsch, V.; Fernandez, L.; Daudt, A. W.; Curado, M. P.; Chen, C.; Castellsague, X.; Ferro, G.; Brennan, P.; Boffetta, P.; Hashibe, M., Sexual behaviours and the risk of head and neck cancers: a pooled analysis in the International Head and Neck Cancer Epidemiology (INHANCE) consortium. *Int. J. Epidemiol.* **2010**, *39* (1), 166–181.
223. O'Leary, J. J.; Browne, G.; Johnson, M. I.; Landers, R. J.; Crowley, M.; Healy, I.; Street, J. T.; Pollock, A. M.; Lewis, F. A.; Andrew, A.; Cullinane, C.; Mohamdee, O.; Kealy, W. F.; Hogan, J.; Doyle, C. T., PCR in-situ hybridization detection of HPV-16 in fixed Caski and fixed SiHa cell-lines. *J. Clin. Pathol.* **1994**, *47* (10), 933–938.
224. Sakurai, M. K., J.; Nishio, M.; Yamamoto, K.; Okuda, T.; Kawano, K.; Nakanishi, N., TMC-205 a new transcriptional up-regulator of SV40 promoter produced by an unidentified fungus, fermentation, isolation, physico-chemical properties, structure determination and biological activities. *J. Antibiot.* **2001**, *54* (8), 628–634.
225. Parsons, P. G. H., C.; Fairlie, D. P.; West, M. L.; Danoy, P. A. C.; Sturm, R. A.; Dunn, I. S.; Pedky, J. Ablett, E. M., Tumor selectivity and transcriptional activation by azelaic bishydroxamic acid in human melanocytic cells. *Biochem. Pharmacol.* **1997**, *53* (11), 1719–1724.
226. Sowa, Y. O., T.; Minamikawa, S.; Nakano, K.; Mizuno, T.; Nomura, H.; Sakai, T., Histone deacetylase inhibitor activates the WAF1/Cip1 gene promoter through the Sp1 sites. *Biochem. Biophys. Res. Commun.* **1997**, *241* (1), 142–150.
227. Ueda, H. N., H.; Hori, Y.; Fujita, T.; Nishimura, M.; Goto, T.; Okuhara, M., FR901228, a novel antitumor bicyclic depsipeptide produced by chromobacterium violaceum No 968. I. Taxonomy, fermentation, isolation, physico-chemical and biological properties, and antitumor activity. *J. Antibiot.* **1994**, *47* (3), 301–310.
228. Johnstone, R. W., Histone-deacetylase inhibitors: novel drugs for the treatment of cancer. *Nat. Rev. Drug Discov.* **2002**, *1* (4), 287–299.
229. Furumai, R.; Komatsu, Y.; Nishino, N.; Khochbin, S.; Yoshida, M.; Horinouchi, S., Potent histone deacetylase inhibitors built from trichostatin A and cyclic tetrapeptide antibiotics including trapoxin. *Proc. Natl. Acad. Sci. USA* **2001**, *98* (1), 87–92.
230. Vigushin, D. M.; Ali, S.; Pace, P. E.; Mirsaidi, N.; Ito, K.; Adcock, I.; Coombes, R. C., Trichostatin A is a histone deacetylase inhibitor with potent antitumor activity against breast cancer in vivo. *Clin. Cancer Res.* **2001**, *7* (4), 971–976.
231. van Alphen, R. J.; Wiemer, E. A.; Burger, H.; Eskens, F. A., The spliceosome as target for anticancer treatment. *Br. J. Cancer* **2009**, *100* (2), 228–232.
232. Tazi, J.; Durand, S.; Jeanteur, P., The spliceosome: a novel multi-faceted target for therapy. *Trends Biochem. Sci.* **2005**, *30* (8), 469–478.

233. Auld, D. S.; Southall, N. T.; Jadhav, A.; Johnson, R. L.; Diller, D. J.; Simeonov, A.; Austin, C. P.; Inglese, J., Characterization of chemical libraries for luciferase inhibitory activity. *J. Med. Chem.* **2008**, *51* (8), 2372–2386.
234. Auld, D. S.; Zhang, Y. Q.; Southall, N. T.; Rai, G.; Landsman, M.; MacLure, J.; Langevin, D.; Thomas, C. J.; Austin, C. P.; Inglese, J., A basis for reduced chemical library inhibition of firefly luciferase obtained from directed evolution. *J. Med. Chem.* **2009**, *52* (5), 1450–1458.
235. Poutiainen, P. K.; Palvimo, J. J.; Hinkkanen, A. E.; Valkonen, A.; Vaisanen, T. K.; Laatikainen, R.; Pulkkinen, J. T., Discovery of 5-Benzyl-3-phenyl-4,5-dihydroisoxazoles and 5-Benzyl-3-phenyl-1,4,2-dioxazoles as Potent Firefly Luciferase Inhibitors. *J. Med. Chem.* **2013**, *56* (3), 1064–1073.
236. Braeuning, A.; Vetter, S., The nuclear factor kappaB inhibitor (E)-2-fluoro-4'-methoxystilbene inhibits firefly luciferase. *Biosci. Rep.* **2012**, *32* (6), 531–537.
237. Thorne, N.; Shen, M.; Lea, W. A.; Simeonov, A.; Lovell, S.; Auld, D. S.; Inglese, J., Firefly luciferase in chemical biology: a compendium of inhibitors, mechanistic evaluation of chemotypes, and suggested use as a reporter. *Chem. Biol.* **2012**, *19* (8), 1060–1072.
238. Somanadhan, B.; Leong, C.; Whitton, S. R.; Ng, S.; Buss, A. D.; Butler, M. S., Identification of a naturally occurring quinazolin-4(3H)-one firefly luciferase inhibitor. *J. Nat. Prod.* **2011**, *74* (6), 1500–1502.
239. Bakhtiarova, A.; Taslimi, P.; Elliman, S. J.; Kosinski, P. A.; Hubbard, B.; Kavana, M.; Kemp, D. M., Resveratrol inhibits firefly luciferase. *Biochem. Biophys. Res. Commun.* **2006**, *351* (2), 481–484.
240. Burlingham, B. T.; Widlanski, T. S., An intuitive look at the relationship of K_i and IC_{50} : A more general use for the Dixon plot. *J. Chem. Edu.* **2003**, *80* (2), 214–218.